BIODEGRADABLE POLYMERS FOR DRUG DELIVERY: SYNTHESIS AND CHARACTERIZATION

A THESIS SUBMITTED TO THE
UNIVERSITY OF PUNE
FOR THE DEGREE OF
DOCTOR OF PHILOSOPHY
IN
CHEMISTRY

BY

HIRE SANTOSH LAXMAN

POLYMER SCIENCE AND ENGINEERING DIVISION
NATIONAL CHEMICAL LABORATORY
PUNE-411008, INDIA

DECEMBER 2011

CERTIFICATE

This is to certify that the work incorporated in the thesis entitled **"Biodegradable Polymers for Drug Delivery: Synthesis and Characterization"** submitted by **Mr. Hire Santosh Laxman** was carried out under my supervision. Such material as has been obtained from other sources has been duly acknowledged in the thesis.

Date: **Dr. M. G. Kulkarni**

National Chemical Laboratory, **(Research Guide)**

Pune 411008.

DECLARATION

I hereby declare that the work presented in the thesis entitled **"Biodegradable Polymers for Drug Delivery: Synthesis and Characterization"** submitted for Ph. D. degree to the University of Pune has been carried out under the supervision of **Dr. M. G. Kulkarni** at the Division of Polymer Science and Engineering, National Chemical Laboratory, Pune, India. The work is original and has not been submitted in part or full by me for any degree or diploma to this or any other University.

Date: **Hire Santosh Laxman**

National Chemical Laboratory, **(Research Student)**

Pune 411008.

Acknowledgements

It is with great pleasure and humble thanks to my guide Dr. M. G. Kulkarni (Head, PSE), for his realistic and motivating suggestions and constant encouragement. I am especially appreciative of the amount of freedom he has extended to me over the years, in terms of research topics and areas of investigation. I consider myself to be fortunate to work under his guidance.

It is my pleasure to acknowledge Dr. Saurav Pal, Director, NCL, for permitting me to present this work in form of thesis.

I would like to acknowledge the financial support received from CSIR in the form of Senior Research Fellowships.

I wish to express my warm and sincere thanks to Dr. S.B. Ogale, Dr. Mrs. M. V. Shelke, Dr. Rabah and Dr. Elisabeth for their help, suggestions and discussion on soft lithography.

My sincere thanks go to Dr. Badiger, Mr. M. J. Thakar, Dr. Rathna and Dr. Karmalkar, for the support given to me during this work.

I'm highly obliged to Dr. Rajmohanan, Dr. Ponrathnam, Mr. Pandare, Dr. Lele, Mr. Menon, Mrs. Dhobale, Mrs. Poorvi, Mr. Gaikwad, Mr. Mane, Mr. Giri, Mr. Murgan, Mr. Jadhav, Mr. Pagare and Mr. Ketan for the support extended during the course of work.

I am grateful to all my friends Suresha, Sachin, Ujwal, Dr. Hemant, Dr. Ramesh, Dr. Gahininath, Dr. Amit, Dr. Arun, Dr. Swarnendu, Dr. Kiran, Dr. Narayan, Dr. Mahesh, Dr. Jayant, Dr. Sudhir, Dr. Raman, Dr. Rupali, Dr. Smitha, Dr. Anupa, Dr. Sunita, Dr. Prerana, Dr. Shubhangi, Dr. Jyotsna, Dr. Jiten, Aarti, Nivika, Manjusha, Dr. Harshada, Shamika, Trupti, Satish, Sameera, Swapnil, Sandeep, Vinod, Rafat, Muntazim, Arpita, Neelam, Vishal, Tushar, Venkat, Narhari, Dr. Anu, Anumon, Pawan, Dr. Abhilash, Dr. Nagraj, Ashwini and Vinayak for timely help, co-operation and making my stay at NCL pleasant.

I would like to thank Mr. Dhavale, Mr. Grime, Mr. Kokane, Mr. Mahajan and Mr. Bharati for all the help rendered by them.

Completion of this thesis would not have been possible without the unconditional support and faith bestowed by my wife Rekha and my in-laws.

*Aai, Dada and brother Arun, am overwhelmed to express my feelings for your unconditional support, freedom for career will remain my inspiration throughout my life, your patience, sacrifice, and faith in education gave me the strength to pursue for PhD**...***

Santosh Hire
December 2011

Table of contents

List of tables

Chapter 3

Acid catalyzed synthesis of poly (β-amino esters)

Chapter 4

Synthesis and characterization of sequentially crosslinkable poly (β-amino esters) (SCPBAE)

Chapter 5

Fabrication of biodegradable polymeric scaffolds from sequentially crosslinkable poly (β-amino esters) via soft lithography

Chapter 6

Soft lithography technique to fabricate unusual patterns

List of figures

Chapter 3

Acid catalyzed synthesis of poly (β-amino esters)

Chapter 4

Synthesis and characterization of sequentially crosslinkable poly (β-amino esters) (SCPBAE)

Chapter 5

Fabrication of biodegradable polymeric scaffolds from sequentially crosslinkable poly (β-amino esters) via soft lithography

Chapter 6

Soft lithography technique to fabricate unusual patterns

Abbreviations and symbols

Al_2O_3	Aluminum oxide
$AlCl_3$	Aluminum chloride
AR	Aspect ratio
BPDA	Bisphenol A diacrylate
BP	Boiling point
$CDCl_3$	Deuterated chloroform
CHDMDA	1,4-cyclohexanedimethanol diacrylate
Ch	Channel
CIEF	Capillary isoelectric focusing
Ci	Circle
cP	Centipoise
DDDDA	1,12-dodecanediol diacrylate
DB	Degree of branching
DCM	Dichloromethane
DEGDA	Diethylene glycol diacrylate
DSC	Differential scanning calorimetry
DRIE	Deep reactive ion etched
EGDA	Ethylene glycol diacrylate
FAP	Fluorapatite
$FeCl_3$	Ferric chloride
FTIR	Fourier transform infrared
HDDA	Hexanediol diacrylate
h-PDMS	Hard poly(dimethylsiloxane)
IDDS	Implantable drug delivery system
KBr	Potassium bromide
KF	Potassium fluoride
mPEG-COOH	Methoxyl PEG carboxylic acid
MIMIC	Micromolding in capillaries
M_n	Number average molecular weight
M_w	Weight average molecular weight

NIL	Nanoimprint lithography
NMR	Nuclear magnetic resonance
NMP	N-methyl pyrolidone
NP	Natural phosphate
nTP	Nanotransfer printing
OPLA	Oligomer of lactide
PBAEs	Poly (β-amino esters)
PCL	Poly(ε-caprolactone)
PEI	Poly (ethylene imines)
PEG	Poly ethylene glycol
PETA	Pentaerythritol triacrylate
PEDAMS	Pentaerythritol diacrylate monostearate
PGA	Poly (glycolic acid)
PLA	Poly (lactic acid)
PLL	Poly (L-lysine)
PLLA	Poly (L-lactide)
ppm	Parts per million
PU	Polyurethane
PVA	Poly (vinyl alcohol)
Pz	Piperazine
QDA	Quinol diacrylate
RDDA	Resorcinol diacrylate
RIE	Reactive ion etching
SAMIM	Solvent assisted micro molding
SCPBAEs	Sequentially crosslinkable poly(β-amino esters)
SEM	Scanning electron microscopy
SFIL	Step and flash imprint lithography
Si	Silicon
Sq	Square
TEGDA	Triethylene glycol diacrylate
TMDP	4,4’-trimethylenedipiperidine
TMPTA	Trimethylolpropane triacrylate

TMPAE	Trimethylolpropane allyl ether
TMPMADA	Trimethylolpropane monomethacrylate diacrylate
TMPAEDA	Trimethylolpropane allyl ether diacrylate
TMPTA	Trimethylolpropane triacrylate
TMS	Tetramethylsilane
UV	Ultra violet
VP	Vapor pressure
VPO	Vapor pressure osmometer
μCP	Microcontact printing
μTM	Microtransfer molding

Chapter 1

Thesis overview

Biodegradable polymers play an important role in developing therapeutic devices such as controlled / sustained drug delivery and tissue engineering (Albertson and Varma 2002, Nair and Laurencin 2007, Clapper 2007, Schacht 2003). Biodegradable polymers are generally defined as macromolecular materials capable of conversion into less complex products through chemical reactions, such as simple or enzyme catalyzed hydrolysis over a reasonable period of time (Chandra and Rustgi 1998).

The biodegradable polymers can be classified as natural polymers or synthetic polymers based on their origin. Natural polymers are further classified as polysaccharides, polypeptides and polyesters depending on repeating units. The polysaccharide contains d-glucopyranoside repeating units, e.g. starch, cellulose, chitin and chitosan. Naturally occurring polypeptides contain amino acid repeating units. Amongst naturally occurring polypeptides, Gelatin is extensively used in pharmaceutical and biomedical applications. Naturally occurring polyesters for example poly-β-hydroxybutyrate (PHB) and γ-hydroxy valerate (PHV) are potential candidates for biomedical applications (Chandra and Rustgi 1998). Natural materials are generally biocompatible, and exhibit mechanical properties comparable to native tissues. However these materials also suffer from disadvantages such as limited control over physico-chemical properties, difficulties in modifying degradation rates. Purification and sterilization of these biomaterials after isolation from different sources is rather cumbersome (Dawson et. al. 2008).

In oral drug delivery, cellulose derivatives for example cellulose ethers like ethyl cellulose, methyl cellulose, hydroxypropyl methylcellulose (HPMC) and hydroxypropyl cellulose have been used in the form of coatings. Similarly synthetic polymers such as poly (acrylates), poly (methacrylates), poly (methyl methacrylates), poly (hydroxyethyl methacrylates) and copolymers thereof have been extensively used (Valle et. al. 2009).

Stimuli sensitive polymers are another class of polymers which interact and respond to the environmental conditions such as temperature, light, salt concentration and pH (Dirk 2006). The pH sensitive polymers are used to develop smart delivery systems due to variation of physiological pH in different parts of the body. Most commonly used pH-dependent polymers are methacrylic acid copolymers – Eudragit® L100-55, Eudragit® L100 and Eudragit® S100 which dissolve at pH 5.5, 6.0 and 7.0 respectively. However these polymers are biocompatible but not biodegradable. When polymeric carriers are to

be used in injectable drug delivery systems, biodegradable polymers which degrade into nontoxic and safe products are needed.

The biodegradable aliphatic polyesters, poly (β-hydroxy butyrate), poly (β-malic acid), poly (ε-caprolactone), or poly (α-hydroxy acids) (PLGA) have been extensively investigated for drug delivery and other biomedical applications (Vert 2005, Okada 2002). PLGA and PLLA are used to encapsulate drug in the form of microparticles or nanoparticles to increase the circulation time and bioavailability of drug (Ha and Gardella 2005). New drug delivery systems are developed for chronic diseases and / or conditions that require sustained drug delivery. Commercially available products based on this technology are Lupron® Depot containing the anticancer drug Leuprorelin acetate encapsulated in a poly (lactic-co-glycolic acid) (PLGA) matrix used for the treatment of prostate cancer. Leuprorelin acetate is a superactive luteinizing hormone-releasing hormone (LH-RH) agonist. Trenantone® (Takeda) is a similar product, releasing the drug Leuprorelin acetate over 3 months. The sustained release of drug was achieved initially by drug diffusion from polymeric microspheres followed by polymer degradation (Siepmann and Siepmann 2006).

Development of injectable in situ setting semisolid drug depots has been explored as an alternative delivery system. Biodegradable polymers can be used in the form of injectable matrix or depot for drug delivery and as injectable scaffolds in tissue engineering (Kretlow et. al. 2007). Atrix laboratories developed ATRIGEL® technology where sustained release of Leuprorelin acetate was achieved through in situ formed PLGA depot.

The subsequent generation of drug delivery systems is focused on developing miniaturized targeted devices which offer high spatial and temporal control over drug release. These systems involve the fabrication of small independent reservoir structures or containers that can be manufactured inexpensively, loaded easily with drugs, delivered with minimal trauma, and easily tracked, programmed or controlled (Santini et. al.1999, Randall et. al. 2007). A prototype silicon micro-chip was developed to demonstrate controlled, pulsatile release of single or multiple chemical substances on demand. The release mechanism is based on the electrochemical dissolution of thin anode membrane covering microreservoirs filled with chemicals in solid, liquid or gel form (Santini et. al.

1999). Implantable drug delivery system (IDDS) for example MicroCHIPS have been reported in the literature. In this device macromolecular drugs such as proteins and peptides are stored in their stable form, such as a solid, liquid, or gel. As drugs are stored separately, an implantable system is capable of delivering tens or hundreds of doses of multiple drugs. The drugs can be released in a pulsatile or continuous manner at their optimal therapeutic levels (Maloney et. al. 2004-2005).

In literature the polymer based scaffolds have been developed which can be used in tissue engineering as supports for cell attachment and proliferation (Langer and Vacanti 1993, Hutmacher et. al. 2001[a-b], Xia et. al. 1998-99, Gates et. al. 2005). These biodegradable scaffolds can be simultaneously used as cell support and for controlled delivery of biologically active proteins like growth factors and cytokines (Tessmar and Göpferich 2007). Apart from biodegradability, polymer should satisfy following requirements for processability for example,

a) It has to be liquid so that it can fill the cavities appropriately and replicate the patterns present on mold with high fidelity.
b) It must contain functional groups to enable cross-linking during processing.

Not too many efforts have been made to synthesize polymers for UV-microembossing in the literature.

The photopolymerizable biodegradable diacrylate poly (lactic acid)-b-poly (ethylene oxide)-b-poly (lactic acid) (PLA-b-PEO-b-PLA) macromer was developed for insitu synthesis of hydrogel for fabricating biodegradable scaffolds (Sawhney et. al. 1993). PEG and PLA block macromers containing terminal (meth) acrylate groups. These macromers were photopolymerized to yield highly crosslinked biodegradable materials (Jason et. al. 2007). In another effort to incorporate vinyl functionality in biodegradable aliphatic polyesters, di and triblock copolymers of ε-caprolactone (CL) and glycolide (GA), lactide (LA) with ethylene oxide (EO) bearing terminal vinyl groups were developed. These polymers were further processed by UV- microembossing to fabricate biodegradable scaffolds. However these polymers had to be processed at 65 ºC as these were not liquid at room temperature (Park et. al. 2004, Zhu et. al. 2006).

Photo-patternable biodegradable 2-hydroxylethyl methacrylate (HEMA) conjugated poly (*ε*-caprolactone-*Co*-RS-*β*-malic acid) (PCLMAc) co-polymers were synthesized to

fabricate biodegradable scaffolds. However quantitative conjugation of carboxylic acid groups to HEMA ester is difficult and involves multiple step synthesis. Further, the resulting polymers are not liquid at room temperature and need to be processed at 60 °C (He and Chan 2005).

Liquid photopatternable polyurethane diacrylates were developed to fabricate biocompatible scaffolds by UV-microembossing. The scaffolds fabricated exhibited cytotoxicity due to the presence of unreacted monomers and the photo initiator used during polymer synthesis. The polymers were rendered biocompatible after the residues were leached out by repeated extractions with methanol which itself is not a highly desirable solvent (Shen et. al. 2006). Other examples of photopolymerizable and degradable polymers developed so far include poly (propylene fumarate)s (PPF), photocrosslinkable poly(anhydride)s, poly (ethylene glycol)s and crosslinkable poly (saccharide)s. However synthesis of these polymers involved multiple reactions and purification steps (Brey et. al. 2008[b]).

In this context we intend to develop materials which can be processed by photo crosslinking and also which will exhibit a wide range of degradation profiles. We would also evaluate their processability to assess utility in various applications.

We have identified poly (β-amino esters) which were synthesized as transfection vectors for gene delivery (Lynn and Langer 2000, Lynn et. al. 2001, Anderson et. al. 2003, Green et. al. 2008). These polymers are promising candidates, as they are viscous liquids at room temperature, non-cytotoxic and biodegradable, they lack functionality necessary for processing via UV-microembossing. We would manipulate their structures as to meet these requirements. Each of these applications which involves, synthesis, characterization, processing and evaluation of fabricated structures has been discussed in each chapter individually. In this chapter we present an overview of the work undertaken.

The objectives and scope of the proposed research investigation were

1. Explore the use Lewis acid as a catalyst in the synthesis of poly (β-amino esters) to shorten polymerization time and to extend this methodology to synthesize PLA, PCL based chain extended and poly (β-amino esters) containing hydrophobic pendant chains.

2. Undertake synthesis of trivinyl monomers bearing functional groups for example, acrylate, methacrylate and allyl ether having different reactivity towards Michael addition reaction and reaction with bifunctional amines to yield polymers bearing pendant acrylate, methacrylate and allyl ether groups.
3. To fabricate micropatterned polymeric scaffolds of sequentially crosslinkable poly (β-Amino esters) via UV-microembossing technique.
4. To explore the possibility of exploiting conventional soft-lithography technique to fabricate novel patterns.

The details of the objective of the investigation are presented in *chapter 2*.

In polymer chemistry Michael addition reaction has been successfully applied for the synthesis of different types of polymers. A classic example of Michael addition polymerization is anionic chain growth polymerization of methacrylate monomers. Numerous examples of step growth Michael addition exist. Typical examples include Poly (amido amines), Poly (amino esters)**,** Poly (imido sulfides), Poly (ester sulfides), Poly (aspartamide), Poly (imido ethers), Poly (amino quinone), Poly (enone sulfide) and Poly (enamine ketone). Poly (β-amino esters) were synthesized via conjugate addition of primary or secondary bis amine to diacrylate ester as transfection vectors for gene delivery (Lynn and Langer 2000, Lynn 2001). However the synthesis of poly (β-amino esters) is too sluggish and takes up to 5 days and a decrease in reaction time is desirable.

Chapter 3 describes an improved methodology for the synthesis of poly (β-amino esters) using Lewis acid as a catalyst. The investigation revealed that the Lewis acids such as $AlCl_3$ and $FeCl_3$ brought down reaction time from 5 days to few hours at room temperature without sacrificing the yield and molecular weight of polymer. Hydrophilic diacrylates EGDA, DEGDA, TEGDA, PEGDA and hydrophobic diacrylates BDDA, HDDA, CHDMDA, DDDDA, QDA and BPDA diacrylates were selected for polymerization with bi-functional amines such as piperazine (Pz), 4, 4' trimethylenedipiperidine (TMDP), 5-amino pentanol and 4-amino butanol. It was concluded that tetrahydrofuran; dichloromethane and acetone could be used as solvents for polymerization. Incorporation of 1 mole % Lewis acid such as $AlCl_3$, $FeCl_3$ and $ZnCl_2$ was adequate. Hydrophilic or hydrophobic polymers could be synthesized by the choice of appropriate monomers. This methodology was further extended to synthesize chain

extension polymers of oligo PLA/PCL and to incorporate pendant chains in polymer structure. The polymers were characterized by instrumental techniques such as NMR, IR spectroscopy, gel permeation chromatography (GPC), vapor pressure osmometry (VPO) and differential scanning calorimetry (DSC).

The dissolution studies of poly (β-amino esters) revealed that the polymers are more readily soluble at acidic pH than near neutral or neutral pH. The solubility of poly (β-amino esters) can be effectively manipulated using monomers containing either long chain hydrocarbon groups as in DDDDA or rigid groups as in CHDMDA. The PLA and PCL based polymers exhibited pH dependant degradation where rate of degradation in acidic medium was faster than that at neutral and basic pH. No evidence of retro Michael reaction was noticed during hydrolytic degradation of polymers. The molecular weight of degradation fractions can be manipulated by selecting PLA diacrylates of varying molecular weight. Diltiazem HCl release study from Poly (HDDA-Co-TMDP) microparticles showed that these polymers could be potential candidates for development of chewable, rapidly disintegrating, quick dissolve tablets for immediate release of drug at gastric region.

Photopolymerizable biodegradable polymers are desirable for the fabrication of tissue scaffolds with controlled surface micropatterns using photolithographic techniques. In *chapter 4* we report synthesis of photo crosslinkable poly (β-amino esters) by Michael addition of triacrylate and mixture of diacrylate and triacrylate with amines in stoichiometric proportions (1:1). These polymers were photopolymerized to form crosslinked degradable networks exhibiting degradation from one week to three months. Both linear and branched polymers were synthesized by the appropriate choice of monomers. In the first approach, triacrylates such as trimethylolpropane triacrylate (TMPTA) and pentaerythritol triacrylate (PETA) were selected for Michael addition with amines to yield branched polymers. In the second approach, one of the acrylate groups of TMPTA was replaced by methacrylate or allyl ether group to yield trimethylolpropane monomethacrylate diacrylate (TMPMADA) or trimethylolpropane mono allyl ether diacrylate (TMPAEDA) respectively. Methacrylate and allyl ether groups are poor Michael acceptors and hence did not participate in Michael addition polymerization, which resulted in linear SCPBAEs.

The incorporation of pendant vinyl functionality was varied to evaluate the effect of crosslinking on degradation. This was achieved by reacting mixtures of diacrylate and triacrylate in various proportions with secondary bis-amines keeping total acrylate to amine mole ratio constant (1:1). The ^{1}H NMR and IR characterization techniques were used for polymer structure elucidation. This synthetic approach avoided the need for protection and deprotection of vinyl groups. Subsequently these polymers were photo-crosslinked using photointiator and UV- radiations. It was observed that in poly (TMPAEDA-Co-TMDP) the conversion of allyl groups in to crosslinked product is lower than that in acrylate and methacrylate groups due low reactivity of allyl ether groups (Heatley et. al. 1993). Curing proceeded rapidly in first 10 min and leveled off after 15 mins. Hence for all subsequent curing experiments polymers were exposed to UV light for 15 mins. The gel content was analyzed to determine the weight fraction of insoluble polymer. Polymers bearing acrylate and methacrylate groups showed comparable gel contents in the range 89 to 94 %. However polymers containing less reactive allyl ether groups showed lower gel content (78 %) (Heatley et. al. 1993). Copolymers were synthesized wherein the ratio of methacrylate diacrylate to diacrylate was varied from 10:90 to 100:0. The gel content decreased with decreasing methacrylate content. However the difference in gel content was less than 10 %. The effect of pendant vinyl group using either acrylate; methacrylate or allyl ether on degradation rate of crosslinked polymers was investigated. It was observed that the degradation of the polymers was controlled by the hydrophobicity of the polymer rather than the degree of crosslinking. The results revealed that the degradation rate could be manipulated upto 3 months based on the choice of monomers. The polymer degradation results indicated that these polymers could be useful for the applications where in polymers need to degrade over varying time spans (Brey et. al. 2008[a]). The uncrosslinked polymers were liquids and also soluble in organic solvents hence could be processed using soft lithography techniques.

In *chapter 5* we report the performance of sequentially crosslinkable poly (β-amino esters) (SCPBAEs) in UV-microembossing. These polymers offer following advantages, these are a) liquid, b) contain functionality necessary for thermal or photo curing and c) after crosslinking yield biodegradable polymers with wide range of degradation profiles.

We selected silicon masters with three different types of pattern geometry, 1) channels, 2) squares and 3) circles varying in aspect ratio and pattern density. These silicon masters were used to fabricate PDMS molds via replica molding technique. SCPABEs synthesized by us were evaluated using these PDMS molds by UV-microembossing. These scaffolds could be used for tissue engineering of tubular organs such as blood vessels and esophagus. The fabrication of small independent microreservoir structures or containers is desired for the development of micro-chip based drug delivery system. Further these microreservoirs can be loaded with drugs, and be easily tracked, programmed or controlled. The results of the evaluation indicated that polymers replicated patterns present on PDMS mold with good fidelity irrespective of polymer structure and extent of crosslinkable functionality present. SCPBAEs synthesized by us were processed in PDMS molds with laterally collapsed cylindrical pillars. It was observed that these lateral collapses of pillars were not directly reflected on the patterns present in polymer film. We got well separated micro wells even for the PDMS molds where lateral collapses of micropillars was noticed. A systematic investigation of laterally collapsed cylindrical micropillars revealed that upper portion of pillars was bent and only tips of the pillars adhered to each other. However the dimensions and position of the micro pillar's base attached to PDMS substrate were unchanged. Hence once the viscous polymer was poured over PDMS mold, it crept down along laterally collapsed micro pillars to fill the cavities. After UV curing of SCPBAEs crosslinked films were peeled from PDMS mold. Micropatterns present on the polymer film surface were complementary to micro pillar's base attached to PDMS substrate. Hence SEM images for UV embossed polymeric films which were fabricated using PDMS molds with laterally collapsed pillars showed well isolated micro wells. However cross section of micropatterned polymer film showed that micro wells formed in polymer were fused with each other within polymer matrix. This however is a limitation of PDMS used and not SCPBAEs resins. This can be overcome by using hard PDMS (h-PDMS) as reported by (Lee et. al 2005).

It was observed that SCPBAEs can replicate patterns with aspect ratio as high as 5.4 and pattern density 0.51. The changes in the polymer structure had no significant influence on the performance of polymers during microfabrication. Thus the polymer structure

essentially influenced the polymer degradation rate. We also observed 5 to 10 % difference in feature size as compared to feature size present on PDMS molds. This difference in pattern dimensions needs to be considered while processing these polymers by UV-microembossing.

Chapter 6 describes a new approach for creating unique, highly ordered, micro patterns. Pattern geometries that can be processed by replication are limited to those that can be obtained by optical lithography. Features such as squares, rectangles, cylinders can be readily fabricated with PDMS stamps. More complex topologies such as spheres or ellipsoids are difficult to fabricate. Such complex patterns are often desired for the fabrication of tissue engineering scaffolds for directed cell growth, microdevices for drug delivery, microbioreactors, microlens arrays and many other applications. Towards this end, mechanical deformation of polymer molds (Xia et. al. 1996), liquid filled cavities (Chronis et. al. 2003), thermal reflow processes (Yang et. al. 2004), gel entrapment (Cayre et. al 2004) , silicon mold with high aspect ratio pattern (Giang et. al 2007), elastic contact induced self organized patterning of soft polymer films (Gonuguntla et. al. 2006), deformation of PDMS membrane using air pressure through SU-8 shadow mask (Park et. al. 2009), and patterning through selective inversion of a liquid–liquid bilayer (Léopoldés and Damman 2006), have been investigated in the past. In the context of recent efforts to fabricate more complex patterns, we present in this chapter a simple new approach for the creation of unique highly ordered mixed microcavity pattern. A viscous polymer solution is poured onto a PDMS mold bearing simple geometric pattern replicated from a silicon master. Evolution of solvent vapours through the viscous polymer solution simultaneously with cross-linking, results in the generation of the patterns not present in the parent PDMS mold.The effect of different fabrication parameters such as polymer solution viscosity, film thickness, solvent vapor pressure, pre-curing time and aspect ratio of parent pattern modify the morphology of new patterns not present in the parent mold in a predictable manner which has been attributed to the back pressure of the solvent vapor released during processing.

We further demonstrate that these novel patterns created on the polymer film can be subsequently transferred to another PDMS mold and can then be used to generate multiple copies of the said patterns. These PDMS molds show that the complementary

patterns are also highly regular in their size, shape and placement. We believe that such patterns are interesting for many applications such as sensors, MEMS devices, microlens molding, or to fabricate microbioreactor. It would be interesting to study this approach with PDMS templates of different patterns i. e. microcircles, tapered microstructures, etc. The significant results obtained and recommendations for the further work are summarized in *chapter 7*.

References

Albertson A-C., Varma I. *Advances in Polymer Science*, **2002**, 157, 1.

Anderson D., Lynn D., Langer R. *Angew. Chem. Int. Ed.*, **2003**, 42, 3153.

Brey D., Erickson I., Burdick J. *J. Biomed. Mater. Res.*, **2008[a]**, 85A, 731.

Brey D., Ifkovits J., Mozia R., Katz J., Burdick J. Acta Biomaterialia **2008[b]**, 4, 207.

Clapper J.; Skeie J.; Mullins R., Guymon C. *Polymer*, **2007**, 48, 6554.

Chandra R., Rustgi R. *Prog. Polym. Sci.*, **1998**, 23, 1273.

Chronis N., Liu G., Jeong K., Lee L. *Opt. Express***, 2003**, 11, 2370.

Cayre O., Paunov V., *J. Mater. Chem.*, **2004**, 14, 3300.

Dawson E., Mapili G., Erickson K., Taqvi S., Roy K. *Advanced Drug Delivery Reviews*, **2008**, 60, 215.

Dirk S. *Advanced Drug Delivery Reviews*, **2006**, 58, 1655.

Gates B., Xu Q., Stewart M., Ryan D., Willson C., Whitesides G. *Chem. Rev.* **2005**, 105, 1171.

Giang U.-B., Lee D., King M., DeLouise L. *Lab Chip*, **2007**, 7, 1660.

Gonuguntla M., Sharma A., Mukherjee R. , Subramanian S. *Langmuir*, **2006**, 22,7066.

Green J., Langer R., Anderson D. *Account of Chemical Research*, **2008**, 41, 749.

Ha C-S., Gardella J. A., *Chem. Rev.*, **2005,** 105, 4205.

He B., Chan M. *Macromolecules,* **2005**, 38, 8227.

Heatley, F., Lovell, P.A., McDonald, J. *Eur. Polym. J.*, **1993**, 29, 255.

Hutmacher D. J. Biomat. *Sci-Polym. Ed.*, **2001[a]**,12**,** 107.

Hutmacher D., Schantz T., Zein I., Ng K., Teoh S., Tan K. *J. Biomed. Mater. Res.*, **2001[b]**, 55, 203.

Kretlow J. D., Klouda L., Mikos A. G. *Advanced Drug Delivery Reviews*, **2007**, 59, 263.

Nair L., Laurencin C. *Prog. Polym. Sci.*, **2007**, 32, 762.

Langer R., Vacanti J. P., *Science*, **1993**, 260, 920.

Lee T-W., Mitrofanov O., Hsu J-W. P. *Adv. Fun. Mat.* **2005**, 15, 1683.

Léopoldès J., Damman P. *Nat. Mater.*, **2006**, 5, 957.

Lynn D. , Langer R. *J. Am. Chem. Soc.*, **2000**, 122*,* 10761.

Lynn D., Anderson D., Putnam D. , Langer R. *J. Am. Chem. Soc.*, **2001**, 123, 8155.

Maloney J. M., Santini, Jr. J. T. *Proc IEEE*, **2004**, 2668.

Maloney J. M., Uhland S. A., Polito B. F., Sheppard Jr N. F., Pelta C. M., Santini Jr. J. T. *Journal of Controlled Release*, **2005**,109 ,244.

Okada M. *Prog. Polym. Sci*., **2002**, 27, 87.

Park M. B., Zhu A. P., Shen J. Y., Fan A. L., *Macromol. Biosci.,* **2004**, 4, 665.

Park J. Y., Lee D. H., Lee E. J., Lee S. H. *Lab Chip*, **2009**, 9, 2043.

Randall C. L., Leong T. G., Bassik N. a, Gracias D. H. *Advanced Drug Delivery Reviews*, **2007**, 59 , 1547.

Santini J., Cima M., Langer R. *Nature*, **1999**, 397, 335.

Schacht E. *European Cells and Materials*, **2003**, 5, 58.

Shen J-Y., Chan M., Feng Z-Q, Chan V., Feng Z-W. J. *Biomed. Mater. Res. Part B: Appl. Biomat.*, **2006**, 77B, 423.

Siepmann J., Siepmann F. *Progr Colloid Polym Sci* , **2006** , 133, 15.

Tessmar J. K., Göpferich A. M. *Advanced Drug Delivery Reviews*, **2007**, 59, 274.

Valle E. M. , Gala´n M. A., Carbonell R. G., *Ind. Eng. Chem. Res.* **2009**, *48,* 2475.

Vert M. *Biomacromolecules*, **2005,** 6, 538.

Xia Y., Kim E., Zhao X., Rogers J., Prentiss M., Whitesides G. *Science*, **1996**, 273, 347.

Xia Y., Whitesides G. *Annu. Rev. Mater. Sci.* **1998,** 28, 153.

Xia Y., Rogers J., Paul K., Whitesides G. *Chem. Rev*., **1999**, 99, 1823.

Yan Y., Chan M., Gao J., Yue C. *Langmuir*, **2004**, 20, 1031.

Yang H., Chao C.-K., Wei M.-K., Lin C.-P. *J. Micromech. Microeng.*, **2004**, 14, 1197.

Zhu A., Chen R., Chan-Park M. B. *Macromol. Biosci.*, **2006**, 6, 51.

Chapter 2

Objectives and scope of the work

Biodegradable polymers for example aliphatic polyesters, poly (β-hydroxy butyrate), poly (β-malic acid), poly (ε-caprolactone), or poly (α-hydroxy acids) (PLGA) have been extensively investigated for drug delivery, tissue engineering and other biomedical applications. Sequentially crosslinkable biodegradable polymers which can be used for the fabrication of tissue scaffolds with controlled surface morphology by using lithography techniques particularly soft lithography have not been so for investigated.

Amongst various soft lithography techniques UV-microembossing is of particular interest as it can be carried out at ambient temperature and pressure. Liquid photo crosslinkable polymers are useful to replicate the micropatterns with high fidelity. However liquid polymers hitherto used are not degradable which limits their use for biomedical applications**.**

Photo-patternable biodegradable 2-hydroxylethyl methacrylate (HEMA) conjugated poly (ε-caprolactone-Co-RS-β-malic acid) (PCLMAc) co-polymers were synthesized to process via UV-microembossing. However quantitative conjugation of carboxylic acid groups to HEMA ester is difficult and involves multiple step synthesis. Biodegradable and photo-patternable triblock copolymers of ε-caprolactone (CL) and polar monomers such as glycolide (GA), lactide (LA) or ethylene oxide (EO) with terminal acrylate groups were synthesized for use in UV-microembossing. However these polymers were not liquid at room temperature and hence had to be processed at 60 °C. In another effort liquid polyurethane diacrylates were synthesized to fabricate biodegradable scaffolds via UV-microembossing. However several methanol extractions were required to render these scaffolds biocompatible.

Poly (β-amino esters) synthesized as gene delivery carrier are promising candidates since they are viscous liquids at room temperature, non-cytotoxic and biodegradable. However they lack functionality necessary for processing via UV-microembossing. Poly (β-amino esters) containing only terminal unsaturations were synthesized to incorporate crosslinking sites. Liquid branched PBAEs bearing a greater number of terminal unsaturated acrylate functionality were also synthesized to increase crosslinking density. However terminal acrylate functionality had to be limited to less than 15 % to avoid crosslinking.

.

We report an alternative approach for the synthesis of sequentially crosslinkable poly (β-amino esters) (SCPBAEs) via Michael addition polymerization. These liquid polymers could be processed by UV-microembossing to prepare polymeric scaffolds bearing different shapes such as channels, squares and circles. The degradation rate of crosslinked polymers can be manipulated by the choice of monomers.

Complex patterns such as spheres or ellipsoids are difficult to fabricate using conventional lithographic techniques. Such complex patterns are often desired for the fabrication of scaffolds for drug delivery, directed growth of cell, microlens moulding and MEMS applications. New approached for creating such unique highly ordered combined micro-cavity patterns need to be explored. It would be even more desirable if the patterns thus generated can be subsequently transferred to another PDMS mold and used to generate multiple copies of the said patterns.

The primary objective of the present research work is to develop new methodology to synthesize liquid sequentially crosslinkable polymers which can be processed by soft lithographic technique to design biodegradable scaffolds.

The objectives and scope of research work have been summarized below,

1. Synthesize poly (β-amino esters) by Michael addition reaction.
2. Explore the use of Lewis acid as a catalyst to reduce poly (β-amino esters) synthesis time and characterize polymers synthesized using NMR, GPC and DSC.
3. Synthesize poly (β-amino esters) via Michael addition reaction of oligomers of PLA and PCL diacrylate with secondary bis-amine (Piperazine).
4. Develop synthetic methodology for the synthesis of poly (β-amino esters) with pendant chains. Synthesize novel diacrylate monomers and explore their polymerization with bifunctional amines to yield poly (β-amino esters) containing pendant chains and characterize the same by NMR to confirm incorporation of the pendant functionality.
5. Synthesize trivinyl monomers to prepare sequentially crosslinkable poly (β-amino esters) containing pendant vinyl groups. Polymerization of monomers synthesized with bifunctional amine to yield polymers bearing pendant acrylate, methacrylate and allyl ether groups and confirm the incorporation of pendant functionality using NMR.

6. Synthesize sequentially crosslinkable poly (β-amino esters) containing varying extents of pendant vinyl groups and evaluate molecular weight of the polymers synthesized.
7. Explore possibility of crosslinking polymers containing pendant unsaturations by photo irradiation.
8. Fabricate PDMS molds varying in shape, aspect ratio and pattern density.
9. Fabricate micropatterned polymeric scaffolds from sequentially crosslinkable poly (β-Amino esters) via UV-microembossing technique.
10. Explore the possibility of using conventional soft-lithography technique to fabricate novel patterns, by incorporating solvents and the possibility of replicating the same in PDMS molds

Chapter 3

Acid catalyzed synthesis of poly (β-amino esters)

3.1 Introduction

The Michael addition reaction is conjugate addition reaction of a nucleophile with α,β-unsaturated carbonyl compound to create new carbon-carbon or carbon-heteroatom bond. In polymer chemistry Michael addition reaction has been successfully applied for the synthesis of different types of polymers. A classic example of Michael addition polymerization is anionic chain growth polymerization of methacrylate monomers (Long et. al. 1989).

Linear step growth Michael addition polymerization is another well-explored class of Michael addition reaction. Numerous examples of step growth Michael addition exist; some of these are given below.

3.1.1 Michael addition reactions in polymer synthesis

In literature Michael addition reaction was explored to synthesize elastomeric and thermoplastic polymers. The reaction involves high monomer conversion rate without any side reactions.

3.1.1.1 Synthesis of poly (amido amines)

Ferruti et. al. (1999, 2002) synthesized linear poly (amido amine) through the reaction of primary and secondary diamines with bisacrylamides at 15 to 69 ºC in aqueous medium (figure 3.1). Reaction time varied from hours to days depending on reactivity of monomers and type of solvent used for polymerization. The rate of polymerization was governed by the basicity of the amines and steric hindrance. The polymerization led to high molecular weight polymers when protic solvent was used for reaction (Danusso and Ferruti 1970).

3.1.1.2 Synthesis of Poly (enamine ketone)

The poly (enamine ketone)s are tough thermoplastics synthesized by Michael addition of aromatic diamines with aromatic bis(alkynone)s (figure-3.2). The reaction was carried out in m-cresol (Wilbur and Bonner 1990). In this reaction conjugated acetylene ketone and conjugated acetylene ester are Michael receptors which react with amine nucleophiles.

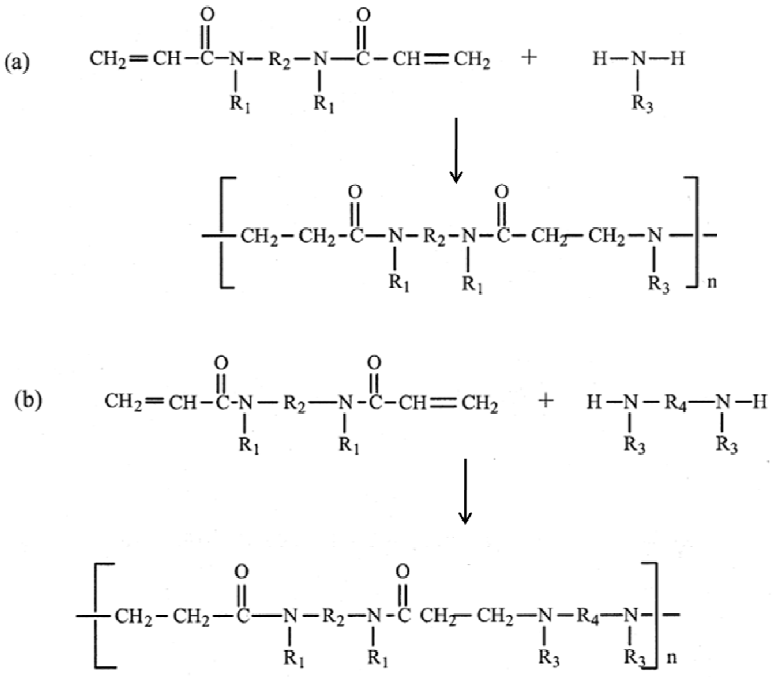

Figure 3.1: Poly (amido amine) synthesis a) primary amine and b) secondary amine (adapted from Ferruti et. al. 2002) .

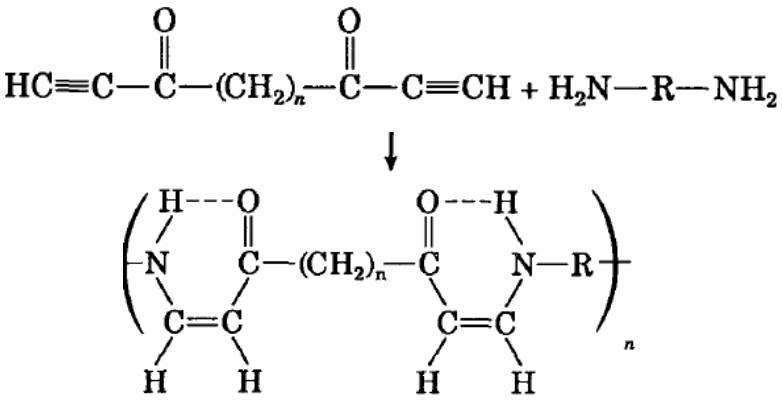

Figure 3.2: Poly (enamine ketone) synthesis (adapted from Wilbur and Bonner 1990)

3.1.1.3 Synthesis of Poly (imido sulfide)

Poly (imido sulfide)s are synthesized by the polymerization of oligomeric or low molar mass dithiols with bismaleimide in presence of triehylamine as catalyst (figure 3.3). Triethylamine deprotonates thiol groups to facilitate addition reaction with maleimide double bond (Mather et. al. 2006).

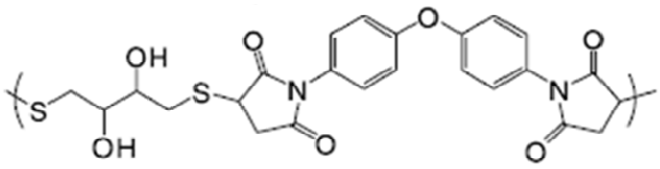

Figure 3.3: Poly (imido sulfide) (adapted from Mather et. al. 2006)

3.1.1.4 Synthesis of Poly (amino quinone)

Poly (amino quinones) are synthesized by the reaction of primary diamines with quinone in the presence of peracetic acid (figure 3.4). Poly (amino quinone)s are useful in developing anticorrosive coating and moisture resistant adhesives (Reddy and Erhan 1994, Mather et. al. 2006).

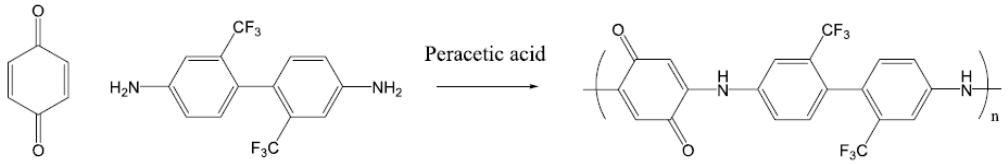

Figure 3.4: Poly (amino quinone) synthesis (adapted from Mather et. al. 2006)

3.1.1.5 Synthesis of Poly (imido ethers)

Poly(imido ethers) are synthesized by the reaction between glycerol or phenolphthalein with aliphatic bismaleimides (figure 3.5). The reaction is performed in NMP or 2-mercaptobenzothiazole as catalyst at 85-115 ºC for 2-3 days (Hulubei and Rusu 2001).

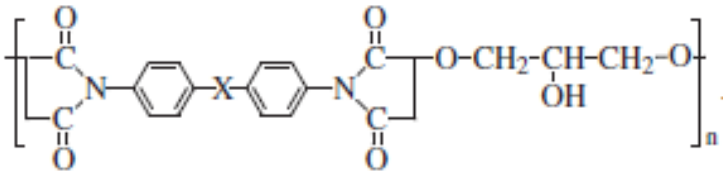

Where X = -CH2-, -(CH_2)- or –O-

Figure 3.5: Poly (imido ethers) (adapted from Hulubei and Rusu 2001)

3.1.1.6 Synthesis of Poly (ester sulfides)

PEG dithiol is reacted with butanediol diacrylate or PEG diacrylate to synthesize Poly (ester sulfides) in presence of triethyl amine as catalyst (figure 3.6). The polymer hydrophilicity can be controlled through the manipulation of PEG chain length (Tomasi et. al. 2002).

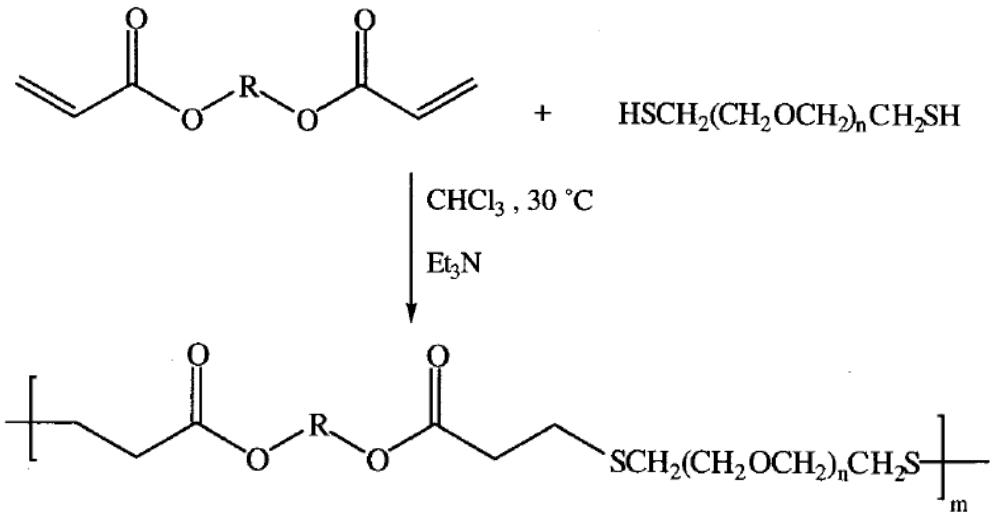

Figure 3.6: Poly (ester sulfides) (adapted from Tomasi et. al. 2002)

3.1.1.7 Synthesis of Poly (aspartamide)s

Poly (aspartamide)s are synthesized by the reaction of diamine with bismaleimide for 3 days at 110 ºC in the presence of catalytic amount of acetic acid (figure 3.7). These polymers exhibit very high glass transition temperature (T_g) near 210 ºC (Mather et. al. 2006).

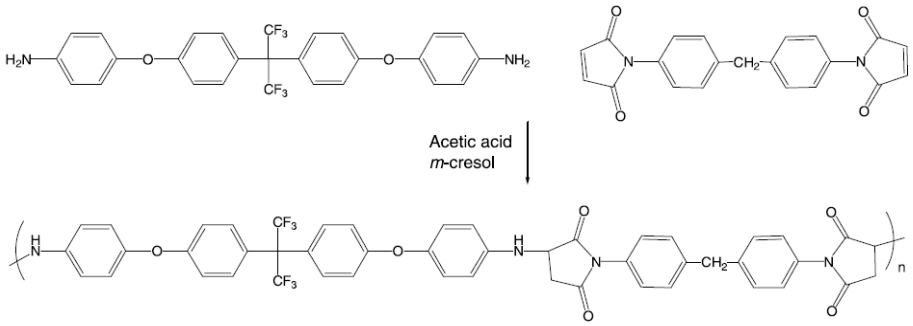

Figure 3.7: Poly (aspartamide)s synthesis (adapted from Mather et. al. 2006)

3.1.1.8 Synthesis of Poly (β-amino esters)

The Poly (β-amino esters) were first synthesized by Chiellini's group via Michael addition of primary amine or secondary bis amine with diacrylates (figure 3.8). These polymers exhibited liquid crystalline nature due to presence of rigid units in main chain (Angeloni et. al. 1985, Laus et. al. 1988).

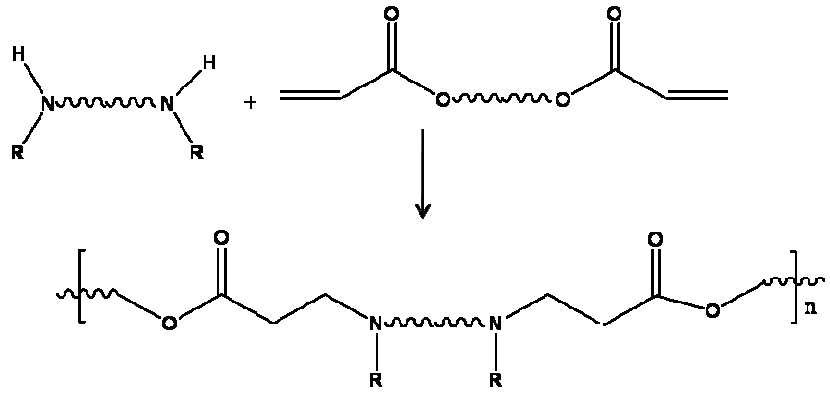

Figure 3.8: Poly (β-amino esters) synthesis

Recently Langer's group synthesized a series of poly (β-amino esters) via conjugate addition of primary or secondary bis amine to diacrylate ester (Lynn et. al. 2000, 2001; Anderson et. al. 2003). Poly (β-amino esters) were investigated as potential transfection vectors for following reasons:

1) The polymers contain requisite amine and readily degradable linkages.

2) Multiple analogues could be synthesized directly from commercially available starting materials.

3) These polymers and their degradation products are less cytotoxic than the conventionally used polymers for gene delivery, such as poly (ethylene imines) (PEI) and poly (L-lysine) (PLL).

These poly (β-amino esters) degrade via ester hydrolysis and not via retro-Michael reaction and avoid regeneration of acrylate group (Lynn and Langer 2000). Hence degradation of these polymers leads to less cytotoxic products as compared to PEI and PLL. However the synthesis of poly (β-amino esters) is too sluggish, takes several days and a decrease in reaction time is desirable.

3.1.2 Catalyzed Michael addition reactions

In literature a range of catalyst has been used to enhance reaction rate and yield of Michael addition reaction. Some of these are discussed below.

3.1.2.1 Natural phosphates

Abrouki et. al. (2002) used natural phosphate (NP) and phosphate doped with potassium fluoride KF/NP) as a catalyst for Michael addition of chalcone derivative with mercaptans (figure 3.9). The reaction takes place at room temperature with very high yield (92-97 %) in 2-20 minutes.

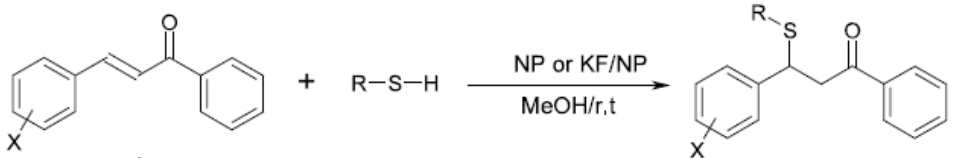

Figure 3.9: Michael addition between chalcone derivative and mercaptans (adapted from Abrouki et. al. 2002)

3.1.2.2 Fluorapatite (FAP)

Zahouily et. al. (2003) reported Michael addition reaction of chalcone derivative with mercaptans catalyzed by fluorapatite in heterogeneous media. The reaction yield varied between 57 to 96 % based on type of chalcone derivatives and thiols used.

3.1.2.3 KF/Al_2O_3

KF/Al_2O_3 was used to catalyze Michael addition reaction between amine (oxazolidinone) and acrylate (figure 3.10). The reaction yield varied from 21 % (chloroform) to 97 % (acetonitrile) based on the type of solvent used (Yang et. al. 2005).

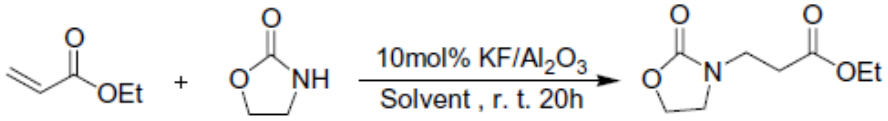

Figure 3.10: Michael addition of ethyl acrylate with oxazolidinone (adapted from Yang et. al. 2005)

3.1.2.4 Bronsted acid

Wabnitz and Spencer (2003) reported bis(trifluoromethanesulfon)imide a strong bronsted acid as catalyst for Michael addition reaction. Various nucleophiles for example carbamates, alcohols, and thiols were used to catalyze the reaction between α,β-unsaturated ketones, alkylidene malonates, and acrylimides (figure 3.11). Reaction rates were high when the reaction was carried out in dichloromethane, acetonitrile or nitromethane and proceeded at room temperature with high yield (66 to 98 %).

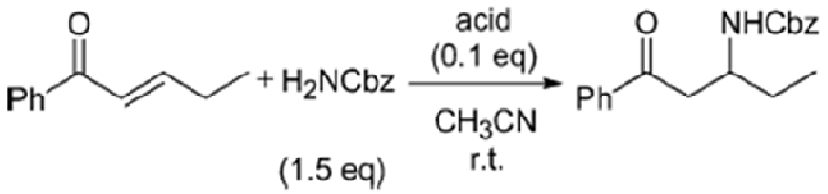

Figure 3.11: Michael addition between benzyl carbamate and 1-phenyl-2-penten-1-one(adapted from Wabnitz and Spencer (2003)

3.1.2.5 Lewis acid

In literature a wide range of Lewis acids was used to catalyze Hetro- Michael addition reactions (Cabral et. al. 1989). Lewis acid such as $FeCl_3$, $AlCl_3$ and $ZnCl_2$ enabled to carry out the reaction at room temperature, in shorter time and at high yield (61 to 91%).

We therefore proposed to use Lewis acid as a catalyst for the synthesis of poly (β-amino esters) containing tertiary amines in their backbone. Conjugate addition of primary or secondary bis amine to diacrylate ester was carried out in the presence of Lewis acids such as $FeCl_3$, $AlCl_3$ and $ZnCl_2$. It was observed that the Lewis acid helped to bring down reaction time from 5 days to few hours at room temperature without compromising polymer molecular weight and yield.

This synthetic methodology was further extended to synthesize Poly (β-amino esters), where PLA and PCL diacrylates of molecular weight (Mn = 620 – 4600) were used as diacrylate blocks and condensed with bi-functional amines to extend the molecular weight of the blocks and also introduce degradable link. The PLA and PCL are most widely utilized class of biodegradable and bioabsorbable polymers for biomedical applications (Chien et. al. 2003, Pan et. al. 2005, Tatsuro et. al. 2006). Degradation of PLLA creates an acidic environment within the microparticles which is often undesirable. The degradation of chain extended PLA/PCL diacrylates with amines leads to poly (β-amino esters) containing PLA/PCL blocks of decreased molecular weights. The scission of the β-amino ester link results in lower acidity. Also the degradation of PLA/PCL polymers generated during degradation can be cleared from the body because of their low molecular weights.

This synthetic methodology was also used to synthesize Poly (β-amino esters) containing pendant chains. To demonstrate this, Poly (β-amino esters) containing stearic acid were synthesized where pentaerythritol monostearate diacrylate was

polymerized with bifunctional amine in the presence of Lewis acid. It has been also shown that the pendant chain content can be manipulated by polymerizing mixture of diacrylates containing varying ratios of pentaerythritol monostearate diacrylate and diacrylate with bifunctional amine. Polymers having hydrophilic backbone with hydrophobic pendant chains and vice- versa can be synthesized depending on the choice of monomers.

The solubility behavior of these polymers at physiological pH shows that typically poly (β-amino esters) are more soluble at acidic pH than at near neutral or neutral pH. The solubility of poly (β-amino esters) can be easily manipulated by the choice of monomers. The degradation studies of poly (β-amino esters) at physiological buffers demonstrate that the rate of degradation is higher at pH 1.2 than at pH 6.8 and 7.8. Polymers reported in this chapter have potential for drug delivery in the form of microparticles, nanoparticles or as polymer film.

3.2 Experimental section

3.2.1 Materials

Acrylic acid, 1,4-butanediol diacrylate (BDDA), 1,6-hexanediol diacrylate (HDDA), ethylene glycol, diethylene glycol, triethylene glycol, 1,4-butanediol, resorcinol, hydroquinone, bisphenol A, 1,4-cyclohexanedimethanol, 1,12-dodecanediol, poly ε-caprolactone diol, pentaerythritol diacrylate monostearate (PEDAMS), poly ethylene glycol diacrylate of MW 258 and 700 (PEGDA258 and PEGDA700), 4,4'-trimethylenedipiperidine (TMDP) Lactide and $Sn(Oct)_2$, were purchased from Aldrich chemicals. Aluminum chloride ($AlCl_3$), zinc chloride ($ZnCl_2$), ferric chloride ($FeCl_3$) and benzoyl chloride were purchased from SD Fine chemicals and used without further purification. All solvents were purchased from Merck India ltd. and purified using standard purification methods.

3.2.2 Characterization

3.2.2.1 Fourier transform infrared spectroscopy (FTIR)

The FTIR spectral studies were carried out using Shimadzu 8300 FTIR spectrometer. The polymer was dissolved in dichloromethane and polymer film was formed on KBr

cell. After complete evaporation of dichloromethane, spectra were recorded over the frequency range 4000 - 400 cm^{-1}, with resolution range of 4 cm^{-1}.

3.2.2.2 Nuclear magnetic resonance spectroscopy (NMR)

NMR (MSL 300 MHz) spectra were recorded on Bruker (Bruker, Karlsurhe, Germany) spectrometer in $CDCl_3$ (Aldrich) as solvent and TMS as internal reference. All chemical shift values are given in parts per million (ppm) with respect to residual proton signal from solvent.

3.2.2.3 Gel permeation chromatography (GPC)

Molecular weights of the polymers were obtained by gel permeation chromatography (GPC) using waters 590 programmable HPLC pump injector with a 100 µl injector loop and four columns in series (500 A^0 to 10^5 A^0, 300 X 7.5 mm, Waters, Milford MA). THF was used as eluent at a flow rate of 1 ml/min. Data were collected using a differential refractometer (waters 410) and processed using the Ezychrome software package. The molecular weights and polydispersity of the polymers were reported relative to polystyrene standards.

3.2.2.4 Vapor pressure osmometer (VPO)

Molecular weights of lactide copolymers and macromers were determined using Knauer Vapor Pressure Osmometer K-7000. Stock solution of lactide polymer (10 mg/ml) was prepared in chloroform (spectroscopy grade) and successive dilutions of polymer were analyzed at 37 °C. Benzil was used as standard for calibration of the instrument. Molecular weight of the sample was calculated using standard procedure.

3.2.2.5 Differential scanning calorimetry (DSC)

The thermal properties such as T_g, T_m, and T_c of the polymers were recorded on the Thermal Analyzer DSC Q 10 (Newcastle, DE, USA). For solid polymers the temperature range selected varied from -70 to 100 °C with heating and cooling rate 10 ^oC/min. For viscous polymers the temperature range was from -80 to 30 ^oC and heating rate of 10 ^oC /min. Three temperature cycles were given for each polymer and T_g and T_m were calculated in second heating cycle. All the data were analyzed using TA Universal Analysis 2000 software package.

3.2.3 Monomer synthesis

3.2.3.1 Synthesis of PLA diol

The dihydroxy-terminated oligomers of Lactic acid (OPLA) were synthesized as reported by Storey et al (Storey et. al. 1997). Briefly 5 g (0.034 mol) of L-lactide and 0.109 g (3.5 mole %) 1,4 butanediol (as macro-initiator) were fed into glass ampoule. 0.014 g, (0.1 mole %) Sn $(Oct)_2$ was added as catalyst. The ampoule was sealed under vacuum and heated at 160 °C for 6 hrs. The reaction mixture gradually turned viscous and finally solidified. The resultant polymer was dissolved in chloroform (20 ml) and precipitated into an excess of diethyl ether / n-hexane (1:3 in volume) mixture. The precipitated product was separated by decantation of the supernatant and thoroughly dried under vacuum. The structure of the purified polymer was confirmed using ^1H NMR spectroscopic technique and molecular weight was measured by VPO. Similarly poly lactide diol (LD) and poly ε-caprolactone (CLD) diol of different molecular weights were synthesized by varying the mole ratio of butanediol.

3.2.3.2 Synthesis of diacrylates

Diacrylates of ethylene glycol, diethylene glycol, triethylene glycol, resorcinol, hydroquinone, bisphenol A, 1,4-cyclohexanedimethanol, 1,12-dodecanediol, poly ε-caprolactone diol, PLAdiols, pentaerythritol monostearate were synthesized by esterification with acryloyl chloride. Briefly, 1 mole diol was condensed with freshly prepared 2.5 mole of acryloyl chloride at 0 to 10 °C for 6 hrs in presences of 2.5 moles of triethyl amine. Tetrahydrofuran (THF) and dichloromethane (DCM) were used as solvent for condensation reaction depending on solubility of diols. When THF was used as solvent, hydrochloride salt precipitated was filtered out and THF layer was concentrated on rota-vapor at 35 °C at reduced pressure. The residue was dissolved in DCM and was extracted three times with brine solution. The organic layer was dried overnight over anhydrous sodium sulfate. When DCM was used as solvent, the product was directly extracted with brine solution and organic layer was dried overnight over anhydrous sodium sulfate. These organic layers were separated from sodium sulphate and monomers were purified using column chromatography.

PLA and PCL diacrylates were directly used for polymerization and were characterized by NMR for purity.

3.2.4 Poly (β-amino esters) synthesis

Polymerization of diacrylate with bi-functional amine was carried out in solution wherein, 2.26 g (1 x 10^{-2} moles) 1, 6-hexanediol diacrylate was dissolved in 40 ml dry DCM (THF or acetone depending on solubility of diacrylates) in a 100 ml round bottom flask. The solution was maintained at 5-10 °C with constant stirring and 13.3 mg $AlCl_3$ (1 x 10^{-4} moles) was added. 2.10 g (1 x 10^{-2} moles) 4,4'-trimethylenedipiperidine was first dissolved in 15 ml dry DCM (THF, acetone) separately and added drop wise to the cooled acrylate solution under nitrogen atmosphere. The reaction mixture was maintained at room temperature for 24 hrs with constant stirring and was extracted thrice with brine solution to remove $AlCl_3$ and unreacted TMDP. In case of THF and acetone, reaction mixture was first concentrated on Rota vapor and residue was dissolved in DCM. The organic layer was separated and dried on anhydrous sodium sulphate. DCM was evaporated under reduced pressure at room temperature. The polymer was precipitated twice in pet ether, and vacuum dried prior to analysis. The polymer was characterized by ^{1}H NMR spectroscopy. The molecular weight (M_w) as determined by GPC was 28900 with respect to polystyrene standard.

3.2.4.1 Variations in polymerization parameters

4 4'-Trimethylenedipiperidine and 1,6-hexanediol diacrylate were selected as an amine and diacrylate respectively for the standardization of reaction parameters.

1. Choice of solvent

Anhydrous acetone, methylene chloride or tetrahydrofuran were used as solvents for polymerization depending upon the solubility of monomers. The polymerization of HDDA and TMDP was carried out in presence of 1mole % $AlCl_3$ as a catalyst in anhydrous methylene chloride, tetrahydrofuran and acetone respectively. The reaction was carried out for 24 hrs. Other reaction conditions were kept constant as per general polymerization method.

2. Choice of catalyst

The polymerizations of HDDA and TMDP were carried out using tetrahydrofuran as a solvent. 1 mole % Lewis acid such as $AlCl_3$, $FeCl_3$ and $ZnCl_2$ was used as catalyst for polymerization.

3. Variation in catalyst mole ratio

The polymerization of HDDA and TMDP was carried out in tetrahydrofuran as a solvent and $AlCl_3$ as a catalyst. The Lewis acid used was 1 mole % and 10 mole % on the basis of monomers. The reaction was carried out for 24 hrs.

4. Effect of time on polymerization

Polymerization of HDDA and TMDP was carried out using general polymerization method described in section 3.2.4. During polymerization 5 ml reaction mixture was collected at fixed time interval using glass syringe. Tetrahydrofuran was removed at room temperature under reduced pressure. The residue was dissolved in dichloromethane and washed thrice with brine solution to remove $AlCl_3$. The organic layer was separated out and dried on anhydrous sodium sulphate. The polymer solution in dichloromethane was concentrated under reduced pressure at room temperature. The polymer was precipitated twice in pet ether, and vacuum dried prior to analysis. The polymers were characterized using GPC.

5. Variation of diacrylate

All polymers were synthesized under identical reaction conditions. 1 mole % $AlCl_3$ as a catalyst, THF was used as a solvent and reactions were carried out at room temperature for 16 hrs.

3.2.5 Chain extension through poly (β-amino esters)

The chain extension of poly lactic acid diacrylate (PLADA) and amines such as butyl amine, lauryl amine, piperazine, 4,4'-trimethylenedipiperadine was carried out via Michael type addition where $AlCl_3$ was used as a catalyst. Briefly, PLA diacrylate (M 3) (2 g, 7.78 x 10^{-4} moles) was dissolved in dry DCM (10 ml) and cooled to 0-10 °C. Catalytic amount of anhydrous $AlCl_3$ (1 mole %) was added under nitrogen atmosphere. Piperazine (0.0673 g, 7.78 x 10^{-4} moles) dissolved in 2 ml dry DCM

separately was added dropwise to the above solution at 0-10 °C. The resulting reaction mixture was stirred for 24 hrs at room temperature. After completion of the reaction DCM was extracted thrice with aqueous brine solution. The organic layer was kept on anhydrous sodium sulphate for drying which was filtered out. The polymer solution was concentrated and precipitated in pet ether and vacuum dried prior to analysis. The structure of the purified polymer was confirmed using ^{1}H NMR spectroscopic technique and molecular weight was measured by GPC.

Similarly biodegradable polymers were synthesized from oligo lactide diol diacrylate (LD) and oligo Caprolactone (CLD) diol diacrylate by reacting with different amines. The molecular weights of oligo PLA and oligo PLADA were determined using vapor pressure osmometer (VPO) at 38 °C where chloroform was used as a solvent. The molecular weights of chain extended polymers were estimated by GPC using four styragel columns, chloroform containing 200-ppm toluene (internal standard) as a solvent and polystyrene as standard. The structures of oligo PLA, oligo PLDA and chain extended polymers were confirmed using ^{1}H NMR.

3.2.6 Synthesis of poly (β-amino esters) containing hydrophobic pendant chains

Stoichiometric amounts of diacrylate (PEDAMS or mixture of PEDAMS and PEGDA) and TMDP were polymerized in presence of 1 mole % $AlCl_3$ as catalyst. Polymerization was performed at room temperature for 16 hrs when DCM was used as a solvent. The reaction mixture was extracted thrice with brine solution to remove $AlCl_3$ and unreacted TMDP. The organic layer was separated and dried on anhydrous sodium sulphate. After filtration the organic layer was evaporated under reduced pressure at room temperature. The polymer was precipitated twice in pet ether, and vacuum dried prior to analysis. The polymers were characterized by using ^{1}H NMR spectroscopy.

3.2.7 Dissolution behavior of poly (β-amino esters) at physiological pH

Polymer was dissolved in chloroform and polymer film was cast by pouring it on flat glass petri-dish surface. Chloroform was evaporated at room temperature. After complete evaporation of chloroform, the polymer film was kept in vacuum desiccator for another 48 hrs till constant weight was achieved. The polymer film thickness was

120 μ. The polymer films were cut in to 1×1 cm^2 and soaked in to 1.25, 5.8 and 6.8 pH buffer solutions to study its dissolution behavior.

3.2.8 Degradation studies of chain extended PLA β-amino esters by molecular weight loss

Degradation rate of the polymers was investigated in 1.25, 6.8 and 7.8 pH physiological buffer solutions.

3.2.8.1 Degradation at pH 1.25 HCl Buffer

200 mg of polymer (P 5) was immersed in pH 1.25 buffer (0.1 N HCl) and was kept at 37 °C for 25 hrs in shaking bath. The samples were collected after 1 hr, 12 hrs and 25 hrs filtered and dried under vacuum till they attained constant weight. The molecular weight was determined by VPO using chloroform as solvent.

3.2.8.2 Degradation at pH 6.8 and 7.8 phosphate buffer

200 mg of polymer (P 5) was immersed in pH 6.8 and 7.8 PBS separately and kept at 37 ° C for 24 hrs in shaking bath. The sample was filtered and dried under vacuum after 24 hrs and molecular weight was determined by VPO using chloroform as solvent.

3.2.9 Encapsulation of Diltiazem HCl in Poly (HDDA-Co-TMDP) microspheres

Diltiazem HCl was encapsulated in polymeric microspheres by w/o/w emulsification method where pluronic F-127 was used as a surfactant. Diltiazem HCL was selected as model drug as it has good solubility over wide pH range. The modified encapsulation technique is briefly discussed below.

900 mg polymer was dissolved in 10 ml dichloromethane 300 mg Diltiazem HCl dissolved in 3 ml 1% w/v aqueous pluronic f-127 solution was added. This solution was homogenized for 1 min at 10000 rpm. The emulsified polymer-drug solution was added dropwise into 100 ml 0.5 w/v % pluronic F-127 aqueous solution with constant stirring at 1000 rpm in a beaker. Stirring was continued until dichloromethane was completely evaporated. The microspheres formed were collected by filtration and washed thrice with distilled water to remove drug and surfactant, adsorbed on the surface of microspheres. These washed microspheres were dried in vacuum desiccator

till constant weight was attained. Dried microspheres were stored in vacuum desiccator until further studies. This encapsulation method yielded 840 mg (70 %) microspheres. The surface morphology and size of the dried microspheres was investigated by scanning electron microscopy (SEM).

3.2.10 Diltiazem content in the polymeric microspheres

The drug content was determined at 237 nm using Shimadzu UV160 IPC UV Visible spectrophotometer. Diltiazem HCl content was determined by dissolving 50 mg of micro particles in 2 ml of 0.1 N HCl solutions. Then the volume was made to 50 ml using 0.1 N HCl. The solution was filtered and diluted further for analysis. Each sample was analyzed in triplicate.

3.2.11 In vitro drug release study from microspheres

The drug release from the micro particles was evaluated by placing the microparticles containing 125 mg Diltiazem HCl in a basket of 900 ml of 0.1 N HCl, pH 5.8 and 6.8 PBS. The dissolution was carried out in Electrolab USP type II apparatus at 100 rpm at 37 ± 0.5°C. The samples were collected after fixed time interval up to 24 hrs and the volume was made upto initial value by adding fresh dissolution medium. The amount of drug released was estimated at 237 nm using UV spectrophotometer. The dissolution tests were done in triplicate.

3.3 Results and discussion

3.3.1 Synthesis of poly (β-amino esters)

The proposed mechanism of Lewis acid catalyzed Michael addition is discussed below. Cabral et. al. (1989) demonstrated that Lewis acid first forms complex with carbonyl oxygen of the diacrylate ester by sharing lone pair of electrons from oxygen atom with strong electron deficient metal atom. This sharing of lone pair of electron with electron deficient metal makes carbonyl group more electron deficient, which tries to pull electrons from π bond, which is in conjugation with carbonyl group, to render C-4 carbon more electron deficient. The electron deficiency at C-4 position helps ease the attack of nucleophile (amine) at this position. Since the formation of

complex takes place at room temperature, the reaction can be carried out at room temperature (figure 3.12).

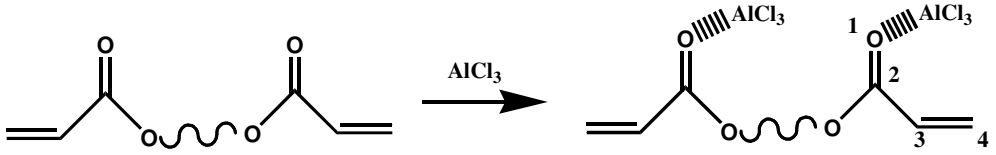

Figure 3.12 : Complexation of O-1 with $AlCl_3$

Prior studies on catalyzed Michael addition reaction, showed that even though C-2 position is more electron deficient than C-4 position, addition of nucleophile is always favored at C-4 position over C-2. This was attributed to the fact that orbital coefficient at C-4 was always greater than that at C-2 (Cabral et. al. 1989, Loncharich et. al 1987).

This observation was further supported by the studies carried out by Heathcock and Oare (1985), who observed that acid catalyzed Michael addition reaction at room temperature proceeds via formation of 1,4 adduct since the adduct is thermodynamically more stable, whereas at –78 °C this reaction proceeds via kinetically more stable enolate route (figure 3.13) and hence yields more 1, 2 addition product.

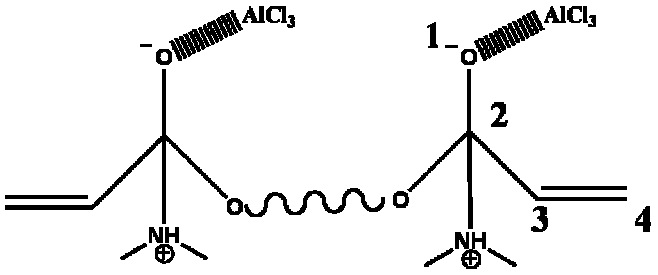

Figure 3.13: Enolate rout to form 1, 2 adduct

Molecular weight and thermal properties of these polymers were evaluated using GPC and DSC techniques respectively.

3.3.2 Effect of variations of polymerization parameters

3.3.2.1 Choice of solvent

HDDA and TMDP were polymerized keeping Lewis acid ($AlCl_3$) and catalyst ratio constant. Different anhydrous solvents such as tetrahydrofuran, dichloromethane and acetone were used for polymerization. Solvent used for polymerization had no effect on polymer molecular weight (table 3.1).

Table 3.1 Synthesis of Poly (HDDA-Co-TMDP)

Sr. No.	Solvent	Mw	PDI	Yield
1	Tetrahydrofuran	28900	1.67	82
2	Methylene chloride	27800	1.82	80
3	Acetone	28000	1.56	76

3.3.2.2 Choice of catalyst

According to Cabral et. al. (1989) $FeCl_3$, $AlCl_3$ and $ZnCl_2$ are good catalysts for Michael addition reaction, as there use results in higher yield under mild reaction conditions.

HDDA was reacted with TMDP using THF as a solvent maintaining catalyst to acrylate ratio 1 mole %. It was observed that as compared to $ZnCl_2$, $AlCl_3$ and $FeCl_3$ yielded polymers having higher molecular weight and higher yield. Reaction carried out in absence of catalyst resulted in very low yield (table 3.2).

Table 3.2: Synthesis of poly (HDDA-CO-TMDP) with Lewis acid variation

Sr.No.	Lewis acid	Mw	PDI	% Yield
1	$AlCl_3$	28900	1.67	86
2	$FeCl_3$	28500	1.58	88
3	$ZnCl_2$	10200	1.92	55
4	Uncatalyzed	*nd*	*nd*	7

nd – could not be determined

Even though $FeCl_3$ was equally efficient catalyst for polymerization it was observed that the polymers synthesized using $FeCl_3$ were light brown in color. Hence we preferred $AlCl_3$ as a catalyst over $FeCl_3$ and $ZnCl_2$ for further studies.

3.3.2.3 Catalyst variation

In this section $AlCl_3$ was used as a catalyst and catalyst ratio was varied as shown in table 3.3 keeping other reaction parameters such as solvent and reaction time constant. It was observed that the molecular weight and yield of the polymer was high when reaction was performed using 1 mole % catalyst.

Table 3.3: Synthesis of poly (HDDA-CO-TMDP) with Lewis acid ratio variation

Sr. No.	$AlCl_3$ mole ratio %	Mw	PDI	Yield
1	1	28900	1.67	82
2	10	16400	2.08	62

We believe the lower molecular weights and yield at high Lewis acid catalyst concentration are a result of the acidic conditions under which the polymer is more susceptible for degradation. To confirm this hypothesis we increased AlCl3 content 1:1 which resulted in still lower molecular weight (Mw 8700) and yield (54 %).

3.3.2.4 Reaction time variation

The effect of time on polymerization and polymer properties was studied. The reaction was carried out for 24 hrs. Polymer samples were collected at different time intervals and characterized using GPC after purification (table 3.4).

The first sample was collected immediately after complete addition of amine in acrylate solution. GPC analysis of this sample showed that molecular weight was 9650 and polydispersity 1.54. The increase in molecular weight was rapid initially up to 5 hrs. Only a small increase in molecular weight (1200) was observed at the end of 24 hrs. Also the increase in molecular weight during this time did not follow a specific trend. The final molecular weight obtained is in good agreement with molecular weight of poly (β-amino esters) reported by Lynn et. al. (2000-2001).

Table 3.4: Effect of time on HDDA and TMDP polymerization

Sr.No	Time	M_w	PDI
1	0 min	9650	1.54
2	5 min	11400	1.87
3	15 min	12300	2.02
4	30 min	11200	1.73
5	1 hr	13200	1.87
6	2 hr	10900	1.59
7	3 hr	15700	1.86
8	4 hr	17200	1.85
9	5 hr	18200	1.72
10	6 hr	17900	1.76
11	7 hr	18700	1.82
12	8 hr	18000	1.87
13	9 hr	15900	1.62
14	10 hr	19500	1.8
15	11 hr	19700	1.84
16	12 hr	19500	1.81
17	24 hr	21900	1.64

3.3.3 Synthesis of poly (β-amino esters)

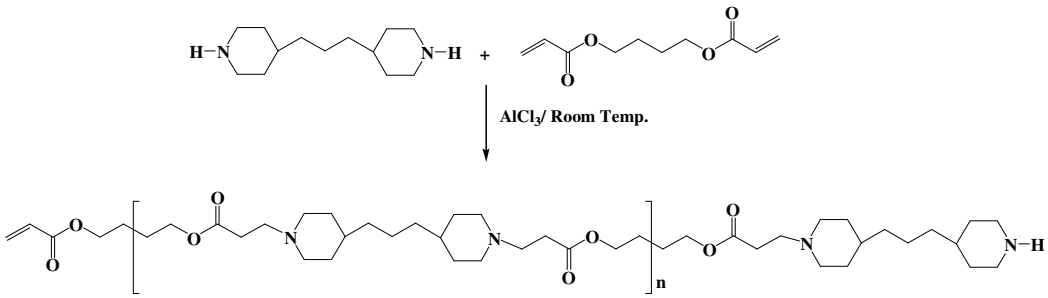

Figure 3.14: Synthesis of poly (HDDA-Co-TMDP)

The polymers were synthesized using equimolar ratios of diacrylate to TMDP in anhydrous dichloromethane; acetone or tetrahydrofuran as a solvent. The solvent was

selected based on the monomer solubility for example for TEGDA, PEGDA either tetrahydrofuran or acetone was used, while in case of CHDMDA, DDDDA, QDA and BPDA dichloromethane was used as a solvent for polymerization (BDDA and HDDA could be polymerized either in dichloromethane or tetrahydrofuran). Anhydrous solvents are used to prevent ester hydrolysis during polymerization (Lynn et. al. 2000).

Table 3.5: Poly (β-amino esters): Synthesis

Polymer	Diacrylate	Molecular weight Mw	PDI	Yield
P1	BDDA	31400	1.68	80
P2	HDDA	28900	1.67	84
P3	CHDMDA	23400	1.53	81
P4	DDDDA	8670	3.0	75
P5	RDDA	18300	1.62	80
P6	QDA	16700	1.70	80
P7	BPDA	14500	1.82	82
P8	EGDA	16600	1.52	68
P9	DEGDA	17000	1.63	60
P10	TEGDA	15400	1.71	64
P11	PEGDA 250	28800	1.67	60
P12	PEGDA 700	12890	1.45	62

1 mole % $AlCl_3$ was used as a catalyst and polymerization was carried out for 24 hrs at room temperature. Both hydrophilic and hydrophobic diacrylates were polymerized with TMDP. The results are listed in table 3 .5.

Polymers synthesized using hydrophilic diacrylates resulted in lower yield (60-70 %) than polymers synthesized using hydrophobic monomers. There is a possibility that some fraction of the polymer may have dissolved in brine solution during purification process. However no attempt was made to optimize the yield.

3.3.4 Chain extended poly (β-amino esters)

3.3.4.1 Synthesis of L-lactide diol

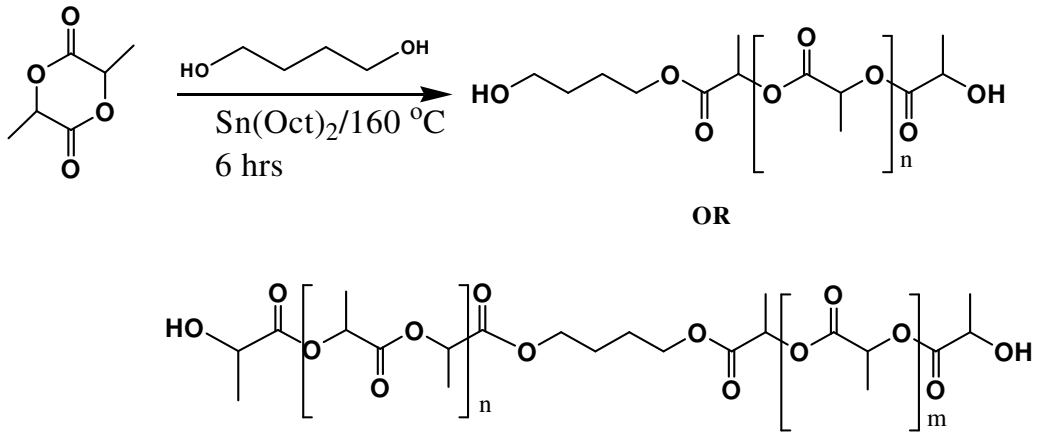

Figure 3.15: PLA diol synthesis

Table 3.6: List of poly-lactide diol (LD) and poly-ε-caprolactone (CLD) diol

Lactide diol	Mole % of 1,4 butanediol*	Molecular Weight (Mn)
LD 1	1	4485
LD 2	2.7	3226
LD 3	3.3	2548
LD 4	4.5	2125
LD 5	5	1925
LD 6	10	1580
LD 7	15	1020
LD 8	20	860
CLD 10	5	530
CLD 11		1925

* Based on L-Lactide initiator, $Sn(Oct)_2$ = 0.1 mol %. CLD 11 is poly-ε-caprolactone (Mn = 530) procured from Aldrich chemicals.

During synthesis of lactide diols (LD), L-lactide was first reacted with 1, 4 butanediol using $Sn(Oct)_2$ as catalyst by ring opening polymerization. Lactide and 1, 4 butanediol ratios were varied between 50:1 to 50:12 moles. Same procedure was used to synthesize caprolactone diol (CLD). Molecular weights of these polymers estimated

by VPO are summarized in table 3.6. Schematic of lactide diol synthesis using lactide and 1,4 Butanediol is shown in figure 3.15.

Under the conditions described above, oligomers bearing terminal hydroxyl groups were formed. When reactions were performed using butanediol upto 15 mole % the oligomers of lactide diols formed were solids. Higher butanediol content resulted in semisolid products.

3.3.4.2 Synthesis of Lactide diacrylate

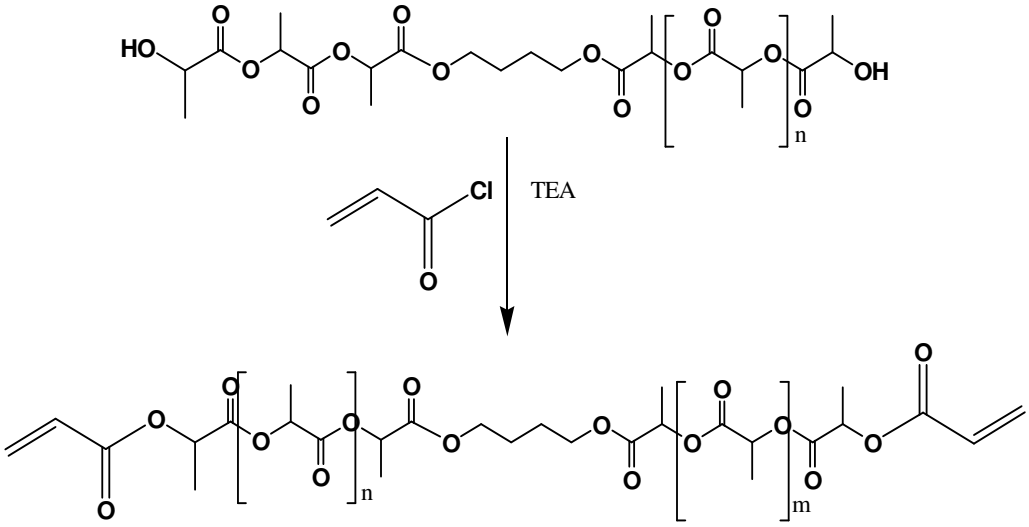

Figure 3.16: Synthesis of PLA diacrylate

Oligomeric lactide diol / ε-caprolactone diols were converted to oligomeric lactide diacrylate or ε-caprolactone diacrylate by condensation with acryloyl chloride. Schematic of this reaction is shown in figure 3.16. The molecular weights are summarized in table 3.7.

Table 3.7: PLA and PCL diacrylates synthesized

Sr. No	LD	Molecular weight (M_n)
M 1	LD 1	4595
M 2	LD 2	3336
M 3	LD 3	2658
M 4	LD 4	2235
M 5	LD 5	2035
M 6	LD 6	1690
M 7	LD 7	1130
M 8	LD 8	970
M 9	LD 9	714
M 10	CLD 10	620
M 11	CLD 11	2035

3.3.4.3 Synthesis of chain extended poly (β-amino esters)

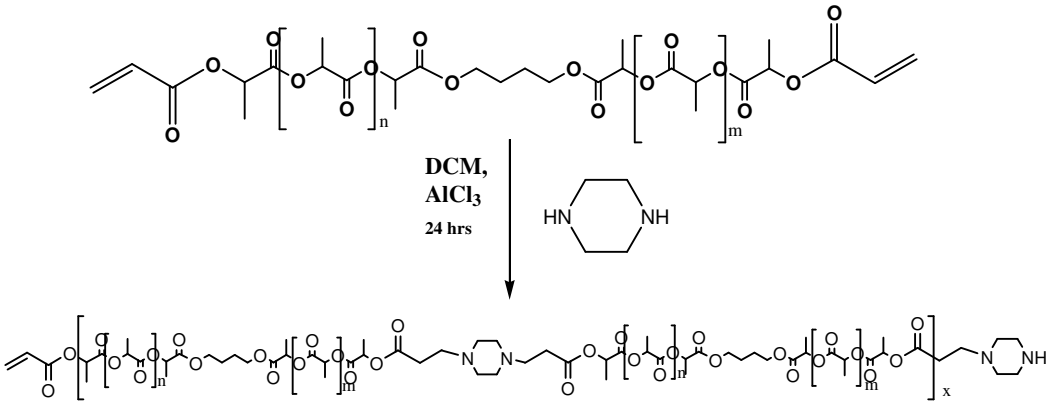

Figure 3.17: Synthesis of chain extended poly (PLA-Co-Pz)

In this section we show that oligomeric PLA/PCL diacrylates can be easily chain extended as to contain more labile β-amino esters links under appropriate conditions using Michael addition approach (figure 3.17). The chain length can be manipulated by manipulating the molecular weight of the oligomeric diacrylate.

Table 3. 8: PLA and PCL based poly (β-amino esters)

Sr.No	M	Amine	Mole. Wt (M_w)
P1	M 3	Piperazine	12,030
P 2	M 3	TMDP	13,680
P 3	M 3	Butyl Amine	13,360
P 4	M 3	Lauryl amine	10,650
P 5	M 4	Piperazine	14,000
P 6	M 5	Piperazine	13,360
P 7	M 5	TMDP	14,101
P 8	M 5	Butyl Amine	12,111
P 9	M 5	Lauryl amine	9910
P 10	M 9	Piperazine	-
P 11	M 9	TMDP	-
P 12	M 9	Butyl Amine	-
P 13	M 9	Lauryl amine	-
P 14	M 10	Piperazine	9290
P 15	M 10	TMDP	11,360
P 16	M 10	Butyl Amine	11,140
P 17	M 10	Lauryl amine	10,290
P 18	M 11	Piperazine	-
P 19	M 11	TMDP	-
P 20	M 11	Butyl Amine	-
P 21	M 11	Lauryl amine	-

Lactide and caprolactone diacrylates were copolymerized with bi functional amines by acid catalyzed Michael addition at ambient temperature for 24 hrs using 1 mole % $AlCl_3$. It was observed that diacrylates having molecular weight (M_n) 4595, 3336, 2035 and 714 did not polymerize. The maximum degree of polymerization obtained for block polymer was 7 and the polymer yield was in the range 70 to 85 %. An increase in the molecular weight of the oligomeric diacrylate resulted in lower degree

of polymerization with the amine because of the lower reactivity of terminal acrylate groups.

3.3.5 Synthesis of poly (β-amino esters) containing hydrophobic pendant chains

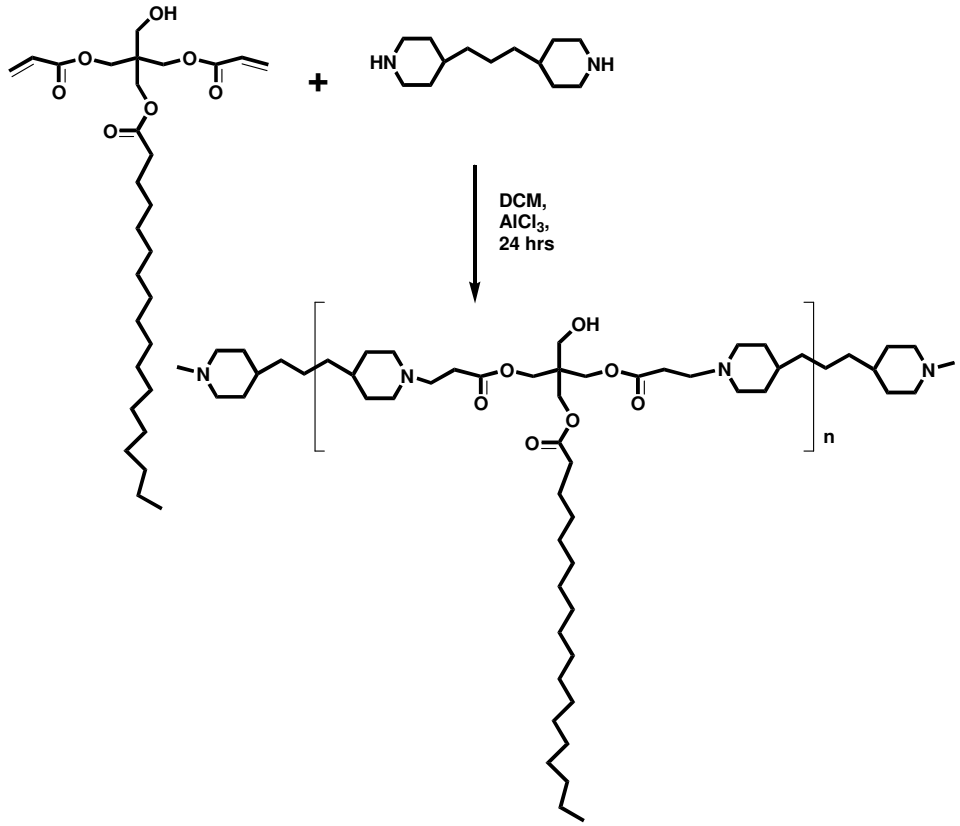

Figure 3.18: Synthesis of poly (PEDMSDA-Co-TMDP)

The poly (β-amino esters) containing hydrophobic pendant chains were synthesized by Michael addition of pentaerythritol monostearate diacrylate with bifunctional amine in the presence of Lewis acid. The extent of incorporation was manipulated by polymerizing mixture of diacrylates containing varying ratios of pentaerythritol monostearate diacrylate and poly ethylene glycol diacrylate with bifunctional amine. Reaction conditions, monomer to catalyst ratio, composition and yield of copolymerization reaction are reported in table 3.9.

The hydrophobicity of the pendant chain can be varied by varying either the length of the carboxylic acid (C_4-C_{18}) or by changing mPEG-COOH of varying molecular weights.

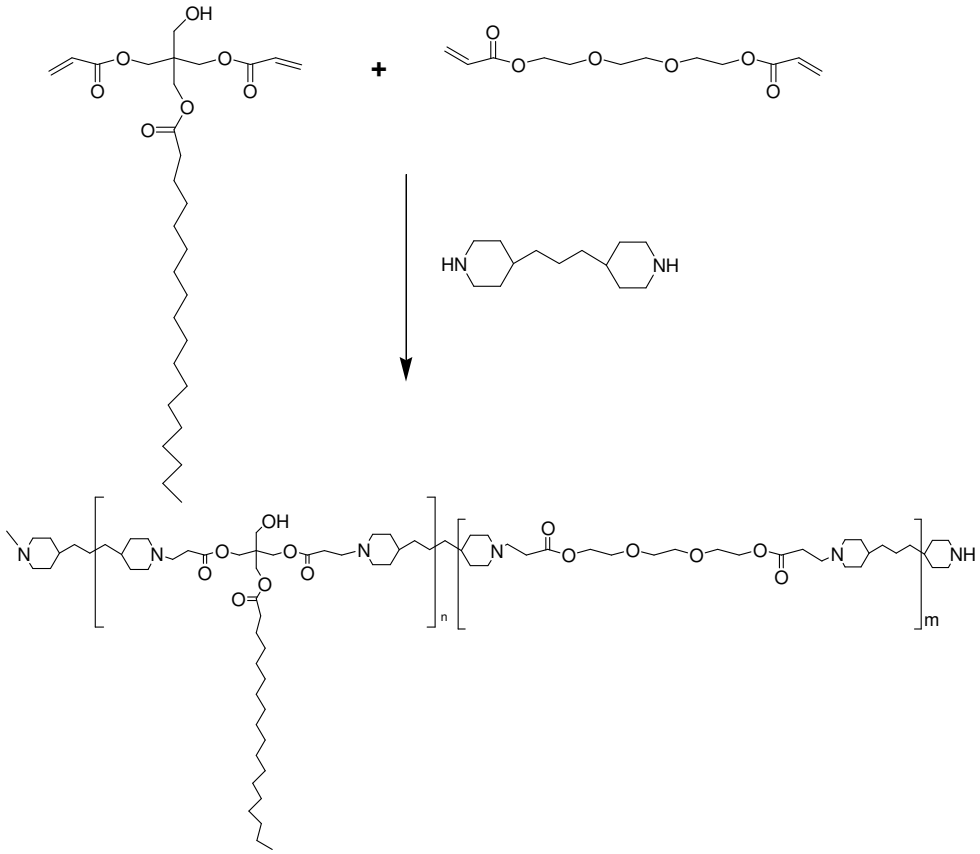

Figure 3.19: Synthesis of polymers with varying degree of pendant groups

When a mixture of PEG diacrylate and PEDAMS was used it was observed that the extent incorporation of PEDAMS in the polymer was the same as in the feed (table 3.9).

Table 3.9: Poly (β-amino esters) containing pendant stearic acid

Polymers	PEDAMS *		PEGDA (258)*		Yield (%)
	In feed	By NMR	In feed	By NMR	
1	100	100	0	0	88.19
2	85	87	15	13	84.45
3	70	66	30	34	83.99
4	50	55	50	45	81.72
5	30	40	70	60	86.39
6	15	25	85	75	75.09

* mole percent where moles of difunctional amine TMDP kept constant 100 mole % w.r.t. total diacrylate moles.

3.3.6 Characterization of monomers and poly (β-amino esters)

3.3.6.1 FTIR of poly (β-amino esters)

A representative FTIR spectrum of poly(HDDA-Co-TMDP) is shown in figure 3.20 where absence of peaks at 1636 cm^{-1} attributed to vinyl unsaturations of diacrylate confirms that polymerization proceeds via Michael type addition. Absence of amide peak at 1680 cm^{-1} in FTIR spectrum further confirms that the polymerization proceeds via 1,4 addition and not via 1, 2 addition. As 1, 2 addition leads to formation of amide bonds as shown in figure 3.13.

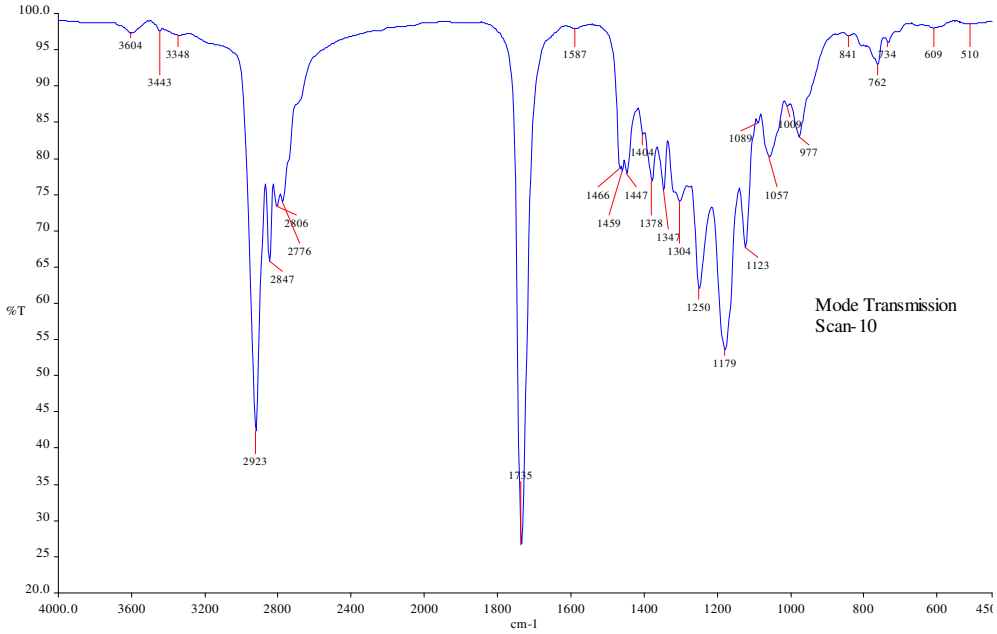

Figure 3.20: FTIR spectrum of the poly (HDDA-Co-TMDP)

3.3.6.2 NMR of poly (β-amino esters)

NMR spectroscopy can also be used to confirm formation of reaction intermediates and end products.

i. Poly (HDDA-Co-TMDP), ^{1}H NMR

Figure 3.21 shows ^{1}H NMR spectrum of poly (HDDA-Co-TMDP). In general the peaks observed were broad because of multiple repeat units. The peak at 4.05 ppm is attributed to 4 protons of k. Peak at 2.89 ppm corresponds to 4 protons of j, peak at 2.67 ppm corresponds to 4 protons of i, peak at 2.53 ppm corresponds to 4 protons of h. Peak at 1.99 ppm corresponds to 4 protons of g. The peak at 1.62 ppm corresponds

to 4 protons of e and 4 protons of f. The peaks at 1.36 ppm and 1.20 ppm correspond to 4 protons of a, 6 protons of b, 4 protons of c and 2 protons of d. This spectrum also confirms that the newly formed tertiary amines in the polymer backbone do not participate in subsequent Michael addition with diacrylate monomer, which would lead to branched or cross linked polymer structure.

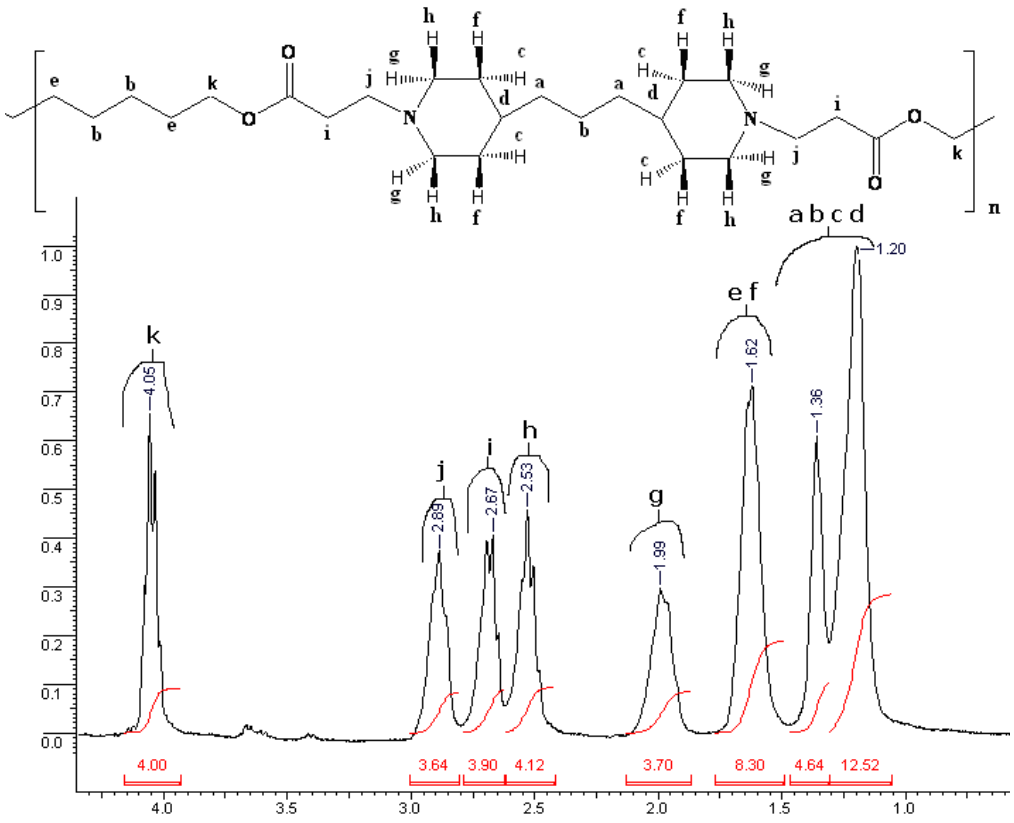

Figure 3.21: ^{1}H NMR spectrum of Poly (HDDA-Co-TMDP)

ii. NMR of chain extended poly (β-amino esters)

a. Poly (PLA-Co-Pz)

In figure 3.22a, spectrum of PLA diol synthesized via ring opening polymerization of L-lactide is shown. Peaks around 4.24 ppm correspond to 4 (-CH_2) groups of 1, 4 butanediol. Thus lactide was converted to lactide diol. Spectrum 3.22b corresponds to PLA diacrylate wherein multiple peaks appear in the region 5.88 to 6.53 ppm which correspond to acrylic protons. ^{1}H NMR spectrum of poly (PLA-Co-Pz) is shown in figure 3.22c. This polymer was synthesized by Michael addition of PLA diacrylate

with piperazine. NMR spectrum of polymer shows disappearance of acrylic proton peaks in the region 5.88 to 6.53 ppm and appearance of broad peaks at 2.60 to 2.80 ppm which corresponds to 12 protons of newly formed -CH_2–N-$(CH_2)_2$ groups. These results confirm the incorporation of piperazine in the polymer backbone and that polymerization occurred by 1,4 addition of amines with acrylate groups of PLA diacrylate.

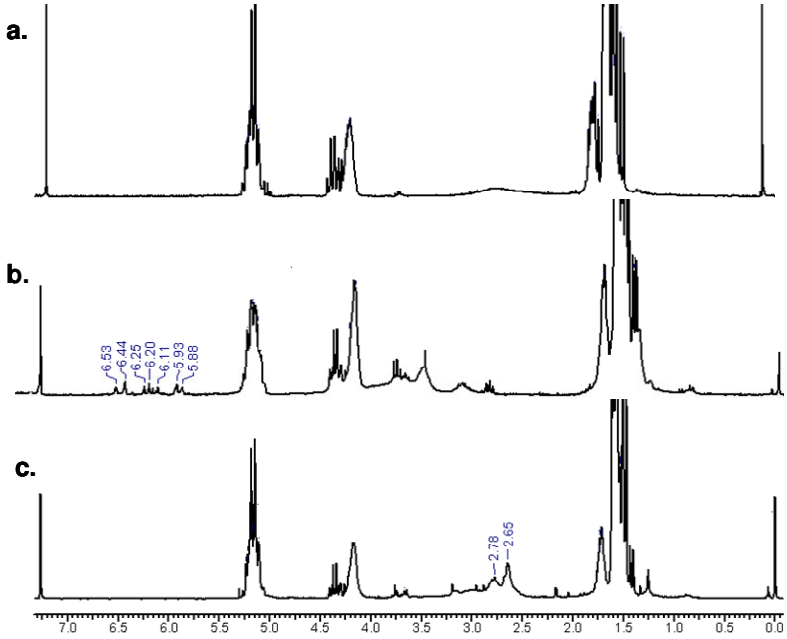

Figure 3.22: ^{1}H NMR of a) PLA diol, b) PLA diacrylate and c) poly (PLA-Co-Pz)

b. Poly (PCL-Co-Pz)

Figure 3.23a shows the NMR spectrum of PCL diol which was converted to corresponding diacrylate by condensation with acryloyl chloride. Spectrum 3.23b shows multiple peaks in the region 5.80 to 6.50 ppm which correspond to acrylic protons and confirm formation of PCL diacrylate. Figure 3.23c shows ^{1}H NMR spectrum of poly (PCL-Co-Pz), disappearance of acrylic proton peaks in the region 5.80 to 6.50 ppm and appearance of peaks at 2.45 to 2.70 ppm which corresponds to 12 protons of newly formed -CH_2–N-$(CH_2)_2$ groups confirm the incorporation of piperazine within polymer backbone and that polymerization occurred via 1,4 addition of amines with acrylate groups of PCL diacrylate.

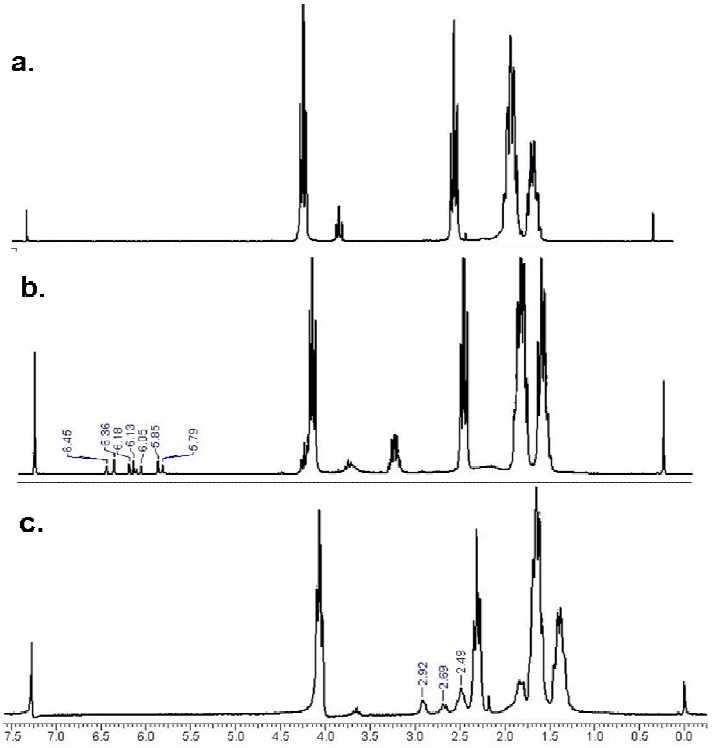

Figure 3.23: ^{1}H NMR of a) PCL diol b) PCL diacrylate c) Poly (PCL-Co-Pz)

iii. Poly (β-amino esters) containing hydrophobic pendant chain

The poly (β-amino esters) were synthesized by Michael addition of pentaerythritol monostearate diacrylate with bifunctional amine. The degree of incorporation was manipulated by polymerizing a mixture containing varying ratios of pentaerythritol monostearate diacrylate and poly ethylene glycol diacrylate with bifunctional amine. Figure 3.24 shows the ^{1}H NMR spectra of poly (β-amino esters) where composition of acrylates, PEDAMS (15% to 100%) and PEGDA (85% to 0%) was varied to manipulate the incorporation of hydrophobic pendant chains. Incorporation of stearyl chain within the polymer was confirmed by NMR analysis. To calculate pendant stearate groups in polymer backbone, protons appearing at 4.1 and 4.2 ppm (highlighted with square in figure 3.24) corresponding to $–CH_2$-O-C=O group of PEDMS and PEGDA respectively were selected for comparison. NMR analysis revealed values that the incorporation of PEDAMS in the polymer was close to that in feed. These results are listed in table 3.10.

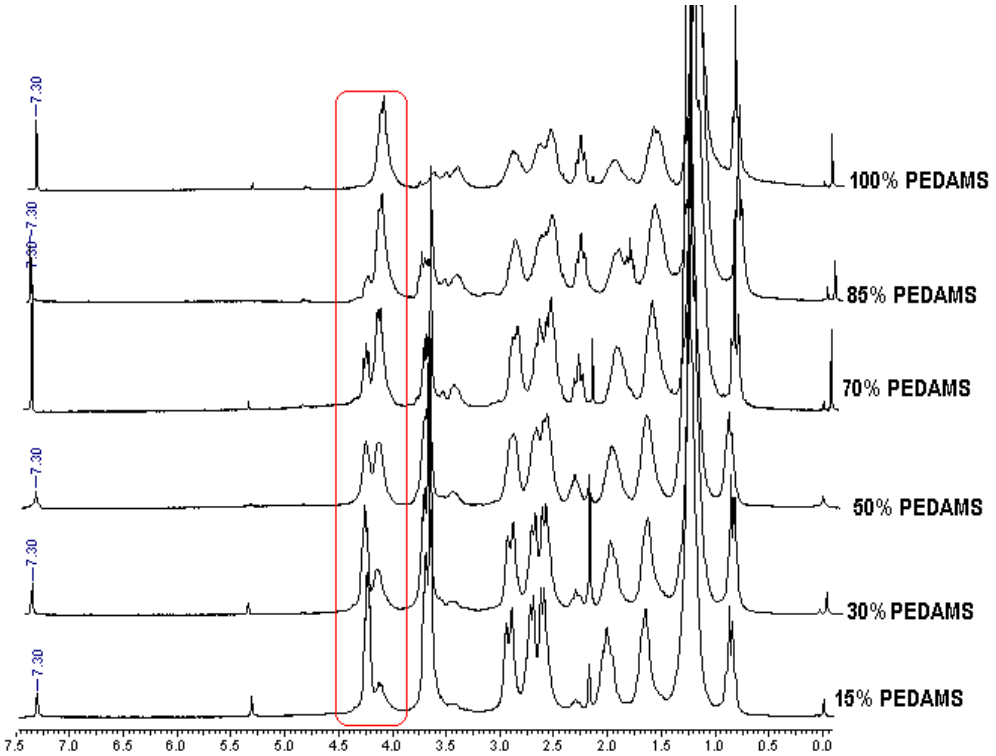

Figure 3.24: ^{1}H NMR of poly (β-amino esters) with pendant stearyl chain

3.3.7 Molecular weight characterization by VPO and GPC

The molecular weights of polymers synthesized in this work were determined using gel permeation chromatography (GPC) and vapor pressure osmometry (VPO). Polymer molecular weights (M_w) ranged from 5200 to 31000 relative to polystyrene standards (table 3.5). Molecular weight distributions of these polymers were monomodal and polydispersity indices (PDI) varied between1.45 to 3.00. Very high polydispersity (7.2.) was reported in previous investigations on PBAEs (Anderson and Langer 2004). The molecular weight build-up is probably restricted due to intramolecular cyclization reaction between amine present on growing end of polymer chain which reacts with acrylate at the other end (Akinc et. al. 2003). Representative molecular weight data are illustrated in table 3.5. Molecular weights of oligomeric PLA and PCL diols and diacrylates were measured using VPO. Molecular weights of chain extended poly (β-amino esters) were measured using GPC (tables 3.6 - 3.9). It was observed from table 3.6 that as the amount of 1, 4 butanediol in the polymer increased, the molecular weight of lactide diol decreased. Thus molecular weight of lactide diol could be controlled by the amount of 1,4 butanediol in feed.

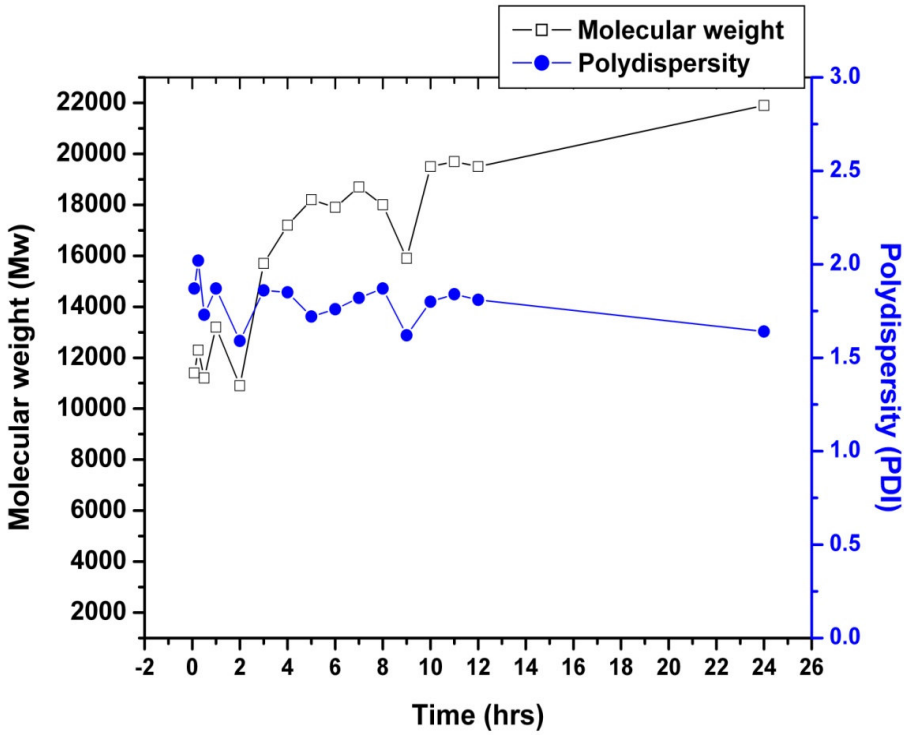

Figure 3.25: Effect of polymerization time on Mw and PDI

Effect of reaction time on molecular weight (M_w) and polydispersity index (PDI) is shown in figure 3.25. Polymerization of TMDP with HDDA was selected to study the course of the reaction. Molecular weight of the polymer increased during first 12 hrs but was practically constant thereafter. PDI initially dropped from 2 to 1.8 in first 12 hrs then to 1.6 after 24 hrs.

3.3.8 Thermal characterization by DSC

The DSC was used to study thermal properties of the polymers and also to demonstrate effect of monomer structure on the physical properties of the polymer. To demonstrate the effect of polymer structure on the physical properties, polymers bearing different backbones as listed in table 3.10 were synthesized. The analysis of these polymers shows that the polymer synthesized using 5-aminopentanol does not show crystallization whereas polymers synthesized using Pz and TMDP exhibit both T_m and T_c. This is due to the presence of rigid piperazine and two piperidine rings in polymer 2 and 3 respectively. Similar observations were reported by Galli et. al. 1983 and Anangeioni et. al. 1985. Poly (β-amino esters) synthesized in this work exhibit very low (-52.90 to -1.59) glass transition temperature. In case of polymer 6

introduction of cyclohexane ring in the polymer backbone restricts the molecular motion resulting in increase in glass transition temperature. These results indicate that the glass transition temperature of the networks can be controlled by the choice of diacrylate and amine.

Table 3.10: Thermal analysis of poly (β-amino esters)

Polymer	Diacrylate	Amine	T_g	T_m	T_c
1	BDDA	5-Amino pentanol	-42.10	_	-
2	BDDA	Piperazine	-34.64	61.40	-5.82
3	BDDA	TMDP	-34.32	47.29	-6.63
4	HDDA	TMDP	-39.47	53.57	-8.27
5	DDDDA	TMDP	-18.02	51.55	--
6	CHDMDA	TMDP	-01.59	57.38	9.82
7	PEGDA258	TMDP	-31.83	-4.37	--
8	PEGDA700	TMDP	-52.90	4.97	--

3.3.9 Polymer dissolution study at different physiological pH

Lynn et. al. 2000 reported that under extreme acidic (pH < 3) or basic (pH > 12) conditions, poly (β-amino esters) degrade rapidly and exclusively to 1,4-butanediol and the bis(β-amino acid) byproducts. The rate of degradation is higher at pH 7.4 than at pH 5.1. Poly(HDDA-Co-TMDP) takes 2 hrs for 80% degradation at 7.4 pH where as at 5.1 pH it required around 25 hrs to undergo 80% degradation .

To study the behavior of pH dependant solubility of polymers at different physiological pH 1.25, 5.8 and 6.8 following polymers were selected.

A) Poly (HDDA-Co-TMDP)
B) Poly (CHDMDA-Co-TMDP)
C) Poly (DDDDA-Co-TMDP)

Solubility results of these polymers at pH 1.25, 5.8 and 6.8 are shown in figure 3.26, 3.27 and 3.28 respectively. The studies revealed that in general poly (β-amino esters) are more readily soluble at acidic pH than at near neutral or neutral pH. The solubility of poly (β-amino esters) can be effectively manipulated using monomers containing either long chain hydrocarbon groups as in DDDDA or rigid groups as in CHDMDA.

As DDDDA is hydrophobic monomer as compared to CHDMDA and HDDA, its rate of dissolution is very slow at pH 1.25. However at pH 5.8 and 6.8 it is practically insoluble. Similarly the polymer containing HDDA shows high rate of dissolution at all pH ranges.

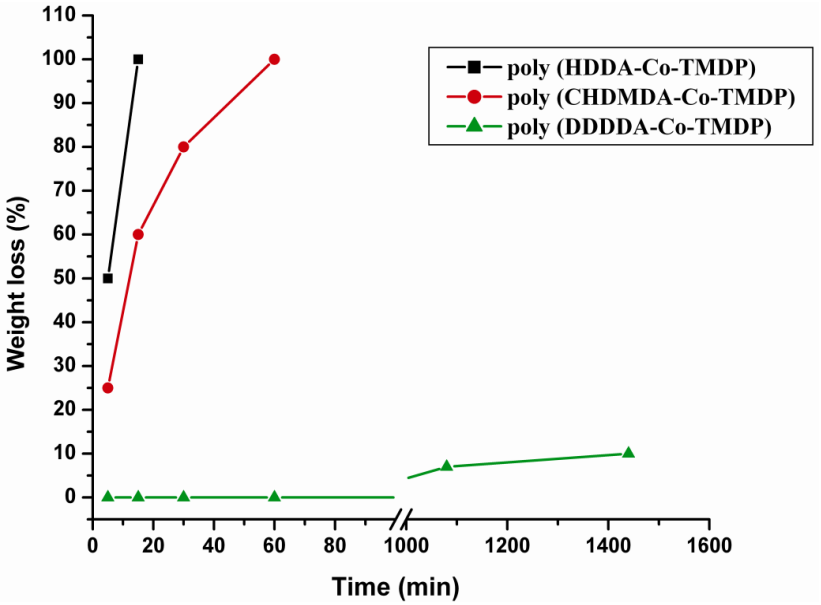

Figure 3.26: Percentage weight loss op polymers at 1.25 pH

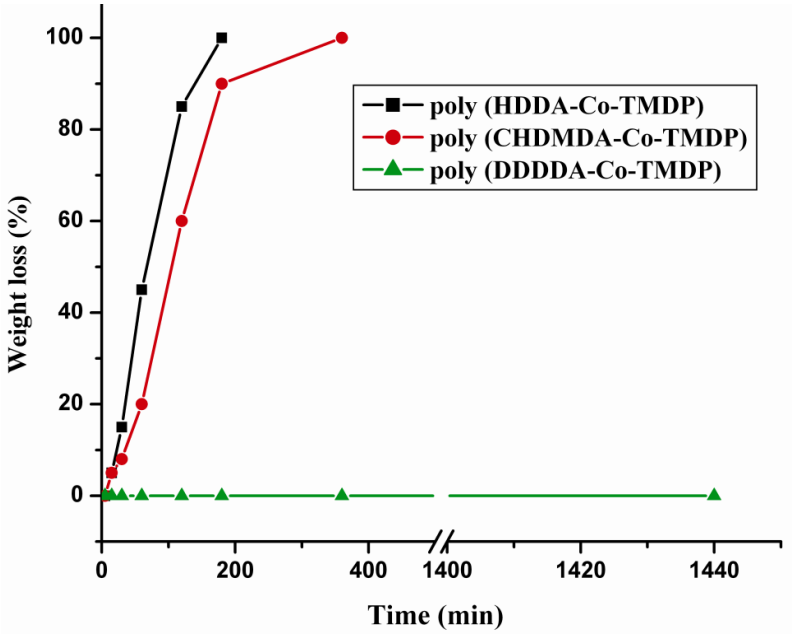

Figure 3.27: Percentage weight loss of the polymers at 5.8 pH

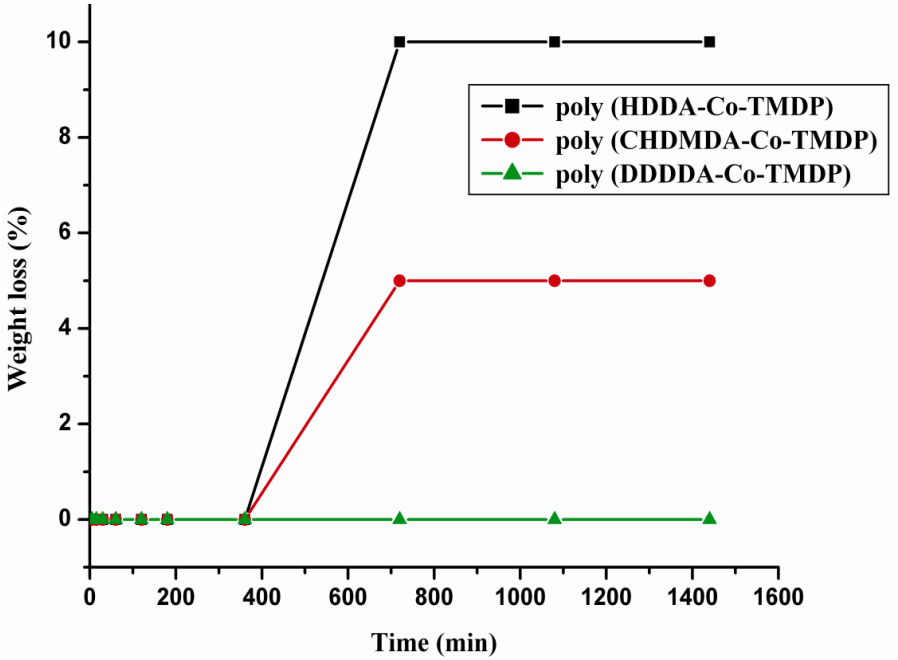

Figure 3.28: Percentage weight loss of the polymers at 6.8 pH

Comparison between dissolution results shown in figures 3.26 - 3.28 and the degradation rates reported by Lynn et. al. (2000) indicates that the polymers first dissolve at acidic pH and then undergo degradation, as dissolution time of polymers is much smaller as compared to degradation time. pH dependent dissolution behavior exhibited by poly (β-amino esters) can be used in developing drug delivery system. These polymers can be used in the form of microparticles, nanoparticles or as film coating on tablet. Especially in oral drug delivery these polymers will help to release drug at acidic pH within few minutes. These polymers could be potential candidates for development of chewable, rapidly disintegrating, quick dissolve tablets or as liquid orals to provide ease of administration and immediate release of drug at gastric region (Kulkarni and Menjoge 2005, 2007).

At neutral pH, polymer degradation rate will govern drug release than dissolution rate. These polymers could be useful in increasing circulation time of polymeric nanoparticles containing the drug (Muthu 2009). As polymers undergo degradation into non-cytotoxic fragments at near neutral pH these can be readily excreted from the body (Duncan and Kopecek 1984, Venkatachalam and Rennke 1978).

3.3.10 Degradation studies of poly (PLA-Co-Pz)

Poly (PLA-Co-Pz)**,** molecular weight (M_w) 14000 was exposed to pH 1.5, 6.8 and 7.8 to study the effect of physiological buffers on the molecular weight and the molecular weight loss was followed by VPO.

Table 3.11: Degradation of poly (PLA-Co-Pz) at pH 1.25 HCl buffer

Time (h)	Mn
0	14000
1	8092
13	4824
25	2667

Table 3.12: Degradation of poly (PLA-Co-Pz) at pH 6.8 and 7.8 PBS

pH	Time (h)	Mn
	0	14000
6.8	24	6240
7.8	24	5986

It was observed that after 24 hrs molecular weight (M_n) of the polymer immersed at pH 1.25 is lowered to 2600 (table 3.11) which is close to the molecular weight of PLA diol (Mn 2125) used for synthesis, whereas at pH 6.8 and pH 7.8, same polymer degraded to half of its original molecular weight 6200 and 6000 respectively (table 3.12). These polymers exhibited pH dependant degradation where rate of degradation in acidic medium was faster than neutral and basic pH. The molecular weight of degradation fractions can be manipulated by selecting PLA diacrylates of varying molecular weight.

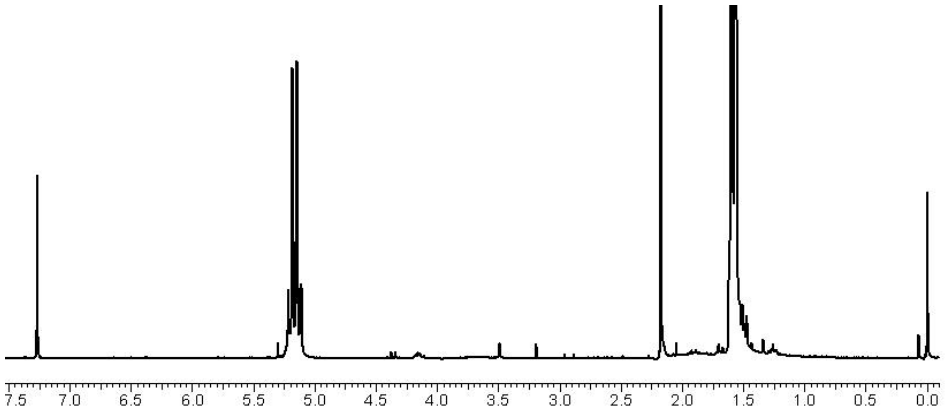

Figure 3.29: ^{1}H spectrum of degraded fraction poly (PLA-Co-Pz)

^{1}H NMR spectrum of degraded fraction of poly(PLA-Co-Pz) shows absence of acrylate groups which confirms that polymers undergo degradation via ester hydrolysis and not via retro Michael addition to yield diacrylate and amine (figure 3.29). The polymer after hydrolytic degradation leads to OPLA and β-amino acid of the respective amine both these degradation products are non-toxic (Lynn et. al. 2000).

3.3.11 Encapsulation of Diltiazem HCl in polymeric microspheres

3.3.11.1 Morphology and size of polymer microspheres

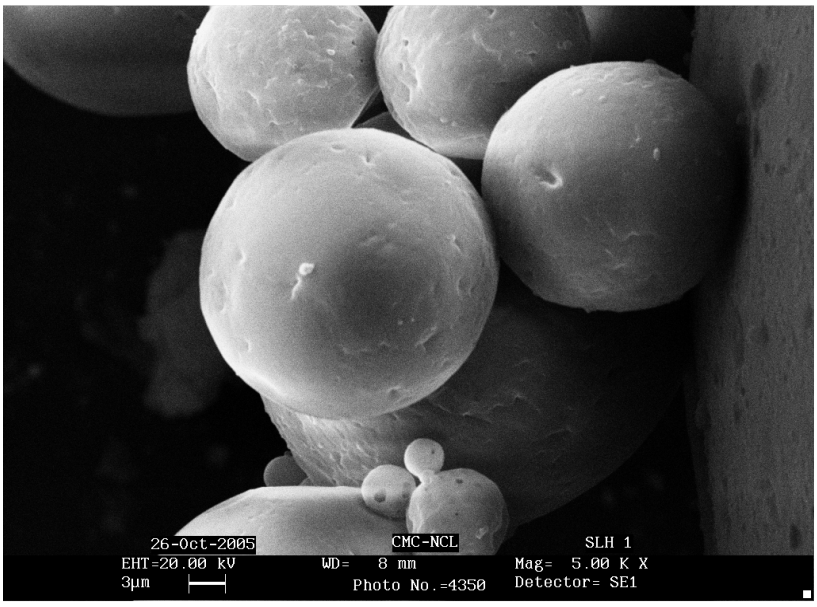

Figure 3.30: SEM picture of the microspheres containing Diltiazem HCl

The microspheres prepared by w/o/w techniques showed very broad size distribution from 5 microns to 300 microns (figure 3.30). The yield of the polymeric microspheres is 70 %.

3.3.11.2 Drug content and encapsulation efficiency

The percentage incorporation of drug in to microsphere was found to be 12.44 %. The encapsulation efficiency of Diltiazem HCL in polymeric microsphere was 34.83 %. The low encapsulation efficiency of drug into polymeric microspheres is due to the high solubility of Diltiazem HCL in the water.

3.3.11.3 Drug release study form microspheres

a) At 0.1 N HCl

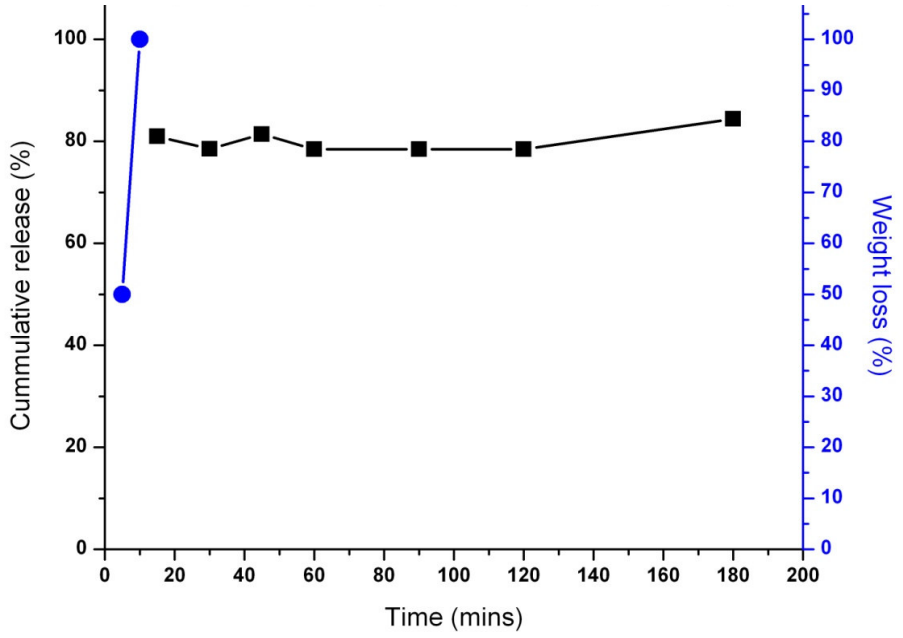

Figure 3.31: Cumulative release (-■-) of Diltiazem HCl and Poly (HDDA-Co-TMDP) weight loss pH 1.25 HCl buffer (-●-)

b) At 5.8 pH

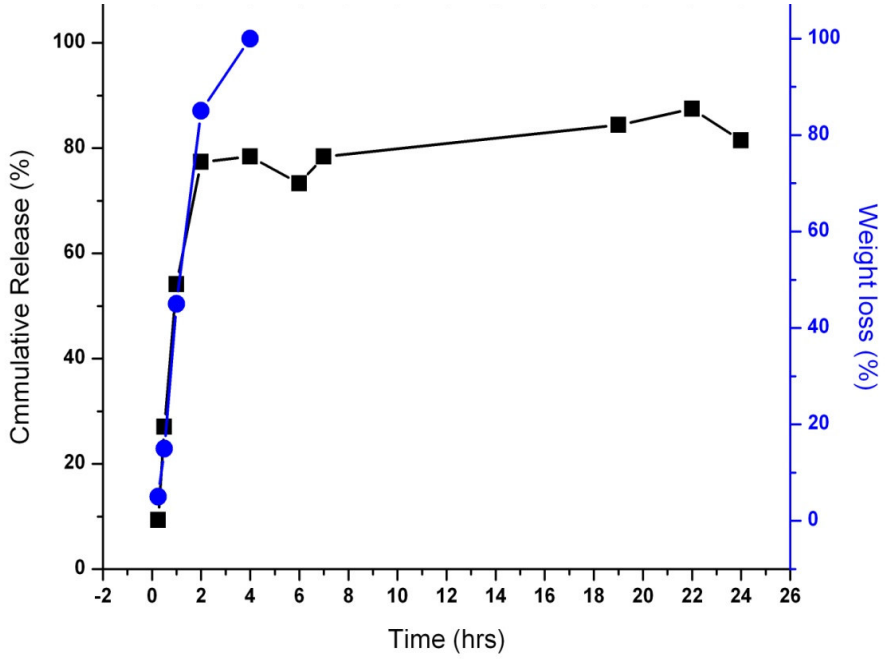

Figure 3.32: Cumulative release of Diltiazem HCl (-■-) and Poly (HDDA-Co-TMDP) weight loss at pH 5.8 PBS (-●-)

c) At 6.8 pH.

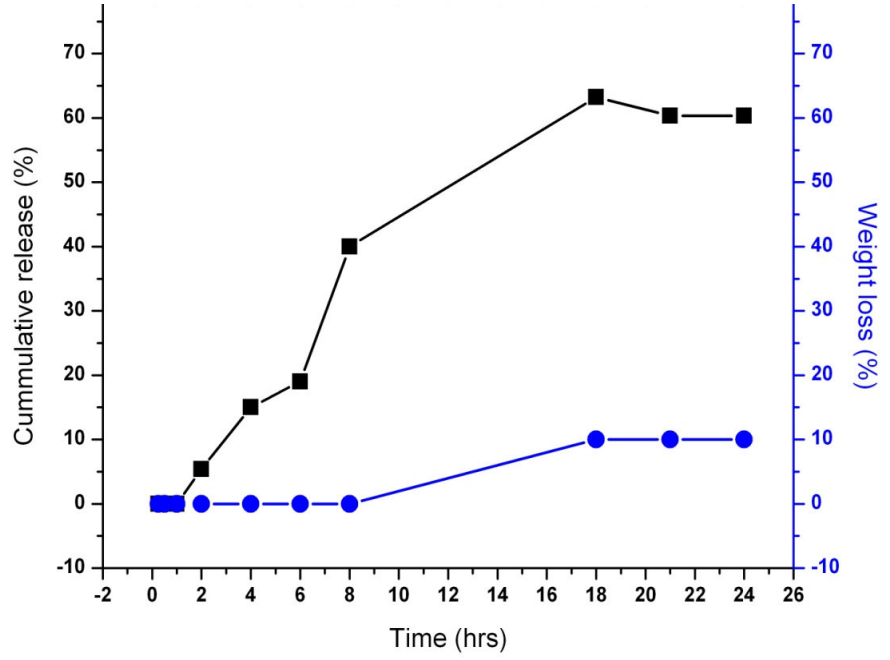

Figure 3.33: Cumulative release of Diltiazem HCl (-■-)and Poly (HDDA-Co-TMDP) weight loss at 6.8 pH PBS (-●-)

The cumulative drug release at pH 1.25 (figure 3.31) and 5.8 (figure 3.32) shows good agreement with the solubility of polymers. But at 6.8 pH it showed sustained drug release (figure 3.33). About 40 % drug was released in 10 hrs and to 60 % in 18 hrs.

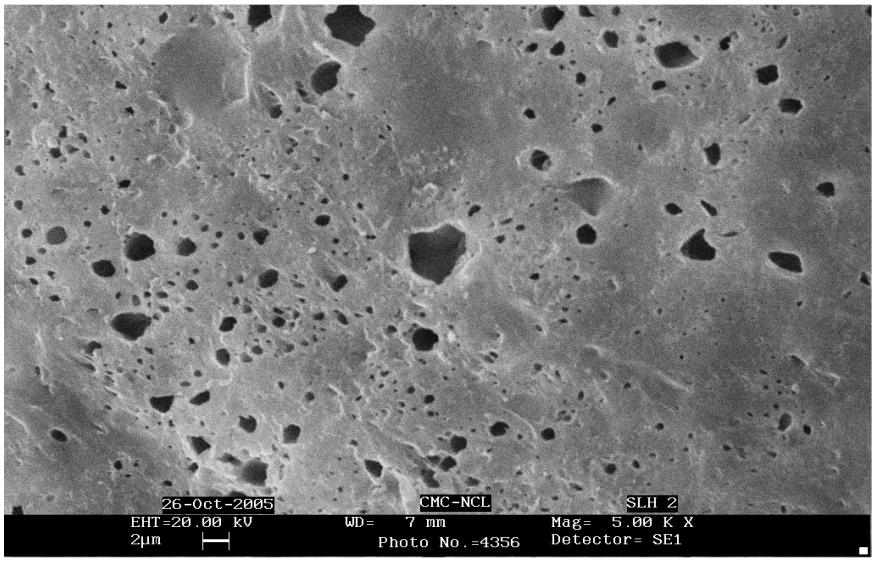

Figure 3.34: SEM image of microsphere surface

To study the reason of drug release surface morphology of dried microspheres was investigated by SEM (figure 3.34). In SEM images it was observed that pores were formed on the surface of the microspheres. This formation of pores leads to diffusion of drug from microspheres in to dissolution medium. Hence even though the polymer microspheres appeared undissolved in release media at pH 6.8 sustained drug release was observed.

3.4 Conclusions

Lewis acid catalysis brought down the polymerization time of poly (β-amino esters) from 5 days to few hours. It was observed that $AlCl_3$ and $FeCl_3$ are better catalysts as compared to $ZnCl_2$. Polymerization can be carried out using anhydrous acetone, dichloromethane and tetrahydrofuran depending on monomer solubility. Lewis acid helps to carry out reaction at ambient temperature without sacrificing yield and molecular weight. This methodology can be used to synthesize chain extended poly (β-amino esters), and incorporate hydrophobic pendant groups by the choice of appropriate monomers. Polymers synthesized in this chapter showed pH dependant solubility and degradation behavior. The degradation of these polymers takes place

via ester hydrolysis. No evidence of retro Michael reaction was noticed during hydrolytic degradation of polymers. The dissolution rate of these polymers is higher in acidic pH as compared to neutral pH. These polymers could be potential candidates for development of chewable, rapidly disintegrating, quick dissolve tablets for immediate release of drug at gastric region.

3.5 References

Abrouki Y., Zahouily M., Rayadh A., Bahlaouan B., Sebti S. *Tetra. Let.*, **2002**, 43, 8951.

Akinc A., Lynn D. M., Anderson D. G., Langer R. *J. Am. Chem. Soc.*, **2003**, 125, 5316.

Akinc A., Anderson D. G., Lynn D. M., Langer R., *Bioconjugate Chem*. **2003,** 14, 979.

Anderson D. G., Lynn D. M.,Langer R. *Angew. Chem. Int. Ed.*, **2003**, 42, 3153 .

Anderson D., Langer R. US Pat Apli. No . 2004/0071654 A1.

Angeioni A. S., Laus M., Castellari C., Galli G., Ferruti P., Chielhi E., *Makromol. Chem.*, **1985**, 186, 977.

Angeloni A. S., Laus M., Castellari C., Galii G., Ferruti P., Chielhi E. *Makromol. Chem*, **1985**, 186, 977.

Bernaerts K. V., Fustin C-A., D'Haese C. B., Gohy J-F., Martins J. C., Du Prez F. E. *Macromolecules*, **2008**, *41*, 2593.

Bradley D.J., McGrath J.E. *Polym. Sci. Part A Polym. Chem.*, **1989**, 27, 4001.

Cabral J., Laszlo P., Mahë L., Montaufier M-T and Randriamahefa L. *Tetrahedron Lett.*, **1989**,30, 3969.

Chien-C. C., Ju-Y. C , How T., Haw-M. H., Sheng-Y. L. *Biomaterials,* **2003**, 24, 1167.

Danusso F., Ferruti P. *Polymer*, **1970**, 11, 88.

Duncan, R. and Jindřich Kopeček *Adv. Polym. Sci.*, **1984**, 57, 51.

Ferruti P., Marchisio M. A., Duncan R., *Macromol. Rapid Commun.,* **2002**, 23, 332.

Filip E. D., *Macromolecules*, **2008**, 41, 2593-2606

Galli G., Laus M., Angeloni A. S., Ferruti P., Chiellhi E., *Makromol. Chem., Rapid Commun.*, **1983**, 4, 681.

Heathcock C. H., Oare D. A. *J. Org. Chem.*, **1985**, 50, 3022.

Laus M., Angeloni A. S., Galli G., Chielhi E. *Makromol. Chem.*, **1988**, 189, 743.

Loncharich R. J., Schwartz T. R., Houk K. N. *J. Am. Chem. Soc.*, **1987**,109, 14.

Long T.E., Broske A.D., Hulubei C, Rusu E. *Polym. Plast. Technol. Eng.*, **2001**, 40, 117.

Lynn D. M., Langer R. *J. Am. Chem. Soc.*, **2000**,122, 10761.

Lynn D. M., Anderson D.G., Putnam D., Langer R. *J. Am. Chem. Soc.,* **2001**,123, 8155.

Kulkarni, M. G., Menjoge, A. R. U. S. Patent, 20050137372 A1, 2005.

Kulkarni, M. G., Menjoge, A. R. U. S. Patent, 20050136114 A1, **2005**.

Mather B. D. Viswanathan K., Miller K. M., Long T. E., *Prog. Polym. Sci.*, **2006**, 31 487.

Menjoge A. R., Kulkarni M.G. *Biomacromolecules*, **2007**, 8, 532.

Muthu M. S., *Asian journal of pharmaceutics*, **2009**, Oct- Dec, **.**

Konradi R., Pidhatika B., Mühlebach A., Textor M. *Langmuir*, **2008**, 24, 613-616.

Pan J., Subbu S., Feng M., Boey Y. Chiang F., Gan L. *Journal of Controlled Release* **2005**, 110, 20.

Reddy T. A., Erhan S. *Journal of Applied Polymer Science*, **1994**, 51, 159.

Sinsky M., Bass R. ,Connell J., *J. Polym. Sci. Part A Polym. Chem.*, **1986**, 24, 2279.

Storey R.F., warren S.C., Allison C.J., Puckett A.D. *Polymer*, **1997**, 38, 26, 6295.

Storey R. F., Warren S. C., Allison C. J., Puckett A. D., *Polymer*, **1997**, 38, 6295.

Tatsuro O., Shunsuke I., Yuichi O. *Polymer*, **2006**, 47, 429.

Tomasi S., Bizzarri R., Solaro R., Chiellini E. *J. Bioact. Compat. Polym.*, **2002**, 17, 3.

Vaccaro E, Scola DA. *Chemtech.*, **1999**, 29, 15.

Venkatachalam, M. A.; Rennke, H. G. *Circ. Res.*, **1978**, 43, 337.

Wabnitz T. C., Spencer J. B. *Org. Lett.,* **2003**, 5, 2141.

Wilbur J. M., Bonner B. A. *Journal of Polymer Science: Part A: Polymer Chemistry*, **1990**, 28, 3747.

Yang L., Xu L-W., Xia C-G. *Tetrahedron Letters*, **2005**, 46, 3279.

Zahouily M., Abrouki Y., Rayadh A., Sebti S., Dhimanec H., David M. *Tetrahedron Letters*, **2003**, 44, 2463.

Chapter 4

Synthesis and characterization of sequentially crosslinkable poly (β-amino esters) (SCPBAE)

4.1 Introduction

4.1.1 Polymers as biomaterials

Polymers both synthetic and natural play a vital role in the development of biomedical applications which range from packaging to most sophisticated drug delivery devices as listed in table 4.1 (Park et. al. 1994, Gomathi et. al. 2008).

Table 4.1: Biomedical applications of polymers (Park et. al. 1994, Gomathi et. al. 2008)

Polymer	Biomedical application
Poly (vinyl alcohol)s	Water soluble packaging
Poly(ethylene)s	Wrap, packaging, containers, transdermal patch backing, tubes for various catheters, hip-joint, knee-joint.
Poly(propylene)s	Packaging, heat shrinkable films, containers, suture materials.
Poly(tetra fluroethylene)s	Vascular and auditory prostheses, catheters, tubes.
Poly(ester)s	Vascular grafts, resorbable systems.
Poly(vinyl chloride)s	Flexible or semiflexible medical tubes, catheters, inner tubes, components of dialysis installation and temporary blood-storage devices.
Poly(acetal)s	Hard-tissue replacement.
Poly(methyl methacrylate)s	Bone cement, intraocular lenses, contact lenses, fixation of articular prostheses, dentures.
Poly(carbonate)s	Casing for biomedical and pharmaceutical products, syringes, arterial tubules, hard-tissue replacement, hemodialysers, blood pumps, oxygenators.
Poly(ethylene terephthalate)s	Vascular, laryngeal, esophageal prostheses, surgical sutures, knitted vascular prostheses.
Poly(amide)s	Intracardiac catheters, surgical sutures, films for packaging, dialysis device components, heart mitral valves, three-way valve profusion, hydrodynamic syringes, sutures.
Hydrogel	Contact lens, reconstructive joint surgery.
Biodegradable polymers (PGA, PLA, PVA)	Sutures, drug-delivery matrix, adhesives, temporary scaffolding, temporary barrier.
Poly(urethane)s	Adhesives, dental materials, blood pumps, artificial heart, and skin and blood contacting devices.
Silicone rubber	Foam-dressing, valves, catheters, contact lenses, intraocular lenses, finger joints, membranes.

4.1.2 Biodegradable polymers for advanced biomedical applications

The applications of polymers in biomedical technologies which include controlled drug delivery, regenerative medicine, gene therapy, tissue engineering and bio-nanotechnology call for biodegradable materials.

Important characteristics of biodegradable biomaterials are listed below (Nair and Laurencin 2007):

- The material should not lead to sustained inflammatory or toxic response on implantation in the body.
- The material should have acceptable shelf life.
- The degradation time of the material should match the healing or regeneration process.
- The material should posses requisite mechanical properties for the intended application and the variation in mechanical properties with degradation should be commensurate with the healing or regeneration process.
- The material should degrade into non-toxic products, readily metabolized and cleared from the body.
- The material should have appropriate processability for the intended application.

4.1.2.1 Microspheres and nanoparticles based drug delivery

Nanoparticles and microspheres which offer effective protection for pharmaceutically active compounds continue to be extensively investigated for drug delivery. The release rates of incorporated drugs can vary over a wide range from hours to months. Most commonly used biodegradable polymers in such applications are PLA, PGA, and PLGA. Commercially available products based on this technology are listed in table 4.2. Lupron® Depot containing the anticancer drug Leuprorelin acetate encapsulated in a poly (lactic-co-glycolic acid) (PLGA) matrix has been used for the treatment of prostate cancer. Leuprorelin acetate is a superactive luteinizing hormone-releasing hormone (LH-RH) agonist. Trenantone® (Takeda) is a similar product, releasing the drug Leuprorelin acetate over 3 months, and is commercially available since 1995 (Siepmann and Siepmann 2006).

Table 4.2: Pharmaceutical products based on drug loaded, biodegradable microparticles (reproduced from Siepmann and Siepmann 2006)

Drug	Trade name	Company	Application
Leuprorelin acetate	Lupron Depot	Takeda	Prostate cancer
Leuprorelin acetate	Trenantone	Takeda	Prostate cancer
Recombinant human growth hormone	Nutropin depot	Genentech-Alkermes	Growth hormone deficiency
Goserelin acetate	Zoladex	ICI	Prostate cancer
Octreotide acetate	Sandostatin LAR depot	Novartis	GH suppression anticancer
Triptorelin Recombinant	Decapeptyl Posilac	Debiopharm Monsanto	Cancer Milk production in cattle
Risperidone	Risperdal Consta	Janssen	Schizophrenia

4.1.2.2 In situ formed delivery systems

Biodegradable polymers used for drug delivery to date have mostly been in the form of injectable microspheres or implant systems, which make use of microencapsulation techniques using organic solvents. Such systems suffer from the disadvantage that the use of organic solvents can cause denaturation when protein drugs are to be encapsulated. Furthermore, the solid form requires surgical insertion, which often results in tissue irritation and damage (Jeong et. al. 1997). Development of injectable in situ setting semisolid drug depots has been explored as an alternative delivery system. For example these types of polymers can be used in the form of injectable matrix or depot for drug delivery and as injectable scaffolds in tissue engineering (Kretlow et. al. 2007). These implant systems are made of biodegradable poly (anhydride)s and poly (ester)s, which solidify in to semisolid depot once injected into the body. Atrix laboratories developed ATRIGEL ® technology where controlled release of Leuprorelin acetate was achieved through in situ formed PLGA depot. Based on mechanism of solidification these are classified in to four categories: 1)

thermoplastic pastes, 2) in situ gelling organogels, 3) in situ precipitation from solvent and 4) in situ cross-linking (Shikanov and Domb 2006).

Thermoplastic pastes are polymer systems, which are injected into the body as a melt and form a semisolid depot upon cooling to body temperature. In situ gelling organogels are composed of water-insoluble amphiphilic lipids, which swell in water and form various types of lyotropic liquid crystals. Hydrophobic poly (sebacic-*Co*-ricinoleic acid) was synthesized using natural fatty acids. These materials formed in-situ organogel on exposure to aqueous medium and may be used for the release of both hydrophobic and hydrophilic drugs (Shikanov and Domb 2006).

In situ polymer precipitation can be induced by solvent removal, a change in temperature, or a change in pH. Aqueous solutions of both diblock (PEO–PLLA) and triblock (PEO–PLLA–PEO) copolymers exhibit temperature-dependent reversible sol-gel transitions. The hydrogel based on these triblock co-polymers was loaded with bioactive molecules (FITC-labelled dextran, M_n 20,000) in an aqueous phase at an elevated temperature (around 45 ºC), where a sol was formed. In this form, the polymer was injectable. On subcutaneous injection and subsequent rapid cooling to body temperature, the loaded copolymer formed a gel that acted as a sustained-release matrix for FITC dextran. The bioactive molecules entrapped in the polymer matrix demonstrated sustained release in the body first by diffusion and later by the combination of both diffusion and degradation (Jeong et. al. 1997).

Photopolymerization has an advantage in that polymerization can be initiated at physiological temperature (37 ºC) and in biological environment without the use of solvents (Brey et. al. 2008[a]). Photopolymerizable poly (ethylene glycol) diglycidyl fumarate (fumarated PEGDGE) and RGD- conjugated poly (ethylene glycol) monoacrylate (RGD-PEGMA) were developed as injectable hydrogels. The hydrogel was modified with RGD peptide to facilitate the adhesion of the cells on the hydrogel surface (Akdemir et. al. 2008). Photopolymerizable and biodegradable polymers are now being used in a wide range of applications in tissue engineering and in the fabrication of the micro devices bearing complex structures (Anderson et. al. 2006; Brey et. al. 2008[b]).

Specifically in tissue engineering applications, these materials offer advantages because of their ability to assume shapes of irregular tissue defects. However the materials must be able to support suspended cells prior to injection and also throughout the solidification process (Kretlow et. al. 2007).

4.1.3 Advanced diagnostic applications

Micro-fabrication technology has been succefully applied to develop health care related products such as diagnostic (Lab-On-Chip) systems. Cellular microarray technique can be used for high throughput screening of new drugs (Tao and Desai 2003). A cellular microarray consists of a solid support wherein small volumes of broad range of different molecules (small molecules, polymers, antibodies, other proteins, etc.) can be arrayed using robotic technology or soft lithography. Miniaturized cell-based assays with high-throughput capability can be used to identify potentially toxic compounds during drug development process (Fernandes et. al. 2009, Gidrol et. al. 2009).

4.1.3.1 UV-embossed polymeric chip for protein separation and identification

An ultraviolet (UV)-embossed polymeric chip for protein separation by capillary isoelectric focusing (CIEF) and identification by matrix-assisted laser desorption/ionization time-of-flight mass spectrometry (MALDI-TOF-MS) was developed. The polymeric chip was successfully replicated from a soft PDMS rubber mold using UV-embossing. This polyester chip was then used to carry out CIEF to separate proteins (BSA), followed by MALDI-TOF-MS identification (Guo et. al. 2006).

4.1.3.2 Membrane protein arrays for pharmaceutical applications

Membrane proteins play a prominent role in cellular function and therefore attract strong interest in identifying new drug candidates by high-throughput screening. Hydrogel-based (Agarose gel) micro contact printing technique was developed to fabricate arrays of various membrane proteins that are embedded functionally in lipid membranes in a parallel and rapid fashion (Majd and Mayer 2008). Schematic of the technique is shown in figure 4.1.

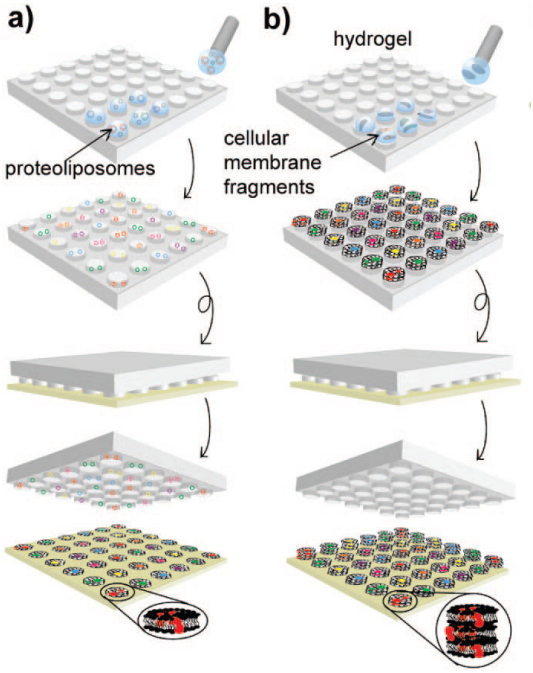

Figure 4.1: Schematic of hydrogel stamping of membranes, a) Storage of small proteoliposomes inside the posts. (b) Preconcentration of large membrane fragments on the posts of the stamp (adapted from Majd and Mayer 2008).

4.1.4 Advanced drug delivery systems

Microfabrication techniques are being explored to develop novel fully implantable drug delivery devices. These devices allow drugs to be delivered at desired locations and rates. An advanced implantable system can be used to precisely control drug delivery (Tao and Desai 2003, Maloney et. al. 2005). A prototype silicon micro-chip was developed to demonstrate controlled, pulsatile release of single or multiple chemical substances on demand. The release mechanism is based on the electrochemical dissolution of thin anode membrane covering microreservoirs filled with chemicals in solid, liquid or gel form (Santini et. al. 1999). Implantable drug delivery system (IDDS) for example MicroCHIPS have been reported in the literature. In this device macromolecular drugs such as proteins and peptides are stored in their stable form, such as a solid, liquid, or gel. As drugs are stored separately, an implantable system is capable of delivering tens or hundreds of doses of multiple drugs. The drugs can be released in a pulsatile or continuous manner at their optimal therapeutic levels (Maloney et. al. 2004-2005).

The subsequent generation of drug delivery systems evolved around developing miniaturized targeted devices which offer high spatial and temporal control over drug release. These systems involve the fabrication of small independent reservoir structures or containers that can be manufactured inexpensively, loaded easily with drugs, delivered with minimal trauma, and easily tracked, programmed or controlled (Santini et. al.1999, Randall et. al. 2007).

Photolithography coupled with self-assembly technique was successfully used to develop monodisperse containers having different 3D polyhedral shapes. These containers can be used for on demand drug delivery and also for cell encapsulation (Randall et. al. 2007). Soft lithography technique was used to develop self folding particulate drug-delivery microdevices and NaCl was used as model drug (Guan et. al. 2007). The fabrication processes is shown in figure 4.2.

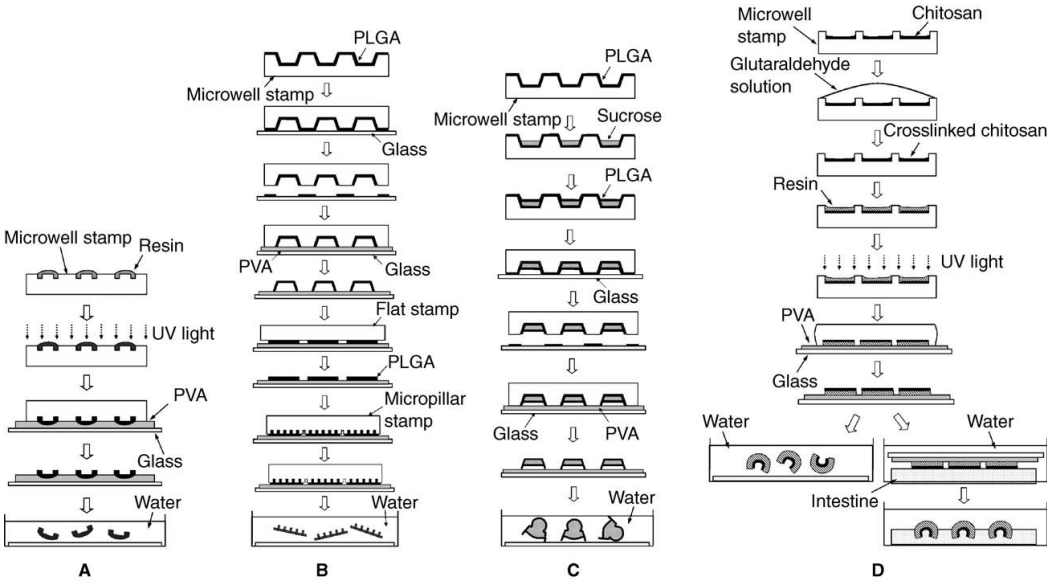

Figure 4.2: Schematic illustration of the fabrication process for A) single and B) multiple reservoirs, C) capsule like microstructures, and D) foldable microstructures (adapted from Guan et. al. 2007).

4.1.5 Biomaterials for tissue engineering

Tissue engineering is a multidisciplinary field which combines both life sciences and engineering sciences, where a combination of cells, bioactive materials such as drugs or growth factors, and biomaterial support system or scaffold have been used to generate human tissues (Kretlow et. al. 2007). Scaffold design is a crucial part of tissue engineering as it provides room for cell attachment and colonization. In

literature the polymer based scaffolds have been developed which can be used in tissue engineering as support for cell attachment and proliferation (Langer and Vacanti 1993, Hutmacher et. al. 2001[a-b], Xia et. al. 1998-99; Gates et. al. 2005). Tissue engineering scaffolds should, (a) posses interconnected pores to help tissue integration and vascularisation, (b) be biodegradable or bioresorbable, (c) favor cellular attachment, differentiation and proliferation, (d) possess adequate mechanical properties, (e) be non-cytotoxic, (f) be easy to fabricate into desired shapes and sizes (Hutmacher et. al. 2001[b]). The lithography techniques used for scaffold fabrications are discussed in the next chapter.

4.1.6 Polymers used for UV-microembossing

Amongst a wide range of soft lithography techniques used for the fabrication of scaffolds, UV- microembossing has been extensively investigated.

Table 4.3: Composition of embossed samples (adapted from Park et. al. 2003)

Compositions	A	B	C	D	E	F
PEGDA	69	70	69	98	0	34.5
PPGDA	0	0	0	0	69	34.5
TMPTA	29	29	0	0	29	29
DPHPA	0	0	29	0	0	0
EB 1360	2	0	2	2	2	2
Irgacure 651	0.2	0.2	0.2	0.2	0.2	0.2

PEGDA = Poly (ethylene glycol diacrylate) (M_n, 700), PPGDA = poly (propylene glycol diacrylate) (M_n 900), DPHPA = dipentaerythritol pentaacrylate, TMPTA = trimethylolpropane triacrylate, EB1360 = silicone hexaacrylate and Irgacure 651 = 2,2-dimethoxy-2-phenylacetophenone (photo initiator).

Oligomers such as epoxy acrylates, polyester acrylates, or polyurethane acrylates commonly used in UV cured coatings are often used in UV-microembossing. DuPont has developed a family of photopolymers (SURPHEX) for high aspect ratio UV-embossing applications. These photopolymers which are solids or semisolids contain substantial amounts (35-50 wt %) of polymeric binder which has to be subsequently

removed from the site. High molding pressures similar to those used in thermal embossing are needed if these highly viscous photopolymers are to be UV-embossed. Liquid acrylate formulations are desirable for UV-embossing as it helps mould filling at ambient temperature and pressure (Park et. al. 2003).

Liquid, photocurable polymers for example poly ethylene glycol diacrylates (PEGDA) were used to fabricate microstructured scaffolds with high fidelity (Yan et. al. 2004). PEGDA based formulations (table 4.3) were also used for UV-microembossing (Park 2003). However, these liquid polymers are not biodegradable which limits their use.

Photopolymerizable biodegradable polymers are required for the fabrication of scaffolds with controlled surface micropatterns using photolithographic techniques (Park et. al. 2004). Biodegradable aliphatic polyesters such as poly (β-hydroxy butyrate), poly (β-malic acid), poly (ε-caprolactone) and poly (α-hydroxy acids) (PLGA) have been extensively investigated for tissue engineering and other biomedical applications as they possess requisite mechanical properties and biocompatibility (Vert 2005, Okada 2002). However lack of vinyl functionality in these materials crucial for crosslinking following UV-microembossing limits their use in lithographic applications.

The photopolymerizable biodegradable diacrylate poly (lactic acid)-b-poly (ethylene oxide)-b-poly (lactic acid) (PLA-b-PEO-b-PLA) macromer was developed for the insitu synthesis of hydrogel for fabricating biodegradable scaffolds (Sawhney et. al. 1993). Jason et. al. (2007) developed PEG and PLA block macromers containing terminal (meth) acrylate groups. These macromers were further photopolymerized to yield highly crosslinked biodegradable materials. In another effort to incorporate vinyl functionality in biodegradable aliphatic polyesters, di and triblock copolymers of ε-caprolactone (CL) and glycolide (GA), lactide (LA) and ethylene oxide (EO) bearing terminal vinyl groups were developed (figure 4.3). These polymers were further processed by UV- microembossing to fabricate biodegradable scaffolds. However these polymers had to be processed at 65 ºC as these were not liquid at room temperature (Park et. al. 2004, Zhu et. al. 2006, He et. al. 2006).

Photo-patternable biodegradable 2-hydroxylethyl methacrylate (HEMA) conjugated poly (ε-caprolactone-Co-RS-β-malic acid) (PCLMAc) co-polymers were synthesized to fabricate biodegradable scaffolds. However quantitative conjugation of carboxylic

acid groups to HEMA ester is difficult and involves multiple step synthesis. Further, the resulting polymers are not liquid at room temperature and need to be processed at 60 °C (He and Park 2005).

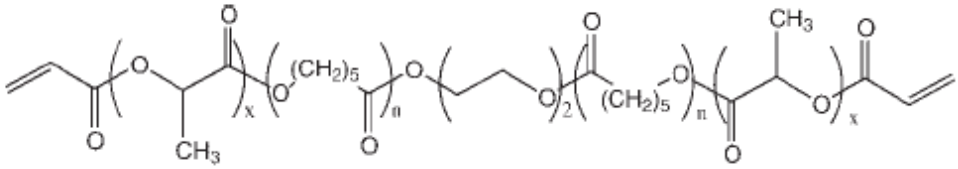

1 - 3

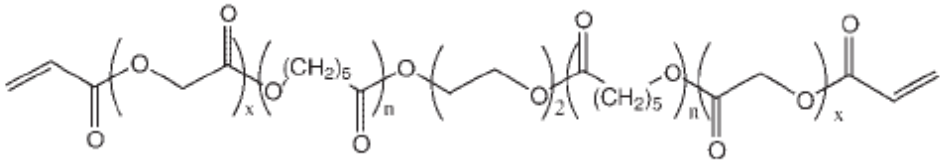

4 - 6

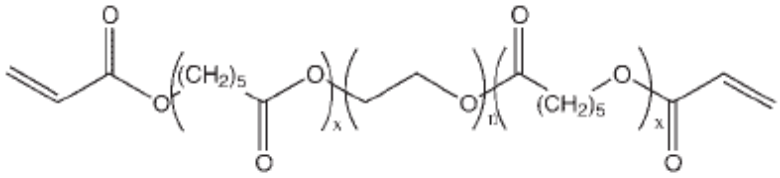

7 - 9

Figure 4.3: Triblock copolymers of PLA-b- PCL-b-PLA for polymers 1–3, PGA-b-PCL-b-PGA for polymers 4–6 and PCL-b-PEO-b-PCL for polymers 7–9 (figure adapted from Park et. al. 2004).

Liquid photopatternable polyurethane diacrylates were developed to fabricate biocompatible scaffolds by UV-microembossing. The scaffolds fabricated exhibited cytotoxicity due to the presence of unreacted monomers and the photo initiator used during polymer synthesis. The polymers were rendered biocompatible after the residues were leached out by repeated extractions with methanol which itself is not a highly desirable solvent (Shen et. al. 2006). Other examples of photopolymerizable and degradable polymers developed so far include poly (propylene fumarate)s (PPF), photocrosslinkable poly(anhydride)s, poly (ethylene glycol)s and crosslinkable poly (saccharide)s. However synthesis of these polymers involves multistep reactions and purification steps (Brey et. al. 2008[a]). Ideal polymers to fabricate biodegradable

scaffolds via UV-microembossing techniques must a) be biodegradable, b) be liquid, and (c) have functional groups to enable cross-linking (He and Park 2005).

Poly (β-amino esters) (PBAEs) were explored as transfection vectors for gene delivery (Lynn et. al. 2000-01, Anderson et. al. 2003, Green et. al. 2008)**.** Since the polymers are viscous liquids at room temperature, non-cytotoxic and biodegradable, they appear promising candidates for biodegradable scaffolds. However these polymers cannot be directly used as they lack functionalities which can lead to crosslinking during lithographic processing.

Anderson et. al. (2006) developed viscous photo-crosslinkable PBAEs containing terminal unsaturations, where degradation times of the network varied from a day to 4 months. Brey et al (2008[a]) extended this work to study the influence of macromer molecular weight on mechanical properties, degradation rate and cell adhesion. Investigations showed that since these polymers contained acrylate groups only at terminal position of chains, crosslinking of these polymers resulted in very high sol fraction up to 47% (see table 4.4) which limited their applications in tissue engineering (Brey et. al. 2008[a])**.**

In continuation of this work the effect of macromolecular branching on network properties was investigated. In this approach triacrylate was introduced in the polymerization of diacrylate and amine which helped to lower sol fraction of crosslinked product. Amine to acrylate mole ratio was maintained at 1:1. Liquid branched photo-crosslinkable PBAEs containing upto 15 % triacrylate were synthesized. However at triacrylate contents greater than 15 % cross linked products were formed (Brey et. al. 2008[b]).

Table 4.4: Sol fractions for photopolymerized PBAEs as a function of number of repeat units (table adapted from Brey et al 2008[a])

Macromer	Ratio*	n	Mol. Wt.	Sol Fraction (%)
J6	1:1	17.5	6070	47.56 ± 1.1
J6	1.05:1	12.2	4317	36.96 ± 1.0
J6	1.1:1	11.4	4049	24.56 ± 0.3
J6	1.2:1	5.8	2182	12.86 ± 1.9
J6	1.4:1	3.5	1406	2.26 ± 0.3
C12	1:1	13.8	5080	47.26 ± 0.4
C12	1.05:1	10.6	3945	44.96 ± 3.8
C12	1.1:1	8.3	3159	33.86 ± 0.9
C12	1.2:1	5.7	2230	17.46 ± 0.6
C12	1.4:1	3.6	1486	10.96 ± 0.4
E1	1:1	9.1	3982	48.96 ± 0.6
E1	1.05:1	8.0	3531	33.96 ± 0.4
E1	1.1:1	6.9	3111	23.26 ± 0.2
E1	1.2:1	5.7	2596	12.06 ± 0.7
E1	1.4:1	3.6	1768	4.36 ± 0.9

*J = triethylene glycol diacrylate, C = 1,6 -hexanediol ethoxylate diacrylate and E= 1,6-hexanediol diacrylate (E). 1= 3-methoxypropyl amine, 6 = 1- amino 2-methylpropane and 12 = 1-(3-aminopropyl) imidazole,*Acrylate: amine ratio.*

In view of current state of art in the literature, the primary objective of this work is 1) to develop alternate methodology to synthesize photo-cross linkable poly (β-amino esters) where up to 50% pendant acrylate groups could be incorporated to achieve low sol fractions, 2) to demonstrate the utility of the polymers synthesized in the fabrication of biodegradable scaffolds using UV-microembossing technique and 3) study degradation behavior of crosslinked polymers under physiological conditions.

Towards this end we synthesized photo cross linkable poly (β-amino esters) by Michael addition of triacrylate and mixture of diacrylate and triacrylate with amines in stoichiometric proportions. These polymers were photopolymerized to form

crosslinked degradable networks exhibiting degradation from one week to three months.

4.2. Experimental section

4.2.1. Materials

Acrylic acid, methacrylic acid, trimethylolpropane triacrylate (TMPTA), pentaerythritol triacrylate (PETA), trimethylolpropane allyl ether (TMPAE), cyclohexanedimothanol (CHDM), 1, 6 hexanediol diacrylate, piperazine (Pz), 4, 4' trimethylenedipiperidine (TMDP) and 1-hydroxy cyclohexyl phenyl ketone were purchased from Aldrich Chemicals. Aluminum chloride ($AlCl_3$) and benzoyl chloride were purchased from Merck India ltd. and used without further purification. All solvents were purified and dried using standard methods.

4.2.2 Characterization

^1H NMR (MSL 300 MHz) spectrum of polymers was recorded on Bruker (Bruker, Karlsurhe, Germany) spectrometer where $CDCl_3$ (Aldrich) was used as solvent. All chemical shift values are given in parts per million (ppm) and are in reference with residual proton signal from solvent. IR spectra of the polymers were recorded on Perkin Elmer Spectrum-One. GPC measurements were made on waters 590 programmable HPLC pump injector with a 100 µl injector loop and four columns in series (500 A^0 to 105 A^0, 300 X 7.5 mm, Waters, Milford MA). THF was used as eluant at a flow rate of 1ml/min. All samples were analyzed at room temperature using a differential refractometer (waters 410) and processed using the Ezychrome software package. The molecular weight and polydipersity of the polymers were reported relative to monodisperse polystyrene standards.

4.2.3 Synthesis of trivinyl monomers

4.2.3.1 Synthesis of trimethylolpropane mono methacrylate (TMPMA)

In a 250 ml round bottom flask 13.48 g (0.1 moles) trimethylolpropane was dissolved in 100 ml dry tetrahydrofuran to which 10.06 g (0.1 moles) triethyl amine was added. The reaction mixture was cooled to 0 °C in ice bath. 10.453 g (0.1 moles) methacryloyl chloride dissolved in 20 ml dry tetrahydrofuran was added dropwise

over 1 hour with constant stirring under nitrogen atmosphere. The reaction mixture was stirred for another 6 hours. The hydrochloride salt formed was separated by filtration. The residue was washed with excess of tetrahydrofuran. The filtrate was concentrated under vacuum at 35 °C and the monomer was purified by column chromatography using ethyl acetate and pet ether as mobile phase. The structure of the trimethylolpropane monomethacrylate was confirmed by ^{1}H NMR spectroscopy. 5.93 g pure trimethylolpropane monomethacrylate was obtained (yield 29.28 %).

4.2.3.2 Synthesis of trimethylolpropane monomethacrylate diacrylate (TMPMADA)

In a 250 ml round bottom flask 5 g (2.5×10^{-2} moles) trimethylolpropane monomethacrylate was dissolved in 80 ml dry tetrahydrofuran and 6.18 g (6.14×10^{-2} moles) triethyl amine was added. The reaction mixture was cooled to 0 °C in ice bath and 5.55 g (6.14×10^{-2} moles) acryloyl chloride in 20 ml dry tetrahydrofuran was added dropwise over 1 hour. The reaction mixture was further stirred for another 6 hours under nitrogen atmosphere. The hydrochloride salt formed was separated by filtration. The residue was washed with excess of tetrahydrofuran. The filtrate was concentrated under vacuum and monomer was purified by column chromatography using ethyl acetate and pet ether as mobile phase. The structure of the TMPMADA was confirmed by ^{1}H NMR spectroscopy. 4.65 g pure trimethylolpropane monomethacrylate diacrylate was obtained (yield 60%).

^{1}H NMR ($CDCl_3$), 6.45 ppm (2H, alkene proton cis and β to –OCO-), 6.13 ppm (1H, disubstituted alkene proton cis and β to-OCO-), 5.89 ppm (2H, alkene protons trans and α to-OCO-), 5.59 ppm (1H, disubstituted alkene proton trans and β to-OCO-), 0.94 ppm (3H, -CH_2-C$\underline{H}_3$), 1.99 ppm (2H,CH_3-C$\underline{H}_2$-), 1.94 ppm (3H, methyl group attached to quaternary carbon), 4.18 ppm (2H, CH_2-OCO-),

^{13}C NMR ($CDCl_3$) 7.3 ppm (H_3C-CH_2-), 18.1 ppm ($H_3\underline{C}$-C=CH_2-), 23.2 ppm (-$\underline{C}H_2$-CH_3), 40.8 ppm ($\underline{C}$-(CH_2-O-)4), 64 ppm (-$\underline{C}H_2$-OCO-), 125.9 ppm (CH_2=$\underline{C}$-CH_3), 127.8 ppm ($C\underline{H}_2$=CH-COO-) 131.2 ppm (CH_2=$\underline{CH}$-COO-), 135.8 ppm ($C\underline{H}_2$=C-CH_3) 165.7 ppm O=$\underline{C}$-O- of acrylate 166.8 ppm O=$\underline{C}$-O- of methacrylate

4.2.3.3. Synthesis of trimethylolpropane allyl ether diacrylate (TMPAEDA)

In a 250 ml round bottom flask 6.97 g (4.0×10^{-2} moles) trimethylolpropane allyl

ether was dissolved in 100 ml dry tetrahydrofuran and 10.06 g (0.1 moles) triethyl amine was added. The reaction mixture was cooled to 0 ℃ in ice bath. 9.05 g (0.1 moles) acryloyl chloride dissolved in 20 ml dry tetrahydrofuran was added in dropwise manner over 1 hour with constant stirring under nitrogen atmosphere. The reaction mixture was stirred for another 6 hours. The hydrochloride salt formed was separated by filtration. The salt residue was washed with excess of tetrahydrofuran and combined filtrate was concentrated under vacuum. Monomer was purified using column chromatography using ethyl acetate and pet ether as mobile phase. 5.2 g pure trimethylolpropane allyl ether diacrylate was obtained (Yield 44.82 %). The structure of the TMPAEDA was confirmed by ^{1}H NMR spectroscopy.

^{1}H NMR,0.89 ppm (3H, -CH_2-$\underline{C}H_3$), 1.5 ppm (2H, CH_3-$C\underline{H}_2$-), 3.36 ppm (2H, C-$C\underline{H}_2$-O-), 3.92 ppm (2H, vinyl $C\underline{H}_2$), 4.15 ppm (4H, -CH_2-OCO-) 5.19 ppm (2H, $C\underline{H}_2$=CH-), 5.86 ppm (3H, CH_2=C$\underline{H}$-), 6.13 ppm (2H, $\underline{CH}_2$=CH- β and cis to –COO-), 6.36 ppm (2H, $\underline{CH}_2$=CH- β and trans to-COO-)

^{13}C NMR ,7.4 ppm ($\underline{C}H_3$-CH_2-), 22.98 ppm (CH_3-$\underline{C}H_2$-), 41.5 ppm (quaternary carbon attached to -$\underline{C}H_2$-O-), 64.54 ppm (-$\underline{C}H_2$-O- of acrylate group), 69.68 ppm ($\underline{C}H_2$-O- attached to quaternary carbon), 72.23 ppm (-$\underline{C}H_2$-O- allylic), 116.67 ppm (-CH_2=$\underline{C}$H- of vinyl ether), 128.21 ppm (CH_2=$\underline{C}$H- of acrylate), 130.74 ppm ($\underline{C}H_2$=CH- of acrylate), 134.59 ppm ($\underline{C}H_2$=CH-of vinyl ether),165.86 ppm (-$\underline{C}$OO- of acrylate).

4.2.3.4 Synthesis of Cyclohexanedimethanol diacrylate (CHDMDA)

CHDMDA was synthesized by condensation of cyclohexanedimethanol with acryloyl chloride by synthetic methodology described in previous sections. Monomer was characterized using ^{1}H NMR spectroscopy. Peaks in the range 5.8 to 6.5 ppm confirm the diacrylate formation.

4.2.4 Polymer synthesis

4.2.4.1 Synthesis of branched SCPBAEs

Synthesis of poly (TMPTA-Co-Pz)

Synthetic methodology reported by Lynn et. al. (2002) was followed. Briefly, in a 100 ml jacketed reactor 2.96 g (0.01 moles), trimethylolpropane triacrylate was dissolved in 60 ml chloroform. 0.86 g (0.01 moles) piperazine was first dissolved in 20 ml chloroform and added dropwise to the acrylate solution with constant stirring at 53 °C. The reaction mixture was maintained at this temperature for 5 days. It was then cooled to room temperature and extracted thrice with aqueous brine solution. The organic layer was dried over night on anhydrous sodium sulphate. Chloroform was evaporated under reduced pressure. The polymer was precipitated twice in pet ether, and vacuum dried prior to analysis. Poly (TMPTA-Co-Pz) was characterized using ^{1}H NMR and FTIR spectroscopy.

IR spectra showed peak at 1636 cm^{-1} which indicates presence of free acrylate group. In ^{1}H NMR, peaks in the range 5.8 to 6.5 ppm confirm the presence of free acrylate groups. Same procedure was used to synthesize Poly (TMPTA-Co-TMDP), Poly (PETA-Co-Pz) and Poly (PETA-Co-TMDP).

4.2.4.2 Synthesis of linear SCPBAEs

i. Synthesis of poly (TMPMADA- Co-TMDP)

3.00 g, (0.01 mole) Trimethylolpropane monomethacrylate diacrylate was dissolved in 40 ml dry methylene chloride in a 100 ml round bottom flask and 33 mg $AlCl_3$ was added. 2.10 g (0.01 mole) 4, 4'-trimethylenedipiperidine dissolved in 10 ml dry methylene chloride was added dropwise to the acrylate solution with constant stirring at 5-10 °C. The reaction mixture was maintained at room temperature for 16 hours. Methylene chloride was first evaporated under reduced pressure and the polymer was then reprecipitated twice in pet ether and vacuum dried. The polymer was characterized by ^{1}H NMR and IR spectroscopy to confirm the presence of unsaturation. In IR spectrum peak at 1638 cm^{-1} indicates presence of free methacrylate group**.**

^{1}H NMR (200 MHz, $CDCl_3$) ppm

Peak at 0.90 ppm is attributed to 3 protons of -CH_2-$\underline{CH_3}$, peak at 1.0- 1.35 ppm is attributed to 12 protons of –$\underline{CH_2}$-, peaks at 1.43 -1.77 ppm correspond to 6 protons of TMDP -$\underline{CH_2}$-, peak at 1.98 ppm corresponds to 3 protons of CH_2=C-$\underline{CH_3}$, peak at 2.44 – 3.00 ppm corresponds to 12 protons of -N-$\underline{CH_2}$, peak at 3.97-4.18 ppm corresponds to 6 protons of –O-$\underline{CH_2}$, peaks at 5.58 and 6.09 ppm correspond to 2 protons of $\underline{CH_2}$=C-CH_3.

FTIR spectrum of polymer peak at 1638 cm^{-1} indicates presence of free methacrylate group.

ii. Synthesis of poly (trimethylolpropane allyl ether diacrylate-Co-4,4'-trimethylene dipiperidene)

Polymer was synthesized according to the procedure reported for the synthesis of poly (trimethylolpropane monomethacrylate diacrylate- Co- 4,4'-trimethylenedipiperidine). IR spectrum shows peak at 1644 cm^{-1} which confirms the presence of free allyl group.

4.2.5 Polymers containing varying extents of pendant vinyl groups

Polymers containing varying ratios of pendant acrylate, methacrylate and ally ether groups were synthesized by using synthetic methodology discussed in earlier sections. Secondary bifunctional amines were reacted with stoichiometric amounts of acrylate monomers containing mixture of triacrylate and diacrylate. Polymers synthesized using varying ratios of triacrylate and diacrylate mixtures are listed in table 4.5 and 4.6. These polymers were characterized using NMR spectroscopy for composition and to calculate the extent of pendant functionality.

4.2.6 Synthesis of crosslinked polymer film using photo initiator

Polymer and 1 wt % (1-hydroxy cyclohexyl phenyl ketone) photo-initiator were dissolved in methylene chloride. The polymer solution with photo-initiator was poured in to petri-dish to facilitate solvent evaporation. The viscous polymer layer formed after solvent evaporation was subjected to UV irradiation (8.2 X 10^{-6} MW/cm^2, UV-plate making machine, Lamba making system, Mumbai,) for 15 min to yield crosslinked polymer film. The crosslinked polymers were characterized by FTIR

spectroscopy to monitor the conversion of double bond into crosslinked network. These crosslinked films were insoluble in organic solvents such as dimethyl formamide, dimethyl sulfoxide, acetone, tetrahydrofuran, alcohols, ethyl acetate chloroform and dichloromethane. The crosslinked polymers were characterized by IR spectroscopy.

4.2.7 Optimization of UV curing time

UV curing behavior of the copolymers was monitored using FTIR spectroscopy. A drop of polymer solution in methylene chloride containing 1 wt % (1-hydroxy cyclohexyl phenyl ketone) as photointiator was poured on KBr cell. After complete evaporation of the solvent, the viscous polymer layer was exposed to UV light upto 30 min. IR spectra of the cured polymer film at different time intervals were recorded. The results are discussed in the subsequent section.

4.2.8 Gel content

The gel content of crosslinked networks was determined by placing crosslinked polymer discs in methylene chloride overnight (Brey et. al. 2008[a]). After drying the polymer disc under vacuum until constant weight, the gel content was calculated using following equation.

% gel content = [Final weight of sample / Initial weight of sample] × 100

4.2.9 Degradation of crosslinked polymer film by weight loss at pH 7.4

The degradation characteristics of polymer films were evaluated by measuring the weight loss with respect to time. Weighed polymer films were immersed in phosphate buffer of pH 7.4 at 37 °C. Samples were removed periodically, dried in a vacuum desiccator and then weighed to determine the weight loss **(**Yin et. al. 2007, Brey et. al. 2008[a]**).**

4.3 Polymer characterization

4.3.1 ^{1}H NMR spectroscopy

^{1}H NMR (MSL 300 MHz) spectrum of polymers was recorded on Bruker (Bruker, Karlsurhe, Germany) spectrometer and $CDCl_3$ (Aldrich) was used as a solvent. All

chemical shift values are given in parts per million (ppm) and are in reference with respect to residual proton signal from solvent.

4.3.2 FTIR spectroscopy

Polymer solution in DCM was applied on KBr cell. The solvent was evaporated and IR spectrum of the polymer was recorded on Perkin Elmer, Spectrum-One.

4.3.3 Intrinsic viscosity measurements

The intrinsic viscosity of polymer solutions in THF was measured at 25 °C using Ubbelohde capillary viscometer.

4.3.4 Gel permeation chromatography (GPC)

Gel Permeation Chromatography was used to evaluate molecular weights of the uncrosslinked polymers synthesized. GPC was carried out using waters 590 programmable HPLC pump, injector with a 100 µl injector loop and four columns in series (500 A^0 to 105 A^0, 300 X 7.5 mm, Waters, Milford MA). THF was used as eluent at a flow rate of 1ml/min. All samples were analyzed at room temperature. Data were collected using a differential refractometer (waters 410) and processed using the Ezychrome software package. The molecular weights and polydipersity of the polymers were reported relative to polystyrene standards.

4.3.5 Differential scanning calorimetry (DSC)

DSC measurements were performed under nitrogen at a flow rate of 50 ml min^{-1}on TA Instruments; model Q-10 (Newcastle, DE, USA). Polymer sample (3 to 5 mg) was heated from -70 to 50 °C for uncrosslinked viscous polymers and -70 to 250 °C for crosslinked polymers at 10 °C min^{-1} and scanned to calculate the glass transition temperature (T_g) of the polymer in subsequent heating cycles. Three temperature cycles were run for each polymer and T_g was calculated in second heating cycle. All the data were analyzed using TA Universal Analysis 2000 software package.

4.4 Results and discussion

4.4.1 Trivinyl monomer synthesis

Different types of trivinyl monomers were selected for the synthesis of either linear

SCPBAE's or branched SCPBAE's. The commercially available triacrylates for example TMPTA and PETA were selected to synthesize branched SCPBAE as reactivities of all three acrylate groups are identical. Two trivinyl monomers TMPMADA and TMPAEDA were synthesized where out of the three vinyl groups, methacrylate and allyl ether groups are weak Michael acceptors (Fansler et. al. 2007[a,b]). These trivinyl monomers behaved as bi-functional monomer during Michael addition when polymerized with the bi-functional amine. Synthetic methodology for these monomers is shown in figures 4.4, 4.5 and 4.6.

i. Synthesis of trimethylolpropane monomethacrylate diacrylate (TMPMADA)

TMPMADA monomer was synthesized in two steps,

a. Synthesis of trimethylolpropane mono methacrylate

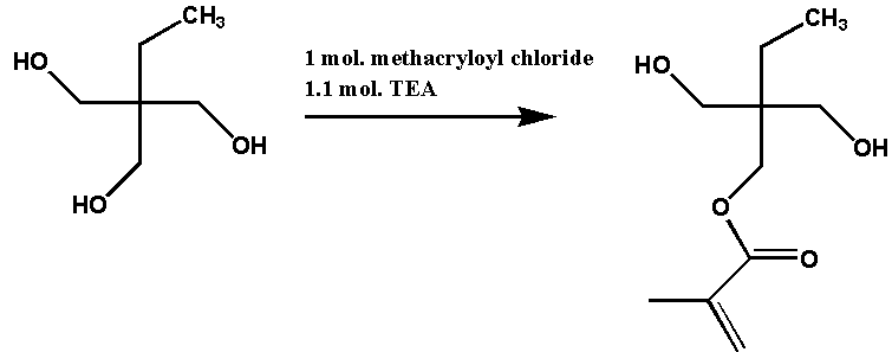

Figure 4.4: Trimethylolpropane monomethacrylate (TMPMA) synthesis

b. Synthesis of trimethylolpropane monomethacrylate diacrylate

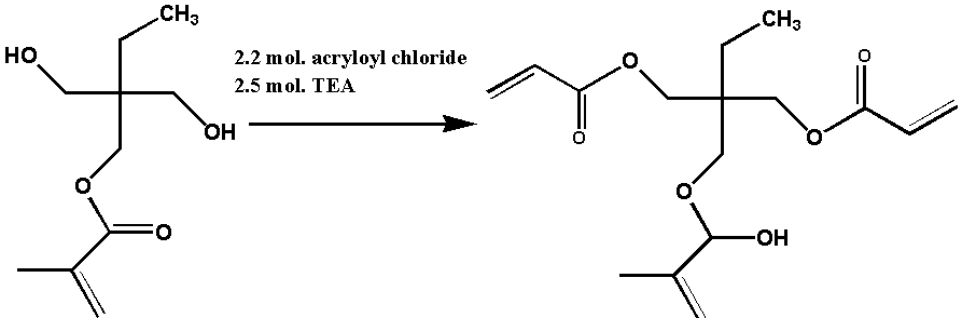

Figure 4.5: Trimethylolpropane monomethacrylate diacrylate (TMPMADA) synthesis

ii. Synthesis of trimethylolpropane allyl ether diacrylate (TMPAEDA)

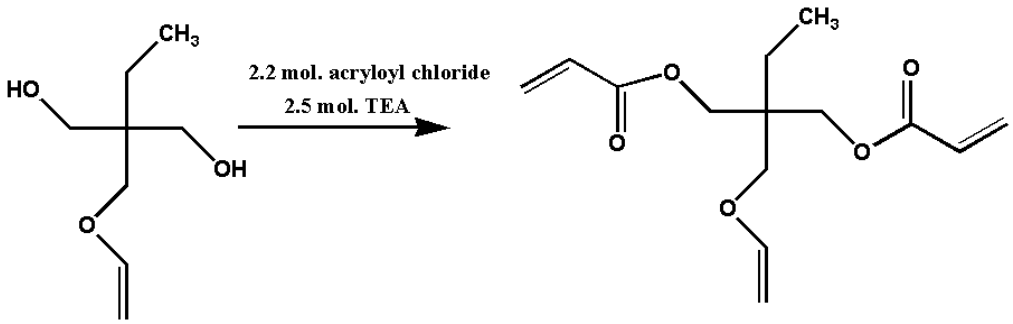

Figure 4.6: Trimethylolpropane allyl ether diacrylate (TMPAEDA) synthesis

4.4.2 Polymer synthesis

Polymers to be used for the fabrication of biodegradable scaffolds by UV-microembossing need to be a) biodegradable and biocompatible, b) liquid to closely replicate microcavities of the parent mold and c) contain functionality necessary for lithographic processing (He and Park 2005). Liquid photopatternable branched PBAE's were prepared by bulk polycondensation. Varying proportions of triacrylate (PETA) were added during condensation of diacrylate and amine to yield solvent soluble branched network. At higher diacrylate to triacrylate ratio (85:15) reaction resulted in gelation (Brey et. al. 2008[b]). This synthesis methodology is similar to the direct condensation of A_3 (triacrylate) and B_2 (amine) system reported by Guo et. al. (2006) who reported that polymerization leads to crosslinking. However if same polymerization were to be carried out by maintaining total monomer concentration less than 10 wt %, a soluble product was reported (Tang et. al. 2005). We therefore synthesized liquid, solvent soluble polymers containing pendant acrylate groups via condensation of triacrylate with amines at concentration lower than 10 wt %.

Three approaches were pursued to synthesize sequentially crosslinkable poly (β-amino esters) (SCPBAE's).

i. Branched poly (β-amino esters)

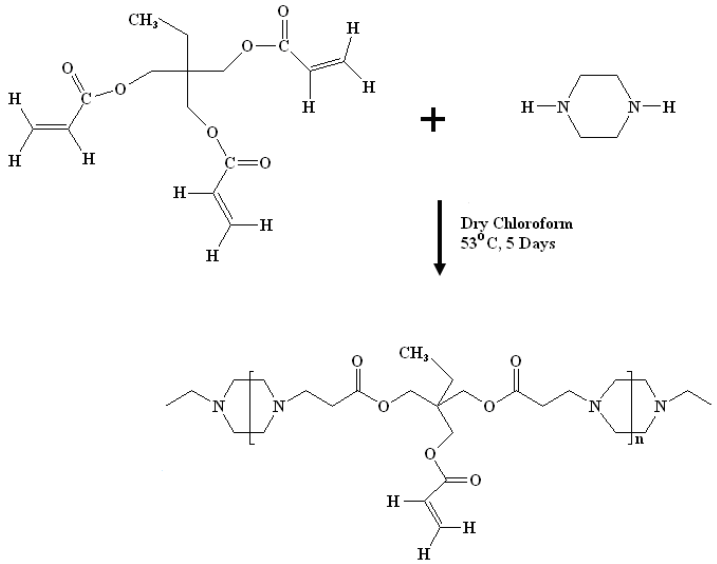

Figure 4.7: Synthesis of poly (TMPTA-Co-Pz)

In the first approach trimethylolpropane triacrylate (TMPTA) and pentaerythritol triacrylate (PETA) were selected for polymerization. These monomers bear three acrylate groups having identical reactivity towards Michael addition with amines which would yield branched polymers. Schematic of polymerization reaction is shown in figure 4.7.

Branched uncrosslinked polymers are desirable for tissue engineering applications, as they help increase adhesion and spreading of Osteoblast cell as it significantly decreases sol fraction of the crosslinked polymers (Brey et. al. 2008[a]).

In the second approach, one of the acrylate groups of TMPTA was replaced by methacrylate as well as allyl ether group to yield trimethylolpropane monomethacrylate diacrylate (TMPMADA) or trimethylolpropane mono allyl ether diacrylate (TMPAEDA) respectively. Methacrylate and allyl ether groups are poor Michael acceptors and hence are not expected to participate in Michael addition polymerization, which would result in linear SCPBAEs (Fansler et. al. $2007_{a,b}$). Schematic of synthesis is shown in figure 4.8.

ii. Linear poly (β-amino esters)

a.

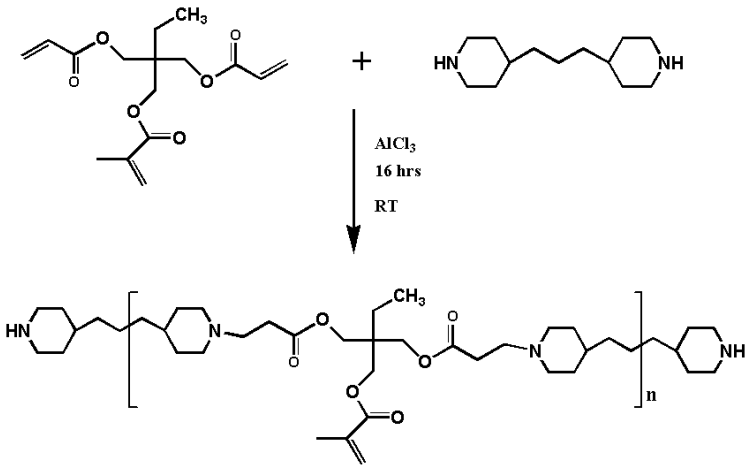

b.

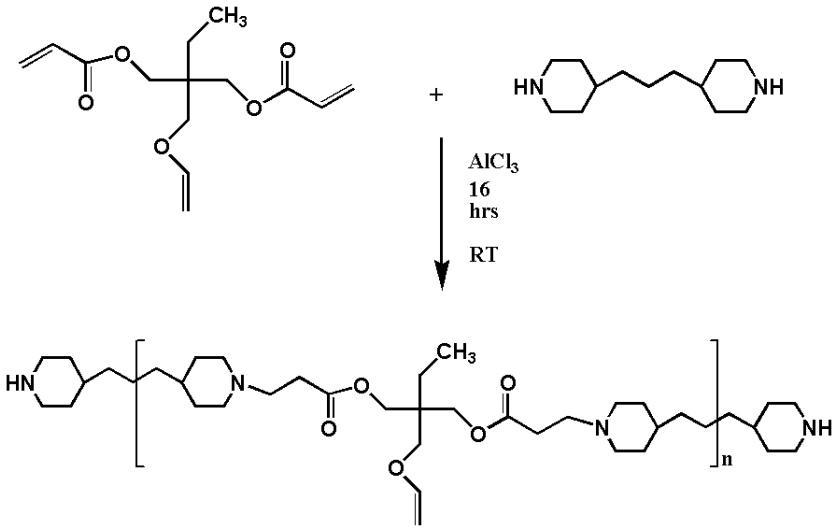

Figure 4.8: Synthesis of a) poly (TMPMADA-Co-TMDP) and b) poly (TMPAEDA-Co-TMDP)

Bulk poly condensation of diacrylates with amine at 100 ºC has been reported in the literature to reduce the reaction time to 5 hrs (Akinc et. al. 2003). However in the present case, since a triacrylate is being used, the reaction leads to crosslinking at higher temperature and monomer concentrations.

Cabral et. al. (1989) reported Lewis acid catalyzed Michael addition. The Lewis acid particularly $AlCl_3$ and $FeCl_3$ catalyze addition of amine nucleophiles to acrylates with good yield (72 to 96 %) at room temperature. For the reaction between TMPMADA and TMPAEDA with amine, we used $AlCl_3$ as the catalyst. Lewis acid first forms a

complex with carbonyl oxygen of the diacrylate ester by sharing lone pair of electrons from oxygen atom with electron deficient metal atom (figure 4.9).

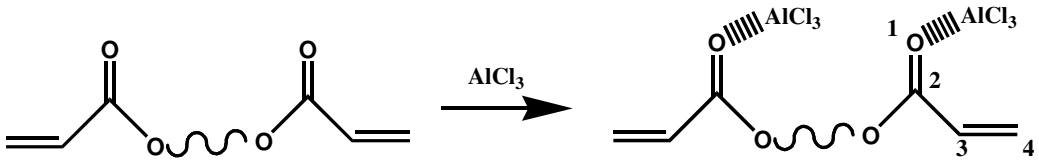

Figure 4.9: Lewis acid complex formation

This makes carbonyl group more electron deficient, which pulls electrons from π bond, in conjugation with carbonyl group and makes C-4 carbon further electron deficient. The electron deficiency at C-4 position accelerates the attack of nucleophiles. Since complex formation takes place at room temperature, the reaction can be carried out at room temperature.

iii. Poly (β-amino esters) bearing varying ratios of pendant vinyl groups

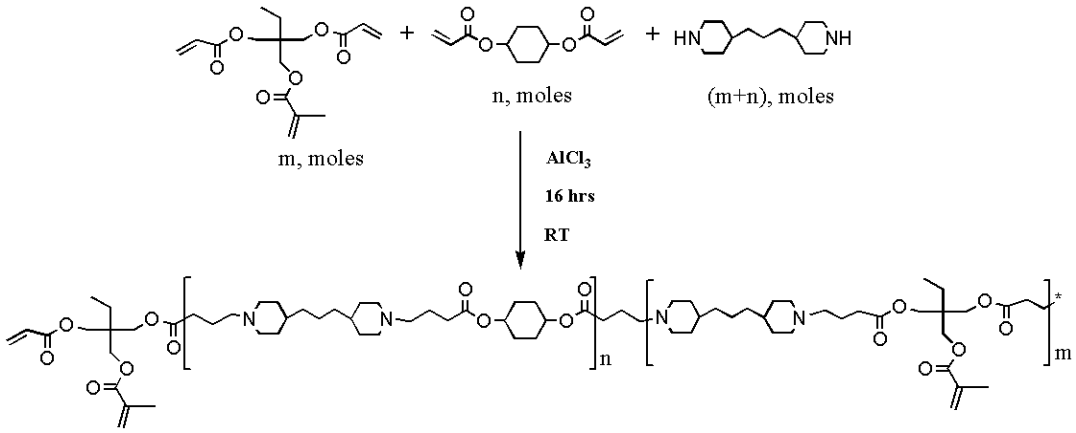

Figure 4.10: Poly (TMPMADA-Co-TMDP-Co-CHDMDA) synthesis

In the third approach mixtures of diacrylate and triacrylate in various proportions were condensed with secondary bis-amines keeping total acrylate to amine mole ratio constant (1:1). Objective was to vary of pendant vinyl functionality content in the polymer backbone as shown in figure 4.10. Polymers containing varying amount of pendant vinyl groups (50 to 5%) were synthesized (see table 4.5 and 4.6).

Table 4.5: Poly (β-amino esters) characterization

Sr. No	Polymers	Mol wt Mw	PDI	% Yield	% Gel content
P1	Poly (PETA-Co-Pz)[a]	15800	10.68	85	89
P2	Poly (PETA-Co-TMDP)[a]	21300	3.30	83	92
P3	Poly (TMPTA-Co- Pz)[a]	24695	3.14	85	94
P4	Poly (TMPTA-Co-TMDP)[a]	29267	3.18	82	93
P5	Poly (TMPAEDA-Co-TMDP)[b]	12310	1.81	74	78
P6	Poly (TMPMADA-Co-TMDP)[b]	16330	3.68	81	91
P7	Poly (TMPMADA (25%)-Co-TMDP (50%)-Co-CHDMDA (25%))[b]	15052	1.76	78	89
P8	Poly (TMPMADA (12.5%)-Co-TMDP (50%)-Co-CHDMDA (37.5%))[b]	16132	1.94	80	86
P9	Poly (TMPMADA (5%)-Co-TMDP (50%)-Co-CHDMDA (45%))[b]	18520	1.83	83	82

a. Uncatalyzed polymerization at 53°C up to 120 hrs.

b. Catalyzed polymerization at room temperature up to 16 hrs.

All polymers were isolated as clear viscous liquids at room temperature with light yellow color. These polymers were soluble in organic solvents such as tetrahydrofuran, dichloromethane, chloroform, acetone and ethanol. Polymers were stored in methylene chloride at 8-10 °C. The polymer structure and composition were confirmed using ^{1}H NMR and IR spectroscopy. GPC was used for molecular weight characterization.

The advantages of the polymers synthesized are, 1) simplicity of synthetic methodology, 2) availability of the amine and acrylate monomers on commercial scale, 3) elimination of protection and deprotection steps as polymerization proceeds via conjugate addition of amine to acrylate, 4) no byproducts formation, and 5) polymerization in the presence of functional groups such as alcohol, ester, ether and tertiary amine (Anderson et. al. 2006).

4.5 Polymer characterization

4.5.1 FTIR spectroscopy of polymers

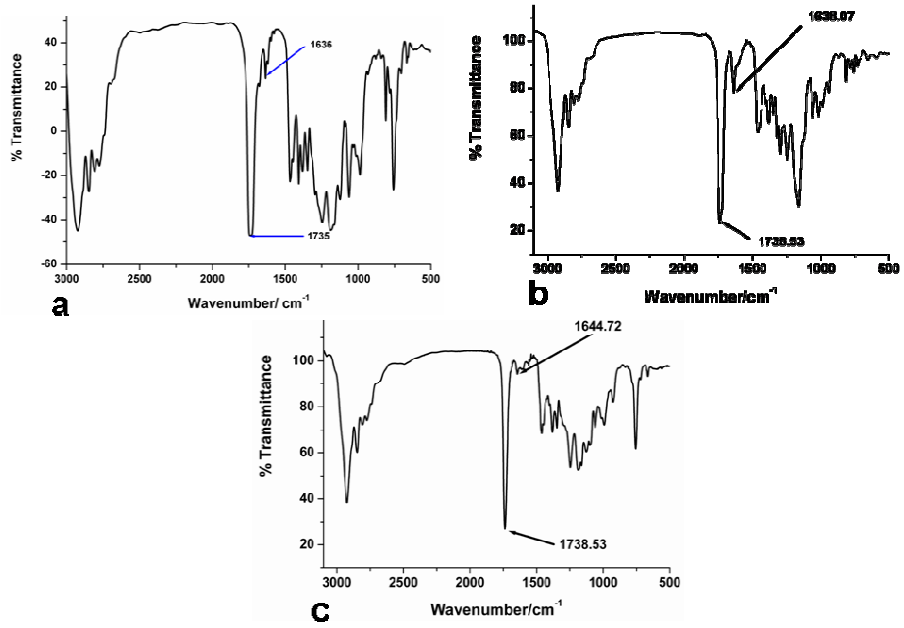

Figure 4.11: IR spectra of a. Poly (TMPTA-Co-TMDP), b. Poly (TMPMADA-Co-TMDP), c. Poly (TMPAEDA-Co-TMDP)

FTIR spectroscopy was used to confirm the presence of pendant vinyl groups in polymer backbone. IR results confirmed that both methacrylate and allyl ether groups did not participate in polymerization as they are weak Michael acceptors. Polymers synthesized were characterized using FTIR spectroscopy (figure 4.11). An absorption band in the range 1636 to 1644 cm^{-1} characteristic of vinyl groups –CH=CH_2 was observed in all cases. IR spectrum 4.11a of poly (TMPTA-Co-TMDP) showed peak at 1636 cm^{-1} corresponding to free acrylate groups. The absorption peak at 1638 cm^{-1} in spectrum 4.11b was attributed to free methacrylate groups of poly (TMPMADA-Co-TMDP). Absorption peak at 1644 cm^{-1} in spectrum 4.11c confirmed the presence of free allyl ether groups in poly (TMPAEDA-Co-TMDP). Absorption band in the region 1736 to 1738 cm^{-1} could be attributed to ester groups present in the polymer backbone. Absence of peak in the region 1680 cm^{-1} confirmed that no amide groups were present in the polymer backbone. Thus results of IR analysis confirm that polymerization proceeds through 1, 4 addition of amine and the acrylate.

4.5.2 NMR spectroscopy

The monomers and polymers synthesized were characterized using ^{1}H NMR spectroscopy. This technique was found suitable to confirm the extent of incorporation of monomers in the polymers.

4.5.2.1 NMR spectroscopy of Monomers

1. ^{1}H NMR of trimethylolpropane mono methacrylate diacrylate (TMPMADA)

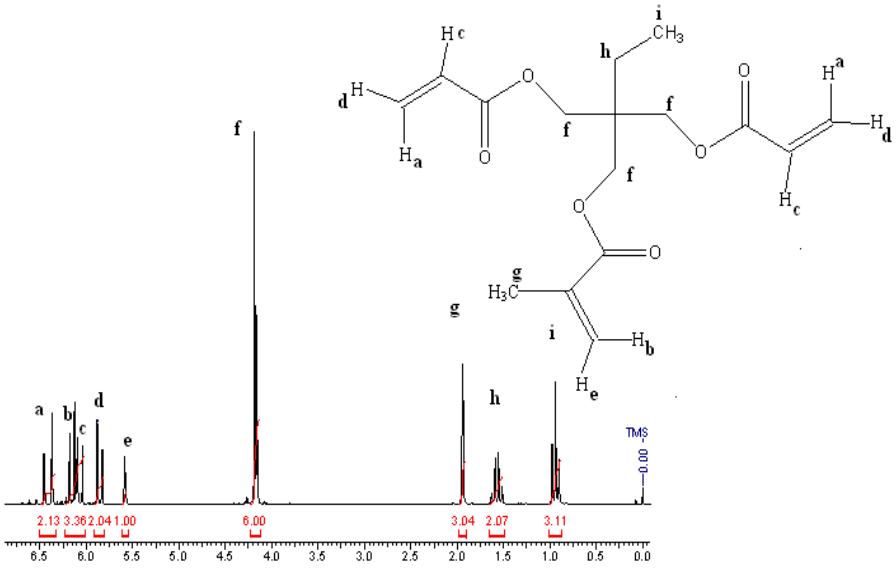

Figure 4.12: ^{1}H NMR spectrum of trimethylolpropane mono methacrylate diacrylate

6.45 ppm (2H, alkene proton cis and β to –OCO-), 6.13 ppm (1H, disubstituted alkene proton cis and β to-OCO-), 5.89 ppm (2H, alkene protons trans and α to-OCO-), 5.59 ppm (1H, disubstituted alkene proton trans and β to-OCO-), 0.94 ppm (3H, -CH_2-C<u>H</u>$_3$), 1.99 ppm (2H,CH_3-C<u>H</u>$_2$-), 1.94 ppm (3H, methyl group attached to quaternary carbon), 4.18 ppm (2H, CH_2-OCO-).

2. ^{13}C NMR of trimethylolpropane mono methacrylate diacrylate (TMPMADA)

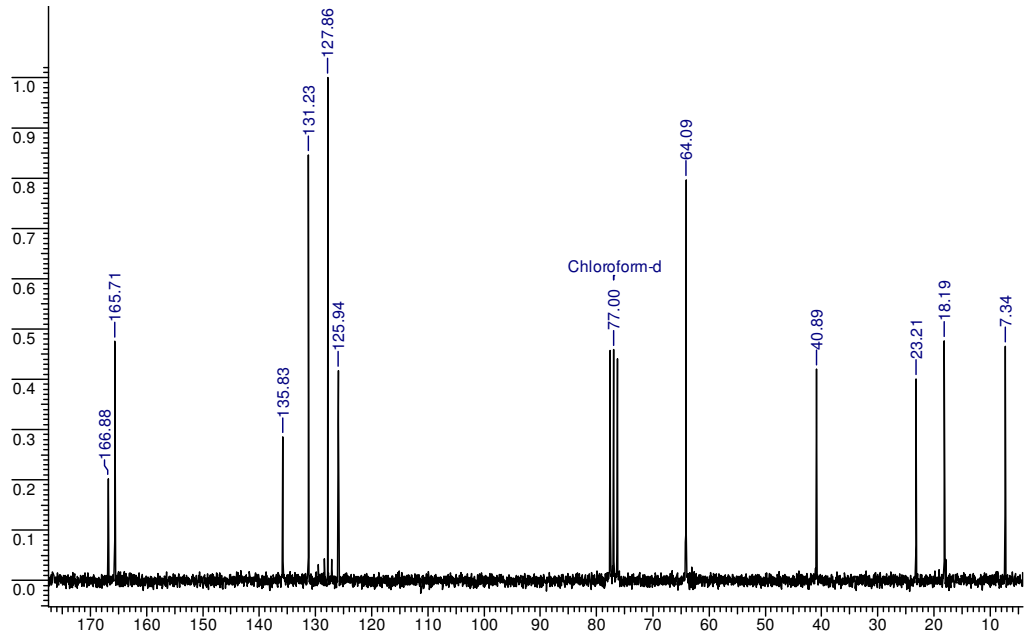

Figure 4.13: ^{13}C NMR spectrum of trimethylolpropane mono methacrylate diacrylate

^{13}C NMR ($CDCl_3$) 7.3 ppm (H_3C-CH_2-), 18.1 ppm (H_3C-C=CH_2-), 23.2 ppm (-CH_2-CH_3), 40.8 ppm (C-(CH_2-O-)4), 64 ppm (-CH_2-OCO-), 125.9 ppm (CH_2=C-CH_3), 127.8 ppm (CH_2=CH-COO-) 131.2 ppm (CH_2=CH-COO-), 135.8 ppm (CH_2=C-CH_3) 165.7 ppm O=C-O- of acrylate 166.8 ppm O=C-O- of methacrylate.

3. ^{1}H NMR of trimethylolpropane allyl ether diacrylate (TMPAEDA)

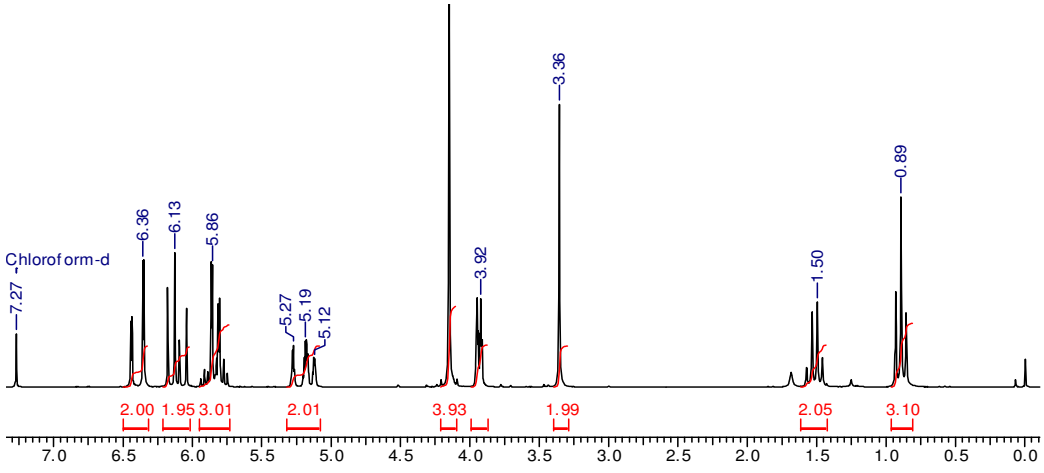

Figure 4.14: 1H NMR of trimethylolpropane allyl ether diacrylate

^{1}H NMR,0.89 ppm (3H, -CH_2-$\underline{C}H_3$), 1.5 ppm (2H, CH_3-$C\underline{H}_2$-), 3.36 ppm (2H, C-$C\underline{H}_2$-O-), 3.92 ppm (2H, vinyl $C\underline{H}_2$), 4.15 ppm (4H, -CH_2-OCO-) 5.19 ppm (2H, $C\underline{H}_2$=CH-), 5.86 ppm (3H, CH_2=C$\underline{H}$-), 6.13 ppm (2H, $\underline{CH}_2$=CH- β and cis to –COO-), 6.36 ppm (2H, $\underline{CH}_2$=CH- β and trans to-COO-)

4. ^{1}H NMR of trimethylolpropane allyl ether diacrylate (TMPAEDA)

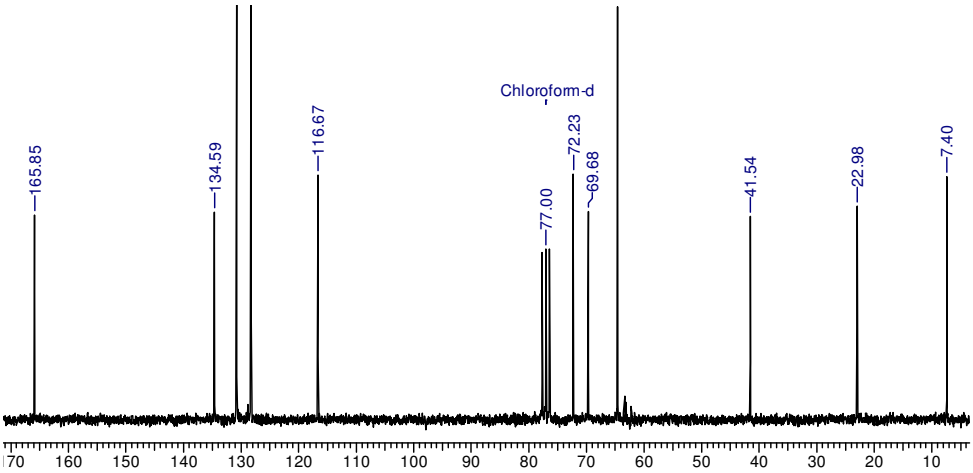

Figure 4.15: ^{13}C NMR spectrum of trimethylolpropane allyl ether diacrylate

7.4 ppm ($\underline{C}$H3-CH2-), 22.98 ppm (CH3-$\underline{C}$H2-), 41.5 ppm (quaternary carbon attached to -$\underline{C}$H2-O-), 64.54 ppm (-$\underline{C}$H2-O- of acrylate group), 69.68 ppm ($\underline{C}$H2-O- attached to quaternary carbon), 72.23 ppm (-$\underline{C}$H2-O- allylic), 116.67 ppm (-CH2=$\underline{C}$H- of vinyl ether), 128.21 ppm (CH2=$\underline{C}$H- of acrylate), 130.74 ppm ($\underline{C}$H2=CH- of acrylate), 134.59 ppm ($\underline{C}$H2=CH-of vinyl ether),165.86 ppm (-$\underline{C}$OO- of acrylate)

4.5.2.2 ^{1}H NMR spectroscopy of SCPBAE's

NMR spectroscopy technique has been extensively used for the characterization of pendant vinyl functionality in polymer chains (Anderson et. al. 2006 and Brey et. al. 2008[a, b]). The consumption of amine group and presence of pendant vinyl groups was easily demonstrated using NMR spectroscopy. The addition polymerization of the acrylate monomer and secondary amine was confirmed by appearance of 12 protons

in the range 2.22 to 2.8 ppm corresponding to newly formed two N-$(CH_2)_3$- groups. The appearance of peaks in the range 5.7 to 6.7 ppm confirms the presence of pendant vinyl functionality within polymer backbone.

1. Poly (TMPTA-Co-Pz); ^{1}H NMR

In the ^{1}H NMR (figure 4.16) of poly (TMPTA-Co-Pz), the peaks at 6.4, 6.13 and 5.75 ppm revealed the presence of pendant acrylate groups in polymer. Thus ^{1}H NMR results indicate that polymerization proceeds via 1,4 addition of amines with acrylates at a stoichiometric ratio 1:1.

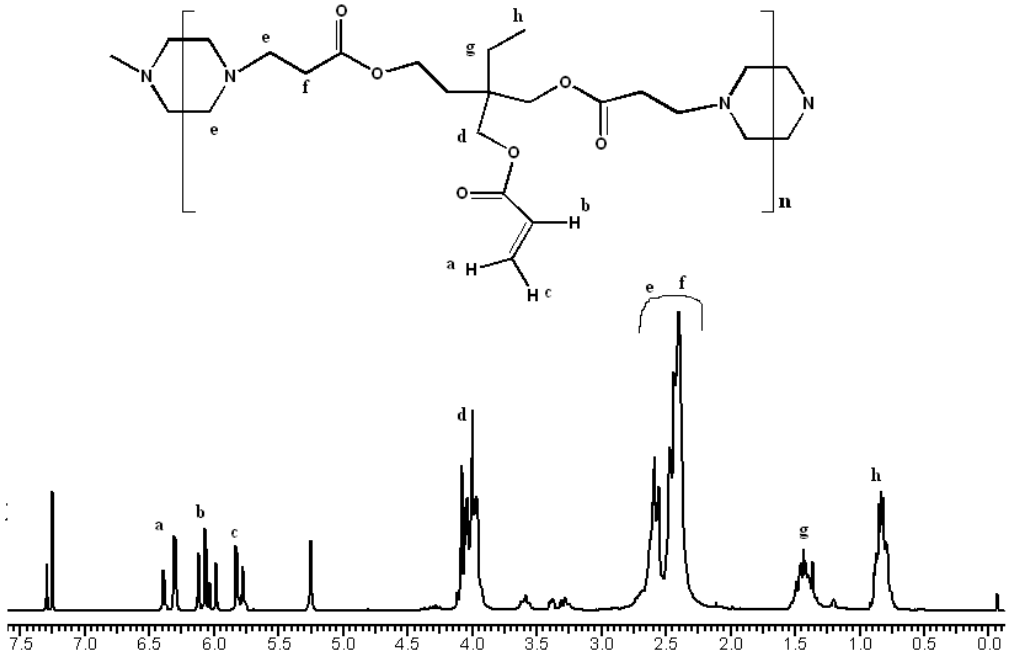

Figure 4.16: ^{1}H NMR of Poly (TMPTA-Co-Pz)

^{1}H NMR ($CDCl_3$): Peak at 0.8 ppm corresponds to -CH_2–$\underline{CH_3}$ protons; peak at 1.48 ppm corresponds to –$\underline{CH_2}$-CH_3. Peaks at 2.22-2.79 ppm correspond to 12 protons of –N-$\underline{CH_2}$ peak at 3.46-3.74 ppm corresponds to 6 protons of O=C-O-$\underline{CH_2}$-, peaks at 5.75, 6.13 and 6.4 ppm correspond to 3 protons of –$\underline{CH}$=$\underline{CH_2}$ group.

2. Poly (TMPTA-Co-TMDP); ^{1}H NMR

TMPTA was reacted with TMDP in stoichiometric proportion 1:1 to synthesize Poly (TMPTA-Co-TMDP). In the ^{1}H NMR (figure 4.17) of poly (TMPTA-Co-TMDP), the peaks at 6.4 , 6.13 and 5.75 ppm revealed the presence of pendant acrylate groups in the polymer. Thus ^{1}H NMR results indicated that polymerization proceeds via 1,4

addition of amines with acrylates in stoichiometric proportions 1:1 of groups leaving rest of the acrylate groups unreacted.

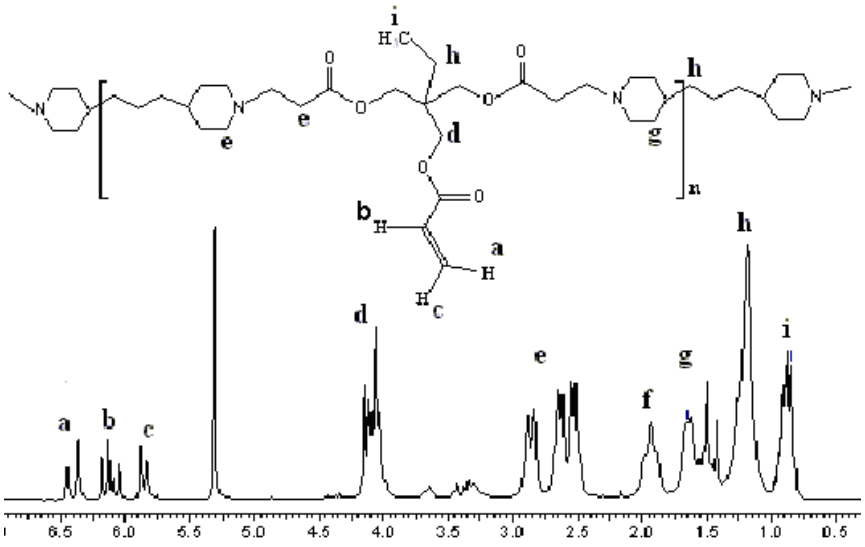

Figure 4.17: ^{1}H NMR of Poly (TMPTA-Co-TMDP)

^{1}H NMR ($CDCl_3$): Peaks in the range of 2.4-2.9 ppm correspond to 12 protons of –N-$\underline{CH_2}$; peak at 3.8 – 4.2 ppm corresponds to 6 protons of O=C-O-$\underline{CH_2}$- peaks at 5.8, 6.18 and 6.35 ppm correspond to 3 protons of –C$\underline{H}$=$\underline{CH_2}$ group.

3. Poly (TMPMADA-Co-TMDP); ^{1}H NMR

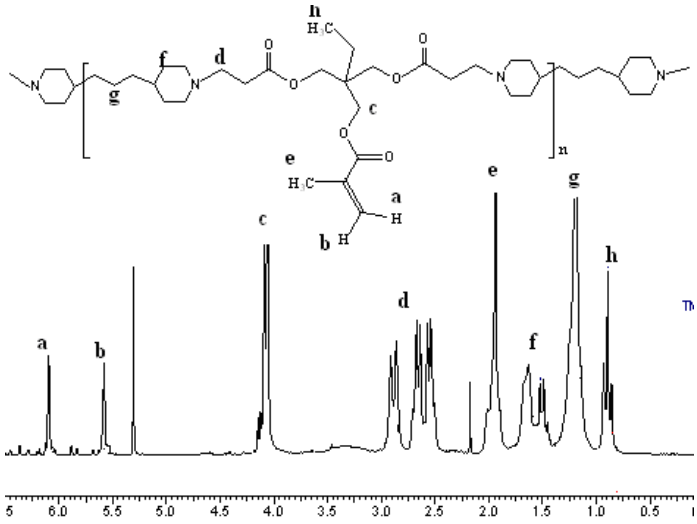

Figure 4.18: ^{1}H NMR of Poly (TMPMADA-Co-TMDP)

^{1}H NMR ($CDCl_3$): Peaks in the range 2.48-2.9 ppm correspond to 12 protons of –N-$\underline{CH_2}$. Peak at 3.8 – 4.2 ppm corresponds to 6 protons of O=C-O-$\underline{CH_2}$-; peaks at 5.6 and

6.18 ppm correspond to 2 protons of $-CCH_3=\underline{CH_2}$ group.

4. Poly (TMPAEDA-Co-TMDP); ^{1}H NMR

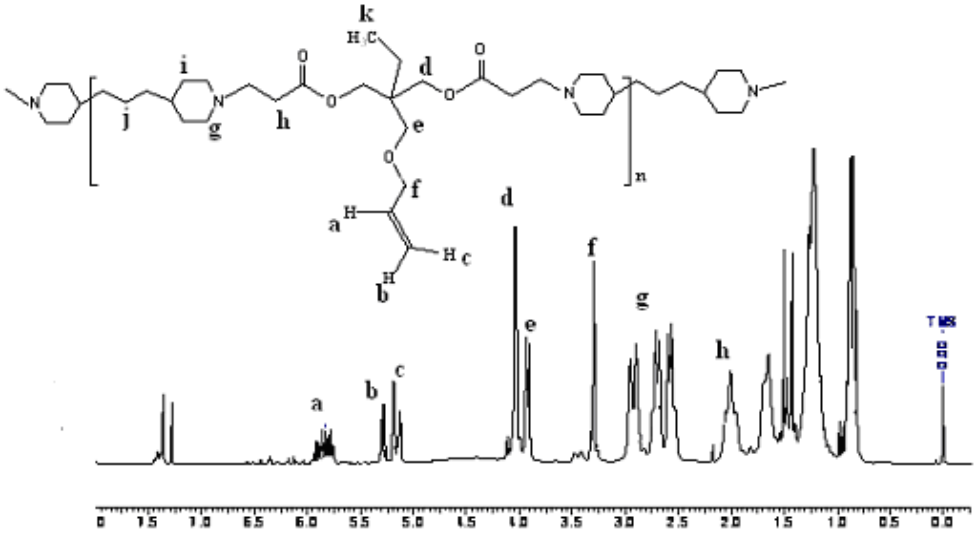

Figure 4.19: ^{1}H NMR of Poly (TMPAEDA-Co-TMDP)

^{1}H NMR ($CDCl_3$): ^{1}H NMR spectrum shows the characteristic peaks of ($C\underline{H_2}=C\underline{H}-CH_2$-O-) allyl group appeared in the range 5 to 6 ppm which confirms the incorporation of pendant allyl groups.

Results of NMR analysis further confirmed that methacrylate and allyl groups did not participate in the addition to amine.

4.5.2.3 ^{1}H NMR of SCPBAE's bearing varying ratios of pendant vinyl groups

As discussed earlier, we used a triacrylate (TMPTA), diacrylate methacrylate (TMPMADA) and diacrylate allyl ether (TMPAEDA) for condensation with amine. The extent of pendant vinyl groups in the polymer was characterized using ^{1}H NMR analysis. The results are discussed below.

Table 4.6: Percentage incorporation of pendant vinyl groups by NMR

Polymers	**In feed**	**By NMR**
Poly (TMPTA-Co-Pz)	50	50
Poly (TMPTA–Co–Pz–Co-HDDA 45 %)	05	08
Poly (TMPTA-Co–Pz–Co-HDDA 25 %)	25	25
Poly (TMPMADA (50%-Co-TMDP 50%)	50	50
Poly (TMPMADA (25%)-Co-TMDP (50%)-Co-CHDMDA (25 %)	25	27
Poly (TMPMADA (12.5%)-Co-TMDP (50%)-Co-CHDMADA (37.5%)	12.5	11
Poly (TMPMADA (5%)-Co-TMDP (50%)-Co-CHDMDA (45 %))	5	6

a. ^{1}H NMR of SCPBAE's with variation in pendant acrylate groups

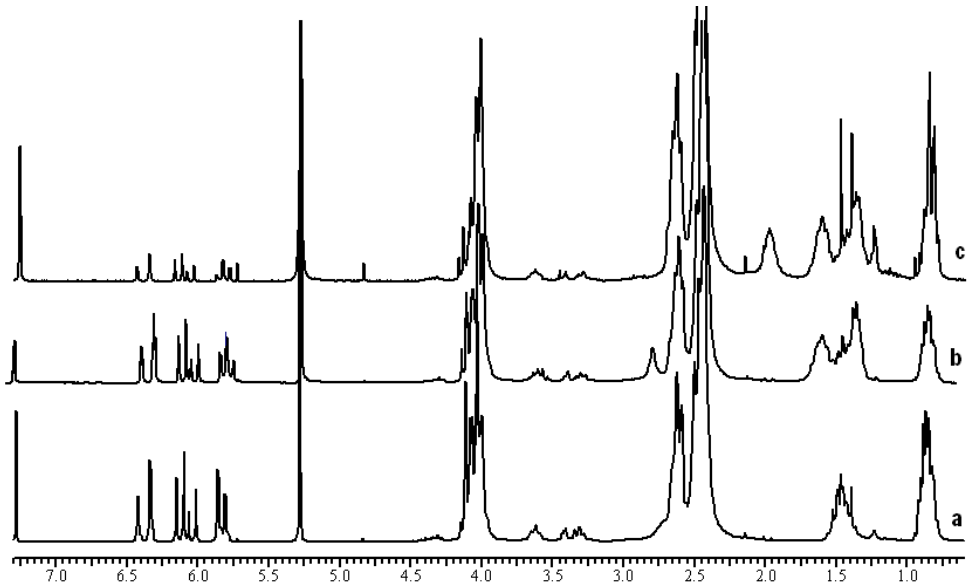

Figure 4.20: Poly(TMPTA-Co-Pz-Co-HDDA) compositions, a. 50;50:00, b. 25:50:25 and c. 5:50:45

The ^{1}H NMR results shown in figure 4.20 clearly demonstrate that pendant acrylate composition in poly (β-amino esters) can be effectively manipulated using synthetic

methodology proposed by us. In figure 4.20 spectra a, b and c corresponds to the polymers containing 25%, 12.5% and 5% TMPTA respectively. The pendant acrylate content was calculated by comparing intensity of vinylic protons at 5.7 – 6.5 ppm ($=CH_2$) of acrylate groups with intensity of methylene protons at 2.2 -2.7 ppm of TMDP attached to nitrogen atom ($-N-CH_2$). The TMDP protons were selected for comparison with acrylate groups because these protons do not interfere with other protons of polymer backbone. Also the TMDP content was constant during synthesis of polymer, varying the ratio of diacrylate to triacrylate. The pendant acrylate content calculated using ^1H NMR closely matches with actual triacrylate feed ratio (table 4.6).

b. ^1H NMR of SCPBAE's containing pendant methacrylate groups

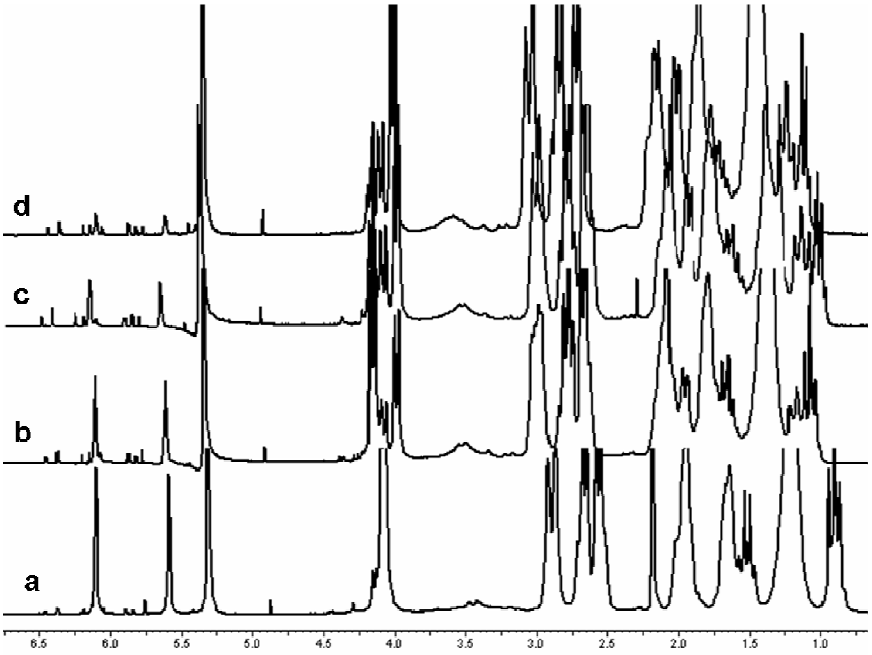

Figure 4.21: Poly (TMPMADA-Co-TMDP-Co-CHDMDA) compositions, a. 50:50:00, b. 25:50:25, c. 12.5:50:37.5 and d. 5:50:45

The ^1H NMR spectra of polymers containing varying ratios of trimethylolpropane monomethacrylate diacrylate (TMPMADA) are shown in figure 4.21. The intensity of peaks at 5.6 and 6.1 ppm which correspond to methacrylate groups, increased with TMPMADA content. The methacrylate content was estimated by comparing intensity of vinyl protons ($=CH_2$) of methacrylate with the intensity of methylene protons of TMDP attached to nitrogen atom ($-N-CH_2$). The TMDP protons were preferred for comparison as they did not interfere with any other groups in the polymer backbone.

The results in table 4.6 confirm that incorporation of methacrylate monomers in the polymers is quantitative.

4.5.2.4 Degree of branching

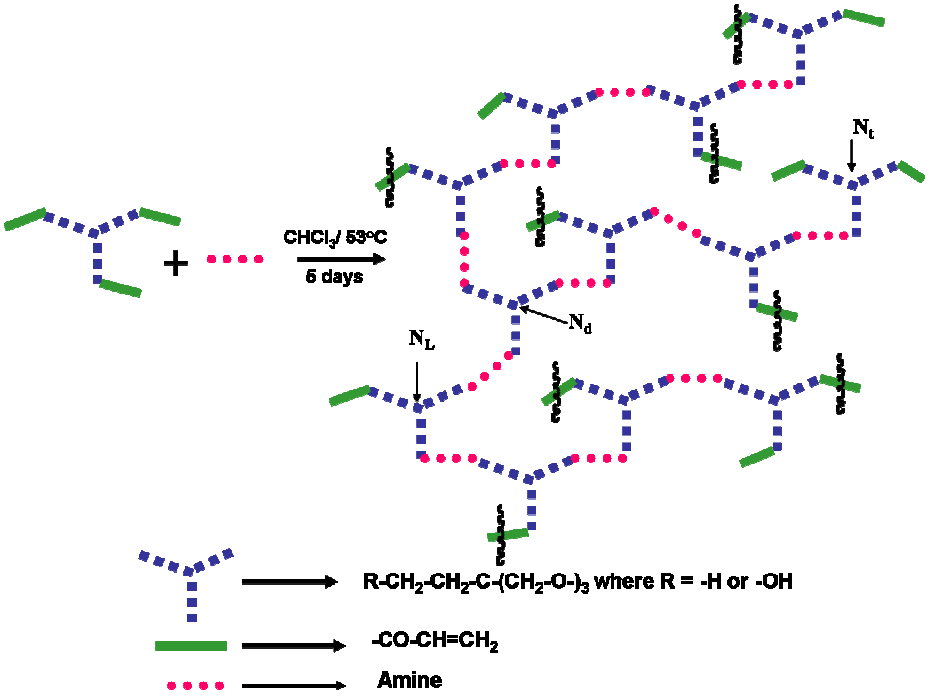

Figure 4.22: Synthesis of branched SCPBAE's containing pendant acrylate groups

The Michael addition of bi functional amine (A_2) with triacrylate (B_3) results in polymers containing three types of structural units: a) N_t - Terminal unit, b) N_L – Linear unit and c) N_d – Dendritic unit (figure 4.22). Degree of branching of the polymers synthesized using TMPTA, PETA, TMPMADA and TMPAEDA was evaluated using ^{1}H NMR spectroscopy. The peaks for the protons in $–CH_2OOC–$ at 3.95 – 4.15 ppm shift to higher values as acrylate groups react with secondary amines. In case of TMPTA and PETA all three acrylate groups have identical reactivity towards amine which leads to three structural units (N_t, N_L and N_d). ^{1}H NMR spectra of these polymers also show three peaks at 4.09 – 4.15, 4.04 – 4.08 ppm and 3.95 – 4.04 ppm attributed to the protons of terminal, linear and dendritic unit respectively (figure 4.23).

However TMPMADA and TMPAEDA behave as diacrylate and reaction with amine results in linear polymers. NMR spectrum of the polymer synthesized using

TMPMADA shows only two broad peaks at 4.10 – 4.15 ppm and 4.00 - 4.10 ppm attributed to the protons of terminal and linear repeat unit respectively. In case of polymers prepared using TMPAEDA the peaks at 3.95 – 4.06 ppm and 4.06 – 4.12 ppm correspond to the protons of terminal unit and linear repeat unit respectively. Based on the integration of the corresponding peaks of the ^{1}H NMR spectra, the content of structural units N_L, N_D and N_t was estimated (table 4.7).

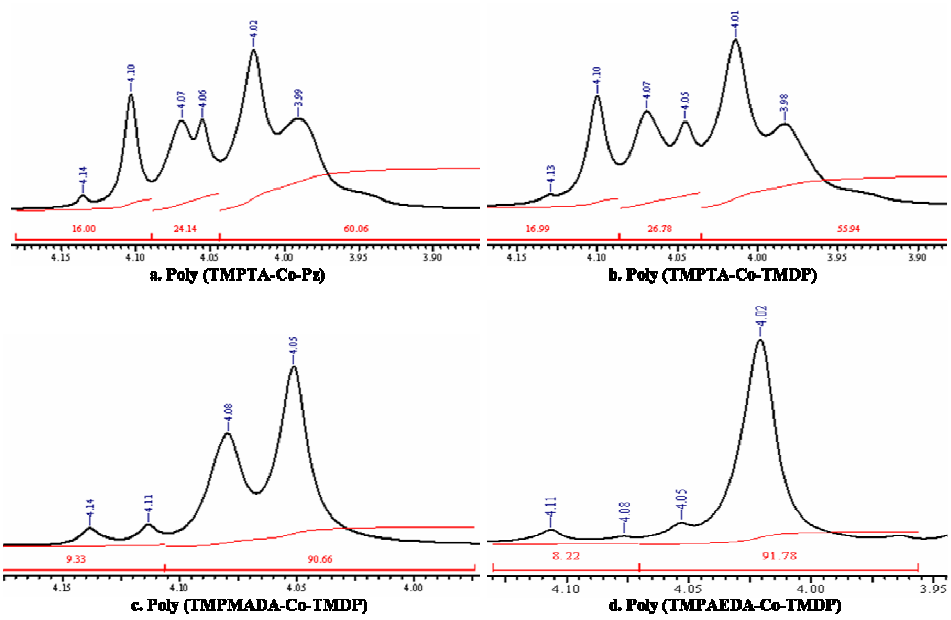

Figure 4.23: Expanded ^{1}H NMR of polymers 3.9 – 4.15 ppm

The analysis revealed that in case of Poly (TMPMADA-Co-TMDP) and Poly (TMPAEDA-Co-TMDP) the percentage of terminal –$\underline{CH_2}$OOC– groups (N_t) is low while that of linear ones (N_L) is high as compared to corresponding values in case of polymers synthesized using TMPTA and PETA acrylates. Both TMPMADA and TMPAEDA behave as diacrylate, hence most of the –$\underline{CH_2}$OOC– groups are present in the polymer backbone as polymer chain grows linearly, resulting in high N_L values and N_d values tend to zero. In case of polymers synthesized using TMPTA and PETA, branched polymers contain more terminal acrylate groups as compared to linear polymers and hence the N_t values are high. Degree of branching was calculated using Frey's equation (Tang et. al. 2005).

$DB = 2\ N_d / (N_L + 2\ N_d)$

Where, N_L – Linear unit, N_d – Dendritic unit, DB – Degree of branching

Table 4.7: Structural analysis of polymers

Polymer	**Structural unit (%)**			**DB (%)**
	N_t	**N_L**	**N_d**	
Poly (TMPTA-Co-Pz)	16	24	60	83.33
Poly (TMPTA-Co-TMDP)	17	27	56	80.57
Poly (PETA-Co-Pz)	23	26	51	79.36
Poly (TMPMADA-Co-TMDP)	9.3	90.7	0	0
Poly (TMPAEDA-Co-TMDP)	8.2	91.8	0	0

4.5.3 Molecular weight determination

The molecular weights of polymers determined by organic phase gel permeation chromatography (GPC), ranged from 12000 to 30000 with polydipersity in the range 1.81 to 10.68 (table 4.5). Very high polydispersity (7.2.) was also reported in previous investigations on PBAEs (Anderson and Langer 2004). The high polydispersity is a result of step growth polymerization. The molecular weight build-up is restricted due to intramolecular cyclization reaction between amine present on growing end of polymer chain reacts with acrylate of the other end (Akinc et. al. 2003). The presence of low molecular weight fraction is an advantage since it lowers the melt viscosity of the polymer which would help in replicating patterns with high fidelity (Brey et. al. 2008[b]).

4.5.4 Solution behavior of PBAEs

The solution properties of the polymer reflect whether it is branched, hyper branched, dendritic or linear (Sato et. al. 2004, Guan 2002).

The relationship between the reduced viscosity (η_{spe}/C) and polymer concentration for poly (TMPTA-Co-Pz) and poly (TMPAEDA-Co-TMDP) is shown in figure 4.24**.** The reduced viscosity of poly (TMPAEDA-Co-TMDP), showed dependence on polymer concentration. However for poly (TMPTA-Co-Pz) the reduced viscosity appeared to be independent of polymer concentration.

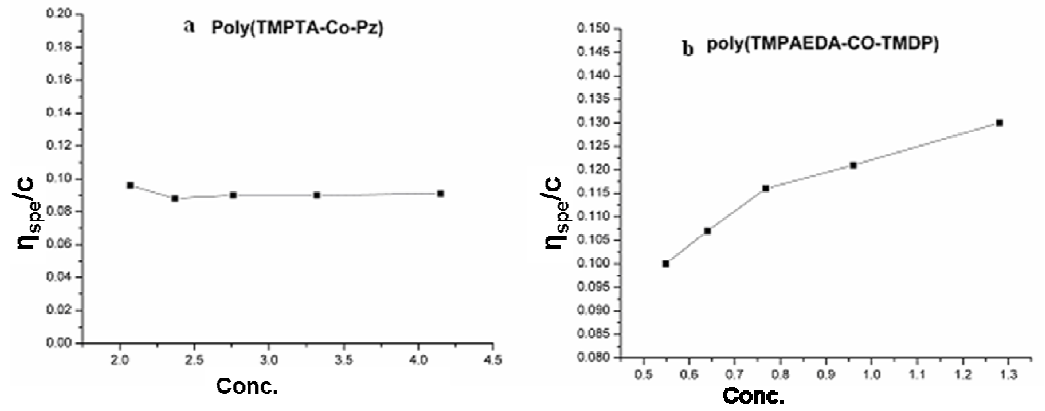

Figure 4.24: Relation between reduced viscosity and polymer concentration, poly (TMPTA-Co-Pz), b) Poly (TMPAEDA-Co-TMDP)

In poly (TMPMADA-Co-TMDP) and Poly (TMPAEDA-Co-TMDP) since the methacrylate and allyl ether groups do not react with the amine, the resulting polymers are linear (figure 4.25a). However in case of polymers synthesized from TMPTA and PETA as reactivity of all three acrylate groups are identical, branched network results (figure 4.25b). This analysis further confirms the nature of the polymer synthesized.

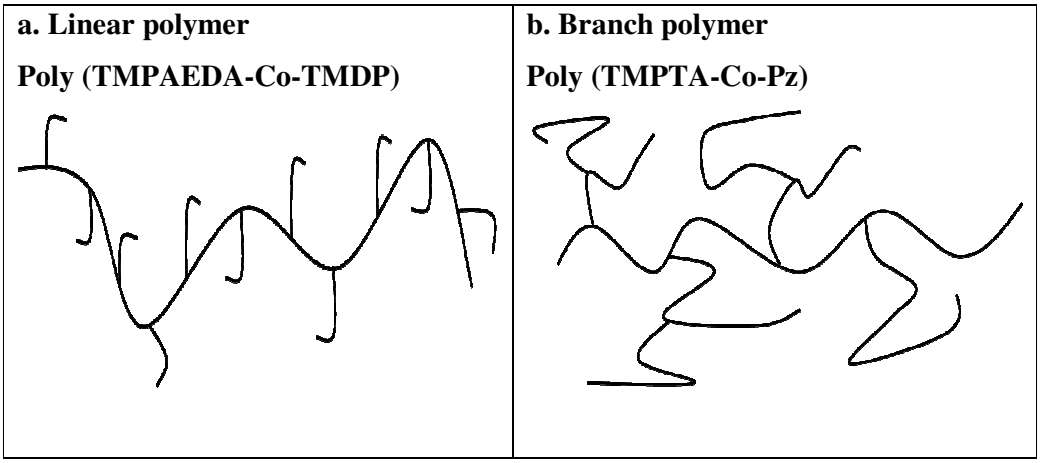

Figure 4.25: Schematic representation of a. linear and b. branch SCPBAE

4.5.5 Second stage polymerization

The pendant vinyl group of polymer can be reacted to undergo intermolecular cross-linking reactions. The cross-linking of viscous biodegradable polymers will find potential applications in soft lithography, drug delivery and tissue engineering.

4.5.6 UV curing of sequentially crosslinkable polymers

FTIR spectroscopy was used to monitor crosslinking behavior of polymers containing pendant vinyl functionality (Brey et. al. 2008[b]). Three polymers Poly (TMPTA-Co-TMDP), poly (TMPMADA-Co-TMDP) and poly (TMPAEDA-Co-TMDP) were selected as representative polymers to demonstrate photo-polymerization behavior of sequentially crosslinkable poly (β-amino ester). These polymers contain different photo polymerizable pendant groups such as acrylate, methacrylate and allyl ether groups respectively. Thin films of polymers containing photo initiator were formed on KBR cell and photo polymerized by UV irradiation of intensity 8 x 10^{-6} MW/cm^2. Polymer film was then exposed to UV radiation for 5, 10, 15, 20 and a 30 min and IR spectrum was run after every UV exposure. Change in peak intensity at 1635 cm^{-1}, 1640 cm^{-1} and 1644 cm^{-1} corresponding to acrylate (figure 4.26), methacrylate (figure 4.27) and allyl ether (figure 4.28) was followed by FTIR spectroscopy.

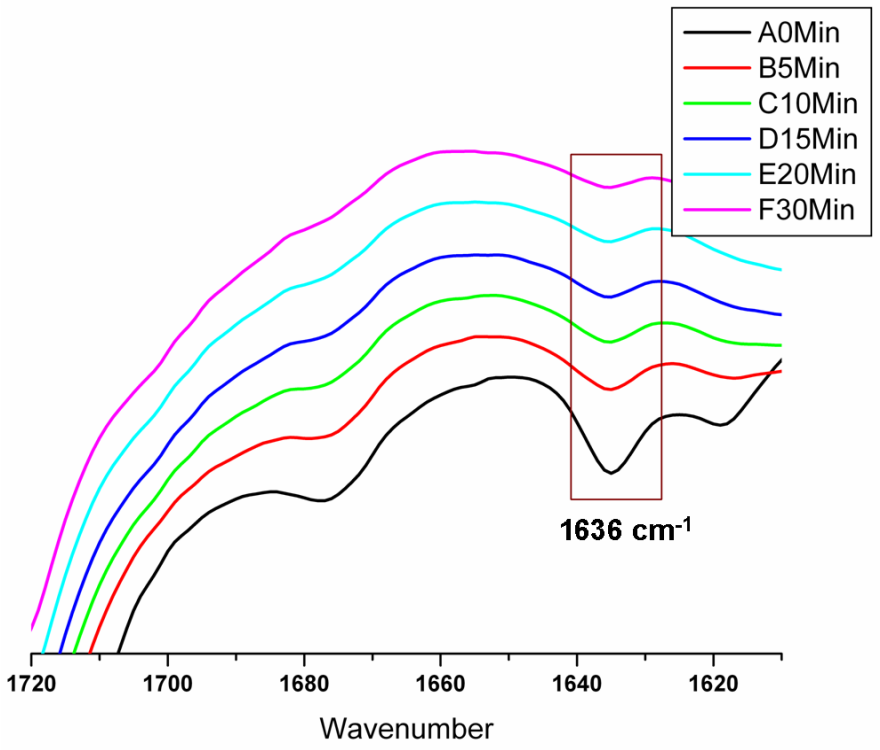

Figure 4.26: UV curing behavior of poly (TMPTA-Co-TMDP)

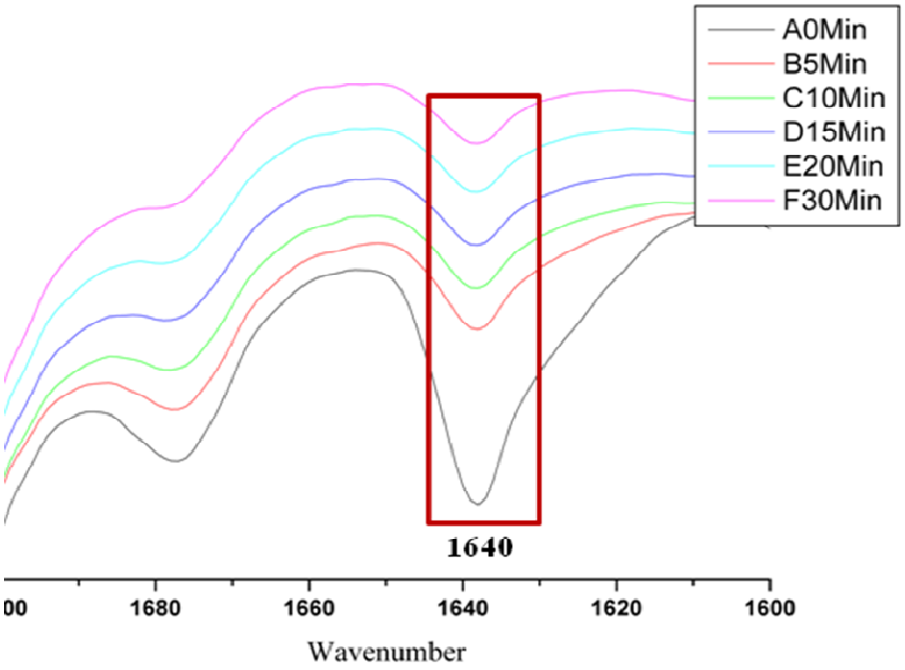

Figure 4.27: UV curing behavior of poly (TMPMADA-Co-TMDP)

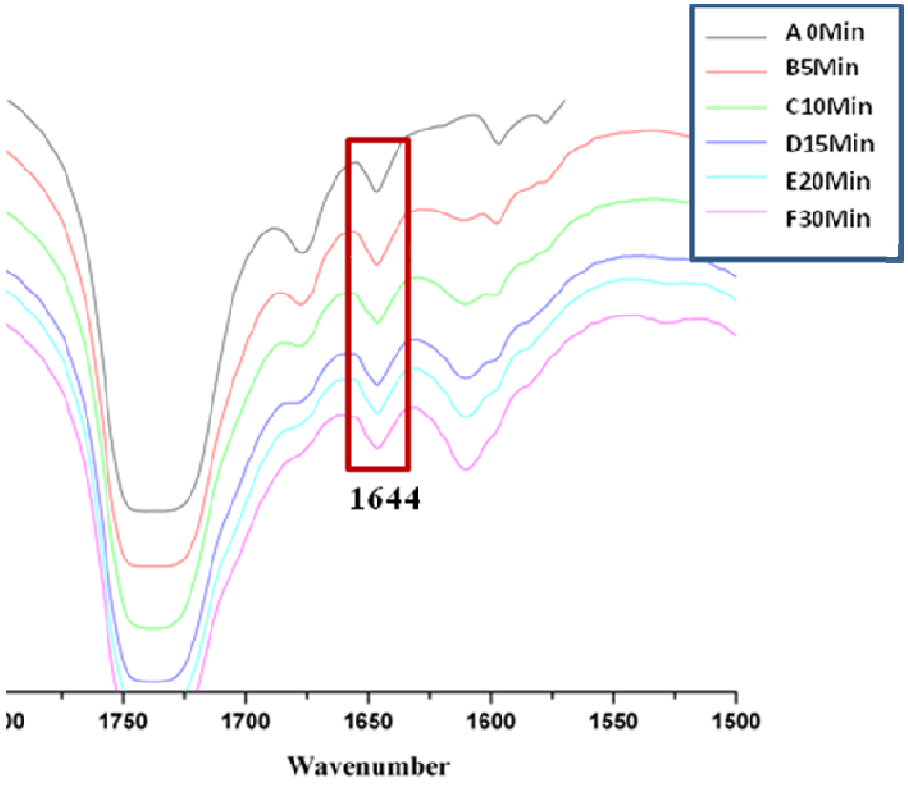

Figure 4.28: UV curing behavior of poly (TMPAEDA-Co-TMDP)

The results show that in poly (TMPAEDA-Co-TMDP) the conversion of allyl groups in to crosslinked product is lower than that in acrylate and methacrylate groups due low reactivity of allyl ether groups (Heatley et. al. 1993). The conversion of methacrylate groups is low as compared to that of acrylate groups due to difference in reactivity and linear nature of methacrylate containing polymers. Reactivity of methacrylate group is low as compared to acrylate group due to steric hindrance created by methyl moiety present on the methacrylate vinyl group (Jason 2007). In case of linear PBAES containing pendant acrylate groups, conversion is poor as compared to that in corresponding branched polymers (Brey et. al. 2008[a]). However this lower conversion of methacrylate functionality did not reflect adversely in gel content of corresponding crosslinked polymers. The sol fractions obtained in case of linear polymers (9 to 12%) are comparable to those obtained in the case of branched polymers (6 to 11 %). Curing proceeds rapidly in first 10 min and levels off after 15 mins. Hence for all subsequent curing experiments polymers were exposed to UV light for 15 min. The rate of photopolymerization can be controlled by the choice of photo-initiator, light intensity and type of double bond (Kretlow et. al. 2007). For practical lithography applications irradiation intensity, initiator type and concentration will have to be optimized so that cure time is only few seconds / minutes (Park et. al. 2004, Shen et. al. 2006). However no attempts were made to optimize curing time, since the objective of this investigation was to demonstrate the concept.

4.5.7 Gel content of crosslinked polymers

Gel content was analyzed to determine the weight fraction of insoluble polymer (table 4.5). Polymers bearing acrylate (P1 to P4) and methacrylate groups (P6 to P9) show comparable gel contents in the range 89 to 94 %. Polymers containing less reactive allyl ether groups showed lower gel content (78 %) (Heatley et. al. 1993). Copolymers were synthesized wherein the ratio of methacrylate diacrylate to diacrylate was varied from 10:90 to 100:0. The gel content decreased with decreasing methacrylate content. However the difference in gel content is less than 10 %. Gel content of the polymers synthesized in this work is higher compared to the linear counterparts reported by Brey et. al. (2008[a]), where acrylate groups are present only at the terminal end of polymer chain which lowers the availability of crosslinker in the system. These polymers exhibit lower gel content (51-77 %) when the macromer molecular weight is higher as compared to those synthesized from macromers (88-

97.8%) of lower molecular weight (table 4.4). The polymers synthesized in the present work contain vinyl groups distributed randomly across the polymer backbone and hence the conversion of polymer chains in to the crosslinked network is very high. For instance in case of polymers containing only 5 % methacrylate functionality the gel content is as high as 82%. In this study it was noticed that the gel content for the linear polymers such as Poly (TMPAEDA-Co-TMDP), Poly (TMPMADA-Co-TMDP), Poly (TMPMADA (25%)-Co-TMDP (50%)-Co-CHDMDA (25%)), Poly (TMPMADA (12.5%)-Co-TMDP (50%)-Co-CHDMDA (37.5%)) and Poly (TMPMADA (5%)-Co-TMDP (50%)-Co-CHDMDA (45%)) show gel content in the range of 78% to 91 % whereas in case of branched polymers such as Poly (PETA-Co-Pz), Poly (PETA-Co-TMDP), Poly (TMPTA-Co- Pz) and Poly (TMPTA-Co-TMDP) it is in the range 92 to 94 %. The relatively higher gel content exhibited by branched polymers is due to presence of higher number of acrylate groups at the terminal end of branched chain which increases the probability of incorporation of greater number of polymer chains within crosslinked network (Brey et. al. 2008[b]).

4.5.8 Degradation of crosslinked polymer film by weight loss at pH 7.4 PBS

The crosslinked poly (β-amino esters) undergoes degradation under physiological conditions by the hydrolysis of ester groups in the polymer backbone to yield poly (β-amino acid), diol molecules and acrylic acid oligomers (Anderson et. al. 2006).

Crosslinked polymers exhibit a range of weight loss patterns (figure 4.29). Polymers synthesized using PETA (P1 and P2) undergo 90 % weight loss within one week whereas polymers synthesized using TMPTA (P3 and P4) undergo identical weight loss over 2-4 weeks. PETA is more hydrophilic than TMPTA because of the presence of free hydroxyl groups. TMPAEDA based polymer (P5) shows 30% weight loss in first week and 90% weight loss after 12 weeks because of the presence of more stable ether groups within crosslinked network which retards the hydrolytic degradation of polymer backbone.

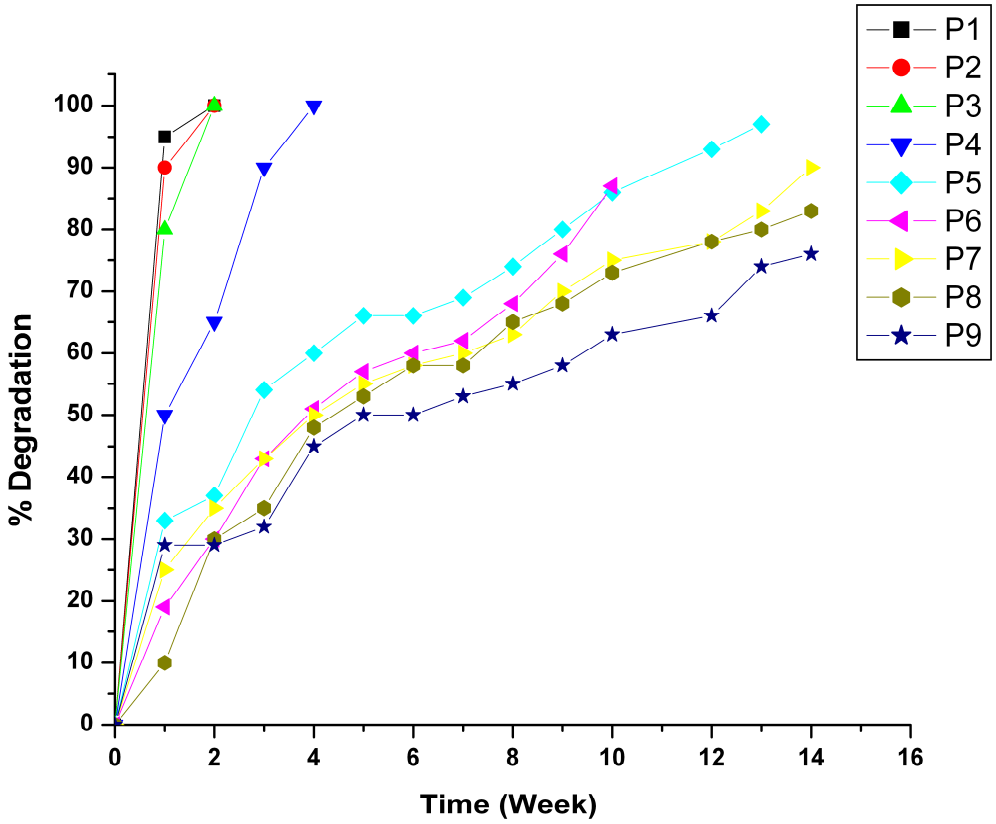

Figure 4.29: Degradation behaviors of crosslinked polymers at pH 7.4 PBS

The effect of amine hydrophobicity on polymer degradation was investigated using piperazine (Pz) and 4 4'- trimethylenedipiperidine (TMDP). TMDP contains an aliphatic spacer and has a more rigid structure as compared to Pz. The polymer synthesized using TMDP (P4) degrades completely in 4 weeks as compared to the polymer based on hydrophilic amine Pz (P3) which degrades completely in 2 weeks. Polymers synthesized using TMPMADA (P6 - P9) undergo only 10-30 % weight loss during first week and 70-80 % weight loss over 3 months. These polymers were synthesized to investigate the effect of increasing hydrophobic content and crosslink density on degradation. Jason et. al. (2007) studied the effect of hydrophobicity on the rate of polymer degradation wherein diacrylate terminated triblock PEG-PLA-PEG polymers were photo cross linked. The hydrophobicity of the polymers was manipulated by varying lactic acid content. With increase in lactide content the molecular weight and hydrophobicity of polymers increased and the acrylate functionality decreased. The acrylate terminated polymers were then crosslinked under UV irradiation. It was noticed that the hydrophobicity of polymers governs the

rate of degradation rather than the crosslink density (Jason et. al. 2007). In the present case hydrophobicity of polymer was manipulated by incorporating hydrophobic monomer (CHDMDA) and crosslink density by varying methacrylate monomer content (Example P6 - P9 in table 4.5). With increase in hydrophobic monomer (CHDMDA) content (0 to 45 %) in the polymer backbone, the methacrylate (TMPMADA) content decreased (50 to 5%). The degradation profile of these polymers revealed that as hydrophobic content of polymer increased, the degradation rate decreased in spite of decrease in the crosslink density (example P6 - P9 in figure 4.29).

These results show that hydrophobicity of the polymer backbone determines the degradation behavior of polymers whereas the pendant vinyl functionality governs crosslinking density necessary for the fabrication of micropatterns. Crosslinked poly (β-amino esters) reported by Brey et. al. (2008[a]) showed a bimodal degradation profile wherein initial mass loss was rapid since these polymers have gel content in the range 51-97.8% as compared to polymers reported herein (78-94%). Also the crosslinked polymers synthesized by Brey et. al. (2008[a]) using triethylene glycol diacrylate (J) showed rapid mass loss as compared to 1,6 -hexanediol ethoxylate diacrylate (C) and 1,6-hexanediol diacrylate (E). However the polymer J6 which is a copolymer of triethylene glycol diacrylate and 1-amino-2-methylpropane at 1.4:1 ratio showed nondegradable polymer fractions (upto 41%) even after 9 weeks. The polymers reported in this work exhibit wide distribution of mass loss which increases with time. The polymer degradation results indicate that these polymers can be useful for the applications which need to degrade over varying time spans (Brey et. al. 2008[a]).

4.6 Conclusions

In this chapter we have demonstrated the methodology for the synthesis of both linear and branched sequentially crosslinkable poly (β-amino ester). The polymers containing acrylate, methacrylate and allyl ether pendant groups were synthesized by the choice of acrylates. The degree of crosslinking was manipulated by reacting varying ratios of mixture of diacrylate and triacrylate with stoichiometric ratio (1:1) of amine. SCPBAEs synthesized in this work exhibit high polydispersity index. These polymers which were crosslinked photo-chemically at room temperature exhibited

high gel content as compared to their linear counterparts reported in literature (Brey et. al. 2008_a). The degradation results revealed that the degradation rate can be manipulated upto 3 months based on choice of monomers. The uncrosslinked polymers are liquids and also soluble in organic solvents hence can be processed using soft lithography techniques (He and Park 2005). This will be demonstrated in the subsequent chapters.

4.7 References

Akdemir Z. S., Akcakaya H., M. Kahraman V., Ceyhan T., Kayaman N., Gungor A. *Macromol. Biosci.*, **2008**, 8, 852.

Akinc A., Anderson D. G., Lynn D. M., Langer R., *Bioconjugate Chem*. **2003,** 14, 979.

Albertsson A.-C., Varma I. K. *Advances in Polymer Science*, **2002**, 157,1.

Anderson D., Langer R. US Pat Apli. No . **2004/**0071654 A1.

Angeioni A. S., Laus M., Castellari C., Galii G., Ferruti P., Chielhi E. *Makromol. Chem.*, **1985**, 186, 977.

Anderson D. G., Lynn D. M., and Langer R. *Angew. Chem. Int. Ed.*, **2003**, 42, 3153.

Anderson D. G., Tweedie C. A., Hossain N., Navarro S. M., Brey D. M., Vliet K. J., Langer R., Burdick J. A. *Materials, Adv. Mater.* **2006**, 18, 2614.

Brey D. M., Erickson I., Burdick J. A. *J Biomed Mater Res.* **2008**[a] , 85A, 731.

Brey D. M., Ifkovits J. L., Mozia R. I., Katz J. S., Burdick J. A. *Acta Biomaterialia*, **2008**[b], 4 , 207.

Cabral J., Laszlo P., Mahe L. T., Montaufier M.-T., Randriamahefa S. L., *Tetrahedron Letters*, **1989**, 30, 3969.

Fansler D. D., Lewandowaski K. M., Wecdland M. S., Gaddam B.N., Heilmann S. M., *US 7276247 B2*, **2007**[a].

Fansler D. D., Lewandowaski K. M., Gaddam B. N. *US 7307106 B2*, **2007**[b].

Fernandes T. G., Diogo M. M., Clark D. S., Dordick J. S., Cabral M.S. *Trends in Biotechnology*, **2009**, 27, 342 .

Galli G., Laus M., Angeloni A. S., Ferruti P., Chiellhi E. *Makromol. Chem., Rapid Commun.,* **1983**, 4, 681.

Gao C., Yan D. *Prog. Polym. Sci.*, **2004**, 29, 183.

Gates B. D., Xu Q., Stewart M., Ryan D., Willson C. G., Whitesides G. M. *Chem. Rev*. **2005**, 105, 1171.

Gidrol X., Fouque´ B., Ghenim L., Haguet V., Picollet-D'hahan N., Schaack B. *Current Opinion in Pharmacology*, **2009**, 9, 1.

Gomathi N., Sureshkumar A., Neogi S. *Current Science*, **2008**, 94, 1478.

Grayson A. C., Shawgo R. S., Johnson A. M., Flynn N. T., LI Y., Cima M. J., Langer R. T. *Proc. IEEE*, **2004**, 92, 6.

Green J. J., Langer R., Anderson D. G. *Accounts of chemical research*, **2008**, 41, 749

Guan Z. *J. Am. Chem. Soc.* **2002**, *124*, 5616.

Guan J., He H., Lee L. J., Hansford D. J. *Small*, **2007**, 3, 412.

Guo X., Park M. B., Yoon S. F., Chun J., Hua L., Newman, Sze S.-K. *Anal. Chem.* **2006**, 78, 3249.

Hutmacher D. W. *J. Biomat Sci-Polym E* **2001**[a] 12, 107.

Hutmacher D. W, Schantz T., Zein I., Ng K. W., Teoh S. H., Tan K.C. *J Biomed Mater Res*, **2001**[b], 55, 203.

He B., Park M. B. *Macromolecules*, **2005**, *38,* 8227.

He B., Wan E., Park M. B. *Chem. Mater.* **2006**, *18,* 3946.

Heatley, F., Lovell, P.A., McDonald, J. *Eur. Polym. J.*, **1993**, 29, 255.

Holter D., Frey H. *Acta Polymer.*, **1997**, 48, 298.

Jason D. C., Jessica M. S., Robert F. M., Guymon C. A. *Polymer*, **2007**, 48, 6554.

Jeong B., Bae Y. H., Lee D. S. & Kim S. W., *Nature*, **1997**, 388, 860.

Kretlow J. D., Klouda L., Mikos A. G. *Advanced Drug Delivery Reviews*, **2007**, 59, 263.

Langer R., Vacanti J. P., *Science*, **1993**, 260, 920.

Laus M., Angeloni A. S., Galli G., Chielhi E., *Makromol. Chem.*, **1988**, 189, 743.

Lynn D. M., Langer R. *J. Am. Chem. Soc.*, **2000**, *122,* 10761.

Lynn D. M., Anderson D. G., Putnam D., Langer R. *J. Am. Chem. Soc.*, **2001**, *123,* 8155.

Majd S., and Mayer M. *J. Am. Chem. Soc.*, **2008**, *130*, 16060.

Maloney J. M., Santini, Jr. J. T. *Proc IEEE*, **2004**, 2668.

Maloney J. M., Uhland S. A., Polito B. F., Sheppard Jr N. F., Pelta C. M., Santini Jr. J. T. *Journal of Controlled Release*, **2005**,109 ,244.

Nair L. S., Laurencin C. T. *Prog. Polym. Sci.*, **2007**, 32, 762.

Okada M. *Prog. Polym. Sci.,* **2002**, 27, 87.

Park M. B.,Yan Y., Neo W. K., Zhou W., Zhang J., Yue C. Y. *Langmuir* **2003,** *19,* 4371.

Park M. B., Zhu A. P., Shen J. Y., Fan A. L., *Macromol. Biosci.,* **2004**, 4, 665.

Randall C. L., Leong T. G., Bassik N. a, Gracias D. H. *Advanced Drug Delivery Reviews*, **2007**, 59 , 1547.

Razzacki S. Z., Thwar P. K., Yang M., Ugaz V. M., Burns M. A., *Adv. Drug Deli. Rev.*, **2004**, 56, 185.

Sato T., Ihara H., Hirano T., Seno M. *Polymer*, **2004**, 45, 7491.

Santini . J. T., Cima M. J., Langer R. T. *Nature*, **1999**, 397, 335.

Sawhney A. S., Chandrashekhar P. P., Hubbell J. A. *Macromolecules*, **1993**, 26, 581.

Schacht E. *European Cells and Materials*, **2003**, 5, Suppl. 1, page 58.

Shalak R., Fox C. F. *Preface. In: Tissue Engineering*, **1988**, eds. Alan R. L., New York, 26.

Shen J-Y., Park M. B., Feng Z-Q., Chan V. , Feng Z-W. *J Biomed Mater Res Part B: Appl Biomater*, **2006**, 77B, 423.

Shikanov A., Domb A. J. *Biomacromolecules*, **2006,** 7, 288.

Siepmann J., Siepmann F. *Progr Colloid Polym Sci* , **2006** , 133, 15.

Tang L.-M., Fang Y., and Feng J. *Polymer Journal*, **2005**, 37, 255.

Tao S. L., Desai T. A. *Advanced Drug Delivery Reviews*, **2003,** 55, 315.

Vert M. *Biomacromolecules*, **2005,** 6, *538.*

Xia Y., Rogers J. A., Paul K. E., Whitesides G. M. *Chem. Rev*., **1999**, 99**,** 1823.

Xia Y., Whitesides G. M. *Annu. Rev. Mater. Sci.,* **1998**, 28,153.

Yan Y., Park M. B., Gao J., Yue C. Y. *Langmuir***, 2004**, *20,* 1031.

Yin L., Huang X., Tang X., *Polymer Degradation and Stability* , **2007**, 92 ,795.

Zhu A., Chen R., Park M. B. *Macromol. Biosci.*, **2006**, 6, 51.

Chapter 5

Fabrication of biodegradable polymeric scaffolds from sequentially crosslinkable poly (β-amino esters) via soft lithography

5.1 Introduction

Whitesides pioneered a number of non-photolithographic microfabrication techniques collectively called soft-lithography (Xia and Whitesides 1998, Xia et.al. 1999). Soft lithography techniques are useful to fabricate devices for optics, microelectronics and BioMEMS applications for example lab-on chip devices, biosensors and scaffolds for cell culture. The techniques can also be used to pattern non-planar surface and replication of three-dimensional structures which are otherwise difficult to pattern using conventional lithography techniques (Xia and Whitesides 1998, Wang et. al. 2006). The first step in soft lithography involves fabrication of elastomeric mold by cast molding of PDMS prepolymer in silicon master. This elastomeric mold can be used repeatedly to pattern materials of interest. Variety of materials can be processed using soft lithographic techniques. However choice of the lithography technique has to be done based on type of material. For example materials which soften at high temperature can be processed via hot embossing technique and a material which dissolves or softens in solvent can be processed by micro printing or solvent assisted micromolding technique respectively. The liquid prepolymers can be processed via microtransfer molding and micromolding in capillary. For UV-microembossing liquid photo-curable polymers are desirable. A short review of soft lithography techniques is presented in subsequent section. In this chapter we will describe results of UV-microembossing evaluation for SCPBAEs reported in the previous chapter.

5.2 An overview of soft lithography techniques

Soft lithographic techniques are promising methods for multiple pattern replications which allow higher throughput, and do not require expensive equipment. The first step in soft lithography involves fabrication of silicon master, which is fabricated by conventional lithography technique. The master once fabricated by conventional lithography can be used repeatedly which makes this technique affordable (Xia et. al. 1999). Soft lithography techniques are summarized in figure 5.1.

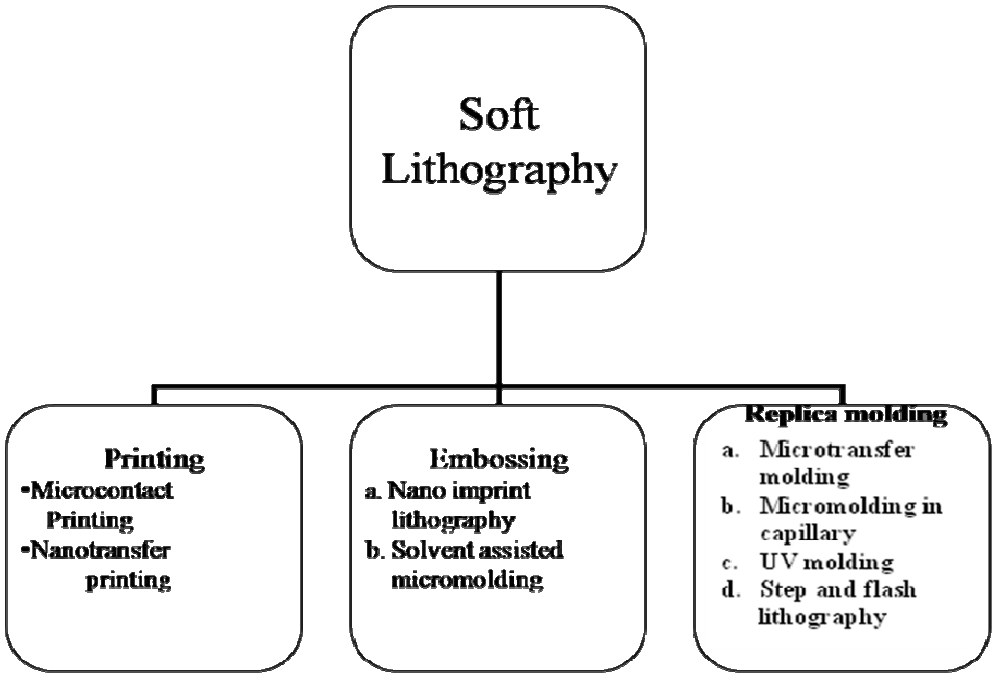

Figure 5.1: Soft lithography techniques (Gates et. al. 2005, Xia and Whitesides 1998)

5.2.1 Printing

Printing includes material transfer from mold on to substrate. It is achieved by two methods, microcontact printing and nanotransfer printing.

5.2.1.1 Microcontact printing

Microcontact printing (μCP) is a technique in which a patterned elastomeric stamp is used to transfer a surface pattern onto a substrate (Xia and Whitesides 1998). The microcontact printing process is depicted in figure 5.2. In this technique PDMS stamp is inked with an appropriate solution, and placed in contact with the substrate to be printed. The stamp makes a contact with the substrate, so that only the protruding features of the stamp touch the surface, and the ink is transferred only to the area of contact with substrate.

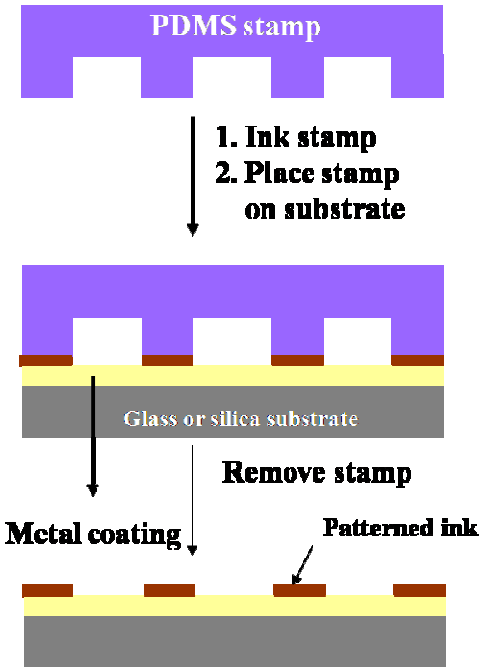

Figure 5.2: Schematic of microcontact printing

5.2.1.1 Nanotransfer printing

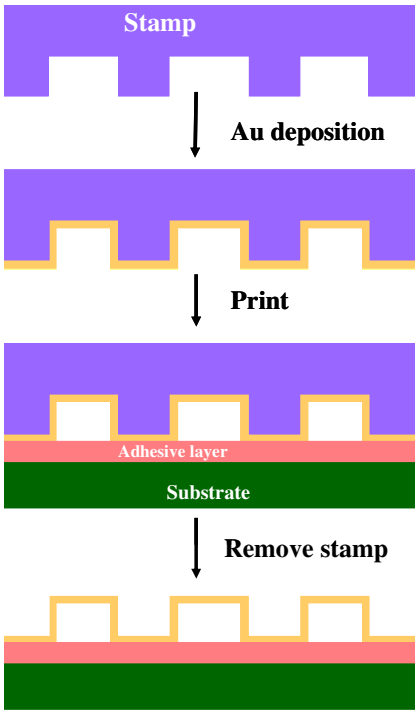

Figure 5.3: Schematic of nanotransfer printing

Nanotransfer printing (nTP) is an advanced technique of printing nanoscale features onto a substrate. A patterned hard or elastomeric stamp is coated with metal. The surface of substrate to be printed has an adhesion layer to facilitate adhesion of the metal. The strength of adhesion between the metal and the stamp is lower than that between the substrate and metal during contact (Gates et. al. 2005). The schematic of nanotransfer printing is presented in figure 5.3.

5.2.2 Embossing

Embossing is a process of imprinting pattern on flat solid soft surface by pressing a mold. The material is embossed thermally, with pressure, or by incorporating a small amount of solvent using a rigid or a soft mold. Two embossing techniques, nanoimprint lithography and solvent assisted micromolding are commonly used (Gates et. al. 2005).

5.2.2.1 Nanoimprint lithography

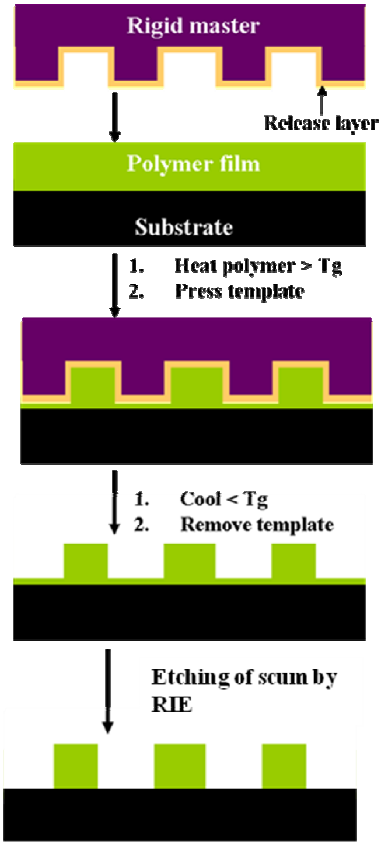

Figure 5.4: Schematic of nanoimprint lithography (NIL)

In nanoimprint lithography (NIL), also called hot embossing, a hard master with release layer is pressed against the polymer on a substrate above the polymer glass transition temperature (T_g). After polymer deformation in the voids of mold, it is cooled below T_g, and the mold is removed. Repeated cooling and heating cycles result in short life of the mold. This can be overcome by embossing the polymer under high pressure at room temperature (Gates et. al. 2005). The process flow is presented in figure 5.4.

5.2.2.2 Solvent assisted micromolding

Solvent assisted micro molding (SAMIM) uses a soft mold usually PDMS and an appropriate solvent to emboss a polymer film. The role of solvent is to soften the polymer so that it can be deformed by the soft mold. After the solvent has evaporated, the mold is removed and a patterned relief structure of the mold is transferred on the polymer film. There is no need to clean the mold since it is cleaned during each cycle after the pattern is transferred (Gates et. al. 2005). The solvent assisted micromolding process is presented in figure 5.5.

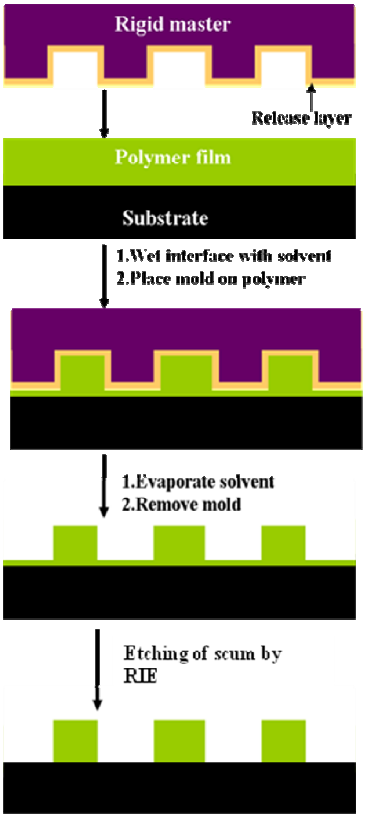

Figure 5.5: Schematic of solvent assisted micromolding

5.2.3 Replica molding

Replica molding involves solidifying liquid precursor in the PDMS mold to create patterns present on original master. Liquid precursor used here can be a prepolymer which could be cured thermally or photochemically.

Replica molding with a soft elastomeric poly (dimethylsiloxane) PDMS mold includes microtransfer molding (μTM) and micromolding in capillaries (MIMIC). Advantages of soft mold are low surface energy of PDMS which facilitates peeling of polymeric replica. Replica molding with a rigid master such as silicon or quartz uses UV- molding step and flash imprint lithography (SFIL) ™. Advantage of rigid mold is that it can withstand pressure used during soft lithography process and no deformation of structure is observed. The mold is thermally stable and chemically inert (Xia 1998; Gates et. al. 2005).

5.2.3.1 Microtransfer molding

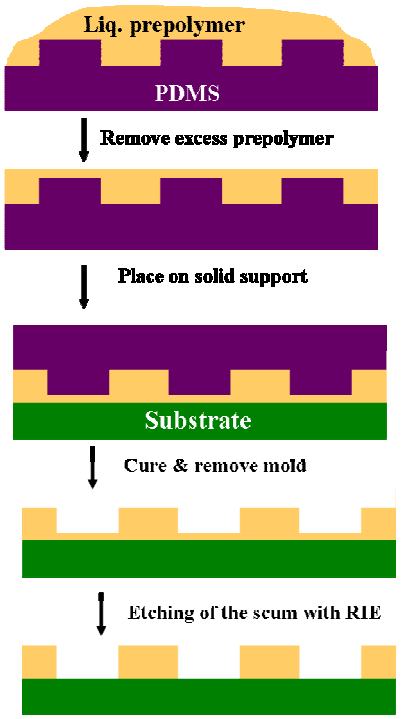

Figure 5.6: Schematic of microtransfer molding (μTM)

In microtransfer molding (μTM), an elastomeric poly (dimethylsiloxane) (PDMS) mold is used. A liquid prepolymer, such as polyurethane (PU) or thermally curable epoxy fills the cavities of the PDMS mold. The excess prepolymer is removed; the prepolymer is placed in contact with a rigid substrate and cured. After curing, the

PDMS mold is removed. The polymer film that remains between the features on top of the substrate (scum) is removed using reactive ion etching (RIE) to separate the feature from the substrate (figure 5.6). This method can create three-dimensional structures and patterns on both planar and curved substrates. Repeating the process can build multilayer structures (Xia and Whitesides 1998).

5.2.3.2 Micromolding in capillary

Micromolding in capillaries (MIMIC) resembles microtransfer molding. The only difference is the soft PDMS mold has microchannels in structure. The PDMS mold is placed onto a substrate, having the channels face down. The liquid prepolymer is placed next to the open ends of the channels, and the capillary forces pull the liquid to fill the channels. The liquid is crosslinked, either by photo or thermal polymerization and then the PDMS mold is removed. The schematic of the process is shown in figure 5.7. In this technique no scum is created and the structures are formed in a single step. The disadvantage of this technique is that only channels can be formed. Feature size is also limited due to slow filling in the channels having small internal dimension (Xia and Whitesides 1998).

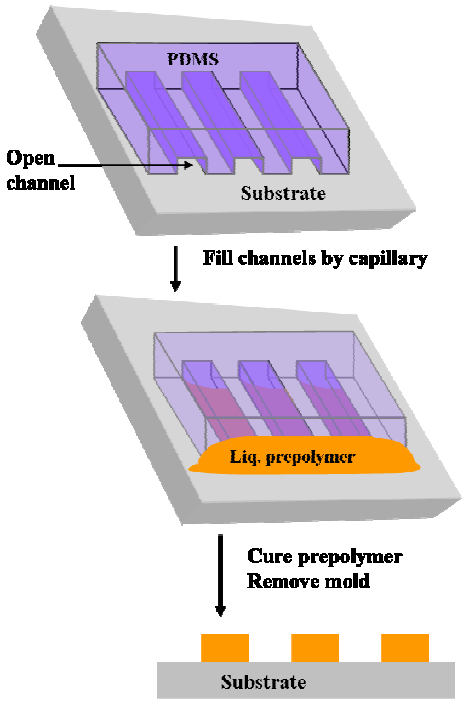

Figure 5.7: Schematic of micromolding in capillaries (MIMIC)

5.2.3.3 UV-microembossing

UV-molding uses both rigid masters and soft PDMS molds. Elevated temperature is used for curing in MIMIC and μTM whereas UV- microembossing uses UV radiation for curing. First step resembles μTM technique where thermally curable PDMS prepolymer is molded onto a silicon master. However in UV-microembossing photocurable prepolymer is placed on the top of PDMS mold and exposed to UV radiation (Xia and Whitesides 1998). UV-micromolding process is presented in figure 5.8.

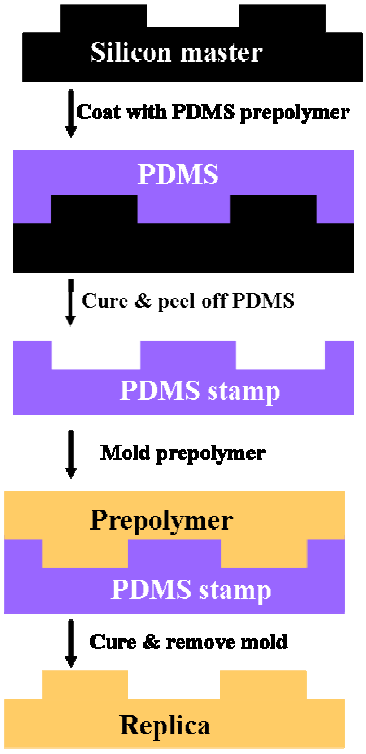

Figure 5.8: Schematic of UV-microembossing

The advantages and disadvantages of conventional lithography vs. soft lithography are listed in table 5.1.

Amongst various soft lithography techniques developed to fabricate polymeric scaffolds, UV- microembossing is of particular interest as it offers following advantages (Park et. al.2003, Shen et. al. 2006, He and Park 2005),

1) UV curing is rapid; its time scale can be manipulated based on UV intensity and type of initiator used.

2) Unlike thermal embossing, UV embossing is usually carried out at room temperature and low pressure (<1bar). This is critical in patterning delicate substrates such as encapsulated protein-in-polymer or water containing hydrogel for biomedical applications.

3) The strength requirements of the mold for such a process are less stringent, and such molds can be duplicated economically from a silicon master.

4) In contrast to photolithography UV embossing can be carried out outside the clean-room environment.

5) It can be used to replicate non planar surfaces.

Table 5.1: Comparison between photolithography vs. soft lithography (adapted from Xia and Whitesides 1998)

Photolithography	**Soft lithography**
Rigid photomask (patterned Cr supported on a quartz plate)	Elastomeric stamp or mold (a PDMS block patterned with relief features)
Photoresists (polymers with photosensitive additives) SAMs on Au and SiO_2	Photoresists. [a,e] SAMs on Au, Ag, Cu, GaAs, Al, Pd, and SiO_2. [a] Unsensitized polymers (epoxy, PU, PMMA, ABS, CA, PS, PE, PVC). [b–e] Precursor polymers(to carbons and ceramics).[c,d] Polymer beads, Conducting polymers, Colloidal materials [a], Organic and inorganic salts, Biological macromolecules.[d] Sol-gel materials.[c,d]
Planar surfaces 2-D structures	Both planar and nonplanar Both 2-D and 3-D structures
*Resolution limit ~250 nm	Resolution limit ~30nm[a,b], ~60 nm[e], ~1 μm[d,e]

a–e Made by (a) CP, (b) REM, (c) TM, (d) MIMIC, (e) SAMIM. PU: polyurethane; PMMA: poly (methyl methacrylate); ABS: poly (acrylonitrile-butadiene-styrene); CA: cellulose acetate; PS: polystyrene; PE: polyethylene; and PVC: poly (vinyl chloride)

** Resolution limits have significantly improved over the last decade.*

5.3 Polymers used for UV-microembossing

An ideal polymer for UV-microembossing should satisfy following requirements,

a) It has to be liquid so that it can fill the cavities appropriately and replicate the patterns present on mold with high fidelity.
b) It must contain functional groups to enable cross-linking during processing.
c) It should be biodegradable and non-cytotoxic so that it can be used in biomedical applications such as drug delivery and tissue engineering.

Not too many efforts have been made to synthesize polymers for UV-microembossing in the literature. A summary of the prior efforts is presented below,

5.3.1 Natural polymers

Natural biomaterials were used for the fabrication of biocompatible scaffolds. These were derived from extracellular matrices for example collagen, fibrinogen, hyaluronic acid, glycosaminoglycans (GAGs) etc and from plants, insects or animal components such as cellulose, chitosan, silk fibroin etc. Natural materials are generally biocompatible, and exhibit mechanical properties comparable to native tissues. However these materials also suffer from disadvantages such as limited control over physico-chemical properties, difficulties in modifying degradation rates. Purification and sterilization of these biomaterials after isolation from different sources is very difficult (Dawson et. al. 2008). Hence efforts have been made to synthesize polymers for lithographic applications.

5.3.2 Synthetic polymers

Oligomers such as epoxy acrylates, polyester acrylates, or polyurethane acrylates commonly used in UV cured coatings are often used in UV embossing. DuPont has developed a family of photopolymers (SURPHEX) for high aspect ratio UV-embossing applications. High molding pressures similar to those used in thermal embossing are needed if these highly viscous photopolymers are to be UV embossed. Liquid acrylate formulations are desirable for UV embossing as it helps mold filling at ambient temperature and pressure (Park et. al. 2003).

Liquid, photocurable polymers for example poly ethylene glycol diacrylates (PEGDA) were used to fabricate microstructured scaffolds with high fidelity (Yan et. al. 2004). PEGDA based formulations were also used for UV microembossing (Park

et. al. 2003). However, these liquid polymers are not biodegradable which limits their use.

Photopolymerizable biodegradable polymers are required for the fabrication of tissue scaffolds with controlled surface micropatterns using photolithographic techniques (Park et. al. 2004, Yan et. al. 2004, He and Park 2005). Biodegradable aliphatic polyesters such as poly (β-hydroxy butyrate), poly (β-malic acid), poly (ε-caprolactone) and poly (α-hydroxy acids) (PLGA) have been extensively investigated for tissue engineering and other biomedical applications as they possess requisite mechanical properties and biocompatibility (Vert 2005, Okada 2002). However lack of vinyl functionality crucial for crosslinking following UV- microembossing in these materials limits their use in lithographic applications.

The photopolymerizable biodegradable diacrylate poly (lactic acid)-b-poly (ethylene oxide)-b-poly (lactic acid) (PLA-b-PEO-b-PLA) macromer was developed for insitu synthesis of hydrogel for fabricating biodegradable scaffolds (Sawhney et. al. 1993). PEG and PLA block macromers containing terminal (meth) acrylate groups. These macromers were photopolymerized to yield highly crosslinked biodegradable materials (Jason et. al. 2007). In another effort to incorporate vinyl functionality in biodegradable aliphatic polyesters, di and triblock copolymers of ε-caprolactone (CL) and glycolide (GA), lactide (LA) with ethylene oxide (EO) bearing terminal vinyl groups were developed. These polymers were further processed by UV-microembossing to fabricate biodegradable scaffolds. However these polymers had to be processed at 65 ºC as these were not liquid at room temperature (Park et. al. 2004; Zhu et. al. 2006).

Photo-patternable biodegradable 2-hydroxylethyl methacrylate (HEMA) conjugated poly (ε-caprolactone-*Co*-RS-β-malic acid) (PCLMAc) co-polymers were synthesized to fabricate biodegradable scaffolds. However quantitative conjugation of carboxylic acid groups to HEMA ester is difficult and involves multiple step synthesis. Further, the resulting polymers are not liquid at room temperature and need to be processed at 60 °C (He and Park 2005).

Liquid photopatternable polyurethane diacrylates were developed to fabricate biocompatible scaffolds by UV-microembossing. The scaffolds fabricated exhibited cytotoxicity due to the presence of unreacted monomers and the photo initiator used during polymer synthesis. The polymers were rendered biocompatible after the

residues were leached out by repeated extractions with methanol which itself is not a highly desirable solvent (Shen et. al. 2006). Other examples of photopolymerizable and degradable polymers developed so far include poly (propylene fumarate)s (PPF), photocrosslinkable poly(anhydride)s, poly (ethylene glycol)s and crosslinkable poly (saccharide)s. However synthesis of these polymers involves several reactions and purification steps (Brey et. al. 2008[b]).

Poly (β-amino esters) were explored as transfection vectors for gene delivery (Lynn et. al. 2000-01, Anderson et. al. 2003, Green et. al. 2008)**.** Since the polymers are viscous liquids at room temperature, non-cytotoxic and biodegradable, they appear promising candidates for biodegradable scaffolds. However these polymers cannot be directly used as they lack functionalities which can lead to crosslinking during lithographic processing.

Anderson et. al. (2006) developed viscous photo-crosslinkable PBAEs containing terminal unsaturations, where degradation times of the network varied from a day to 4 months. Brey et. al. (2008[a]) further extended this work to study the influence of macromer molecular weight on mechanical properties, degradation rate and cell adhesion. Investigation showed that since these polymers contained acrylate groups only at terminal position of chains, crosslinking these polymers resulted in very high sol fraction (47%) which limited their applications in tissue engineering**.** In continuation of this work the effect of macromolecular branching on network properties was investigated. In this approach triacrylate was introduced in the polymerization of diacrylate and amine which helped to lower sol fraction. Amine to acrylate mole ratio was maintained at 1:1. Liquid branched photo-crosslinkable PBAEs containing upto 15 % triacrylate were synthesized. However at triacrylate contents greater than 15 % cross linked products were formed (Brey et. al. 2008[a]).

In previous chapter we described the synthesis and characterization of sequentially crosslinkable poly (β-amino esters) (SCPBAEs). In this chapter we evaluate the performance of these polymers in UV-microembossing. The advantages offered by these polymers are a) they are liquid, b) they contain functionality necessary for thermal or photo curing and c) after crosslinking they yield biodegradable polymers exhibiting wide range of degradation profiles.

We selected silicon master with three different types of pattern geometry, 1) channels, 2) squares and 3) circles varying in aspect ratio and pattern density. These silicon

masters were used to fabricate PDMS molds via replica molding technique. The results of the evaluation indicate that all polymers replicate patterns present on PDMS mold with good fidelity regardless of difference in polymer structure and extent of crosslinkable functionality present. These polymers can replicate patterns with aspect ratio as high as 5.4 and pattern density 0.51. We also observed 5 to 10 % variation in feature size as compared to feature size present on PDMS molds which needs to be considered while processing these polymers by UV-microembossing.

5.4 Experimental section

5.4.1 Materials

1-hydroxy cyclohexyl phenyl ketone was purchased from Aldrich Chemicals and Sylgard ® 184 from Dow Corning. The silicon masters were provided by Dr. Rabah Boukherroub from Institut de Recherche Interdisciplinaire (IRI) France.

5.4.2 Fabrication of PDMS molds

Three types of PDMS molds 1) channels, 2) square pillars and 3) cylindrical micropillars were fabricated from the silicon masters. The rationale behind selecting these patterns is described later. General fabrication process is given below.

Poly (dimethylsiloxane) (PDMS) was used for elastomeric stamp fabrication. The two components were mixed in 10:1 weight ratio, thoroughly mixed and degassed in vacuum for 30 minutes to ensure the removal of the air bubbles created during stirring. After degassing, the prepolymer mixture was poured onto the silicon master and degassed for 5 minutes in vacuum to remove the air bubbles created during pouring. The stamp was cured thermally at 80 °C for 1 hour. After curing PDMS turned into an elastomeric rubber and could be easily removed from the silicon master. These PDMS molds were characterized using scanning electron microscope (SEM).

5.4.2.1 Fabrication of PDMS mold with channels

To fabricate the PDMS mold having channel shape patterns the silicon master with parallel channels (25 μm wall width X 50 μm channel depth X 55 μm channel width) was selected. The PDMS mold was fabricated using general fabrication process described in previous section.

5.4.2.2 Fabrication of PDMS molds with square pillars

Four silicon masters with square trenches were selected to fabricate PDMS molds with square pillars (see table 5.2). Silicon masters with fixed aspect ratio (0.4), feature width (50 μm) and varying pattern density (0.11 to 0.51) were selected to fabricate PDMS molds by general fabrication procedure described in section 5.4.2.

5.4.2.3 Fabrication of PDMS molds with cylindrical pillars

Four silicon masters with circular trenches were selected to fabricate PDMS molds with cylindrical pillars (table 5.2). Silicon masters with varying aspect ratio (2 to 5.4), pattern density (0.11 to 0.51) and feature diameter (3.7 to 10 μm) were selected to fabricate PDMS molds by general fabrication procedure described in section 5.4.2.

5.4.3 UV microembossing of SCPBAEs

A mixture of SCPBAEs and 1 wt % (1-hydroxy cyclohexyl phenyl ketone) photo-initiator was poured in the PDMS mold. The viscous polymer layer formed on the top of PDMS mold was subjected to UV irradiation (8.2 X 10^{-6} MW/cm^2, UV-plate making machine, Lamba making system, Mumbai,) for 15 min. After curing the polymer film was peeled off from the PDMS mold. These polymeric scaffolds were characterized using scanning electron microscope.

5.4.4 Characterization

Scanning electron microscope, Quanta 200 3D, FEI company was used to examine the patterns on PDMS molds and UV-microembossed polymer films.

5.5 Results and discussion

Amongst the family of soft lithography techniques UV-microembossing is particularly suitable for the fabrication of polymeric scaffolds using SCPBAEs. UV-microembossing consists of following steps (i) fabrication of silicon master by conventional lithography, (ii) replica molding of PDMS to fabricate complementary mold and (iii) UV- curing of liquid prepolymer in the PDMS mold. Micro molding technique suffers from few limitations for example, (a) fabrication of silicon masters having small features is difficult, (b) the ability of PDMS to replicate the features of

the master with high fidelity at lower feature size is limited, (c) the distortion of features in the transferred pattern; (d) the swelling of PDMS by the monomers or the solvent used to dissolve polymers; and (e) the ability of the material to fill the PDMS mold completely (Gates et. al. 2005). SCPBAEs synthesized in previous chapter are liquid in nature and eliminate the need for solvent while processing by UV-microembossing. To evaluate the performance of the SCPBAEs we selected three types of PDMS molds with different pattern geometry, 1) microchannels, 2) square pillars and 3) cylindrical pillars (table 5.2). The UV-microembossing was performed in two steps, 1) fabrication of PDMS molds and 2) UV- microembossing of SCPBAEs. Details of the each fabrication step and rationale behind the choice of molds are discussed in subsequent sections.

Pattern density of the micropatterned structure present on both PDMS mold and polymers was calculated using Lee's equations (Lee et. al. 2005).

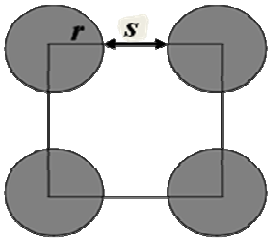

Pattern density (PD)= $\pi r^2 / (s + 2r)^2$

Where r is radius of the circle ($w/2$),

s is distance between two posts

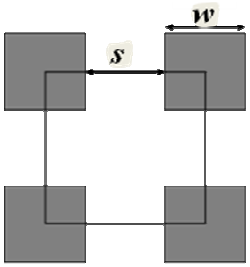

Pattern density (PD) = $w^2 / (s + w)^2$

Where w is width of square

s is distance between two posts

Figure 5.9: Pattern density calculations

5.5.1 Fabrication of PDMS molds

Table 5.2: Pattern dimensions of silicon master and PDMS mold

Patterns	Silicon masters*					PDMS molds#				
	w µm	s µm	d µm	AR d/w	PD	w µm	s µm	d µm	AR d/w	PD
Ch1	25	55	50	2.0		25	55	50	2.0	
Ci1	10	4	25	2.5	0.4	10	4	25	2.5	0.4
Ci2	10	7	25	2.5	0.27	10	7	25	2.5	0.27
Ci3	9.5	2.5	25	2.6	0.45	9.5	2.5	25	2.6	0.45
Ci4	3.7	2.3	20	5.4	0.29	3.7	2.3	20	5.4	0.29
Sq1	50	95	20	0.4	0.11	50	95	20	0.4	0.11
Sq2	50	50	20	0.4	0.25	50	50	20	0.4	0.25
Sq4	50	25	20	0.4	0.44	50	25	20	0.4	0.44
Sq5	50	20	20	0.4	0.51	50	20	20	0.4	0.51

** Pattern dimensions provided by suppliers, # pattern dimensions measured using SEM. Ch - Channels, Ci - Circles, Sq – Squares, AR-Aspect ratio and PD-Pattern density,w- pillar or trench width, s-distance between two pillars or trenches and d-height of pillar or depth of trench.*

PDMS molds were obtained from silicon masters by replica molding. Details of the fabrication technique are discussed in section 5.4.2. The schematic of fabrication process is shown in figure 5.8. The dimensions of the patterns formed on PDMS molds match with the pattern dimensions of silicon masters (table 5.2).

5.5.1.1 Fabrication of PDMS molds with microchannels

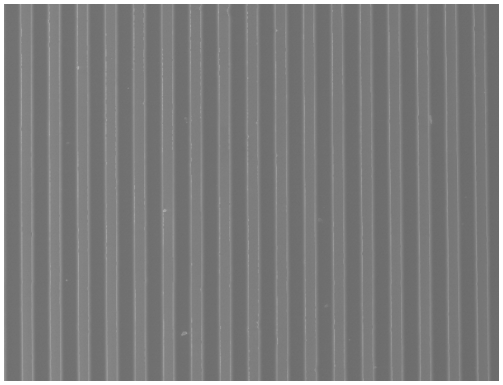

Figure 5.10: SEM images of the molded PDMS microchannels

The polymeric micro channel scaffolds have been used for vasculature and guided nerve generation. These scaffolds can also be used for tissue engineering of tubular organs such as blood vessels and esophagus (He and Park 2005). Shen et. al. (2006) reported that the skeletal muscle cells merged together to form myofibers when cells were seeded on scaffolds having channel width 40 μm. Hence PDMS mold having pattern dimensions, 25 μm wall width X 50 μm channel depth X 55 μm channel width was selected in this study to evaluate performance of the SCPBAEs synthesized by us (figure 5.10).

5.5.1.2 PDMS molds with isolated features

Independent microreservoirs or containers are needed to develop micro-chip based drug delivery system. These microreservoirs can be loaded with drugs, and be easily tracked, programmed or controlled (Randall et. al. 2007; Santini et. al. 1999). To demonstrate the utility of SCPBAEs for above applications we selected PDMS molds having more complex square as well as cylindrical pillars.

1. PDMS mold with square pillars

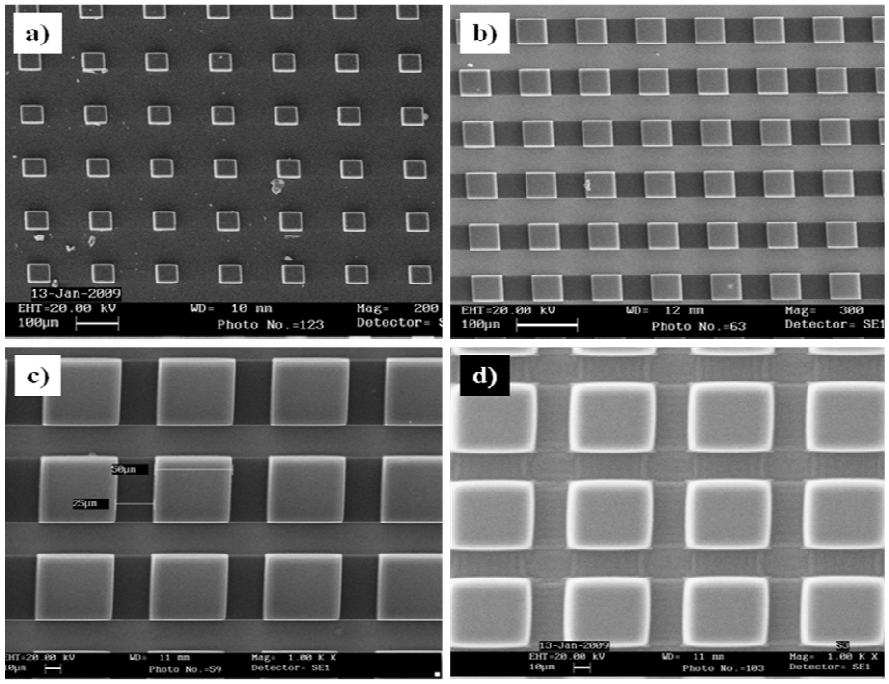

Figure 5.11: SEM images of the molded PDMS square post
a) Sq1, b) Sq2, c) Sq3, d) Sq4

PDMS molds bearing different square pillar geometry were fabricated via replica molding technique from silicon master as per procedure described in section 5.4.2. These molds were used to study the effect of change in pattern density at constant aspect ratio on performance of SCPBAEs. Four PDMS mold were fabricated where aspect ratio was 0.4 and pattern density was varied from 0.11 to 0.51 by varying the distance between two square pillars. No deformation in pattern geometry was observed for PDMS mold (Sq4) with high (0.51) pattern density (figure 5.11). The dimensions of the PDMS molds were measured using scanning electron microscopy (SEM) the results are summarized in table 5.2.

2. PDMS mold with cylindrical pillars

Four PDMS molds (Ci1, Ci2, Ci3 and Ci4) bearing different cylindrical pillar geometries were fabricated via replica molding technique from silicon master as per procedure described in section 5.4.2. The mold dimensions are listed in table 5.2. In PDMS molds Ci1 and Ci2 the pillar diameter (10μ) and aspect ratio (2.5) were kept constant while pattern density was varied from 0.4 to 0.27 to study its effect on pillar stability. It was observed that pillars were stable and no lateral collapse or buckling was observed in PDMS mold (figure 5.12 a-b). In PDMS molds Ci1 and Ci3 pillar diameter was reduced by 0.5 μm (9.5 μm) and pattern density was increased to 0.45 by reducing the distance between two pillars from 4 μm to 2.5 μm while aspect ratio was kept constant (2.5 and 2.7 respectively). Lateral collapse of pillars was observed in case of PDMS mold Ci3 (figure 5.12c). In PDMS mold Ci4 the pillar diameter was reduced to 3.7 μm which results in pillars with high aspect ratio (5.4). We observed collapse of micropillars which formed bundles of five or more micropillars due to combined effect of smaller pillar size and high aspect ratio (figure 5.12d) (Xia and Whitesides 1998).

Lee et. al. (2005) reported that the pattern density plays an important role in lateral collapses of PDMS feature. However results obtained for PDMS processed under experimental conditions used by us suggest that along with pattern density, aspect ratio, feature size and distance between two features also contribute to lateral collapse of micro pillars formed in PDMS molds. No buckling of the pillars was observed in any of the PDMS molds fabricated under these experimental conditions.

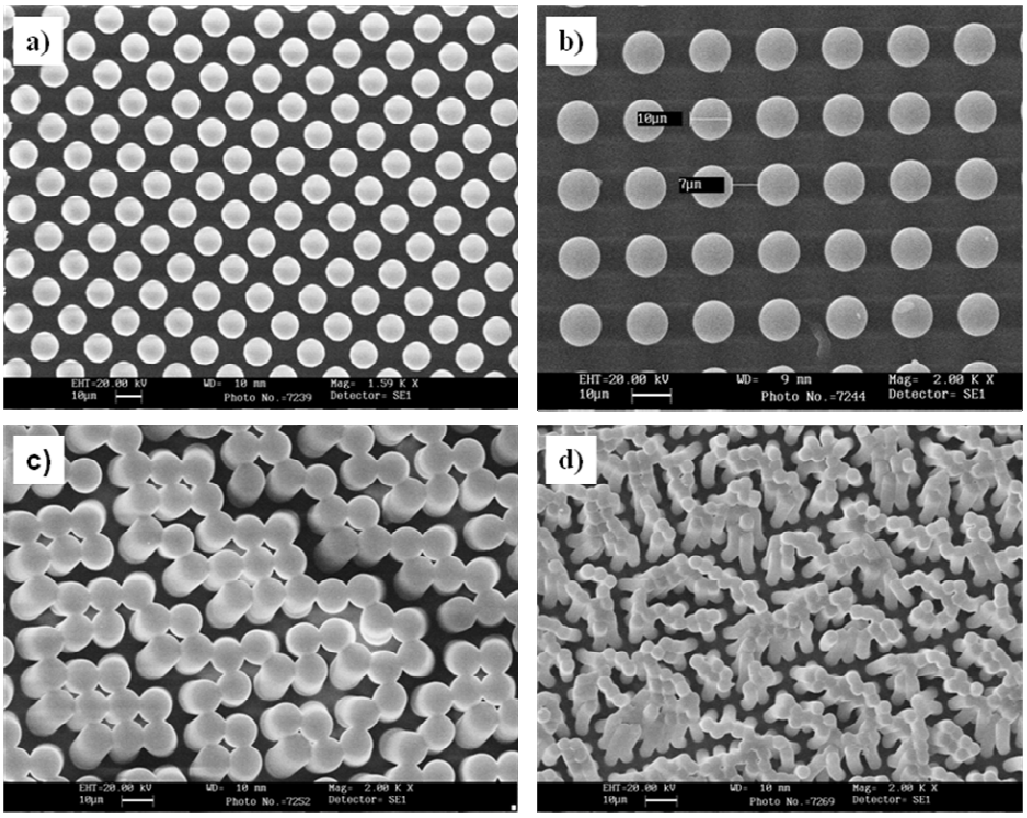

Figure 5.12: SEM images of the molded PDMS circular micro pillars a) Ci1, b) Ci2 , c) Ci3, d) Ci4

5.5.2 UV-microembossing of SCPBAE

UV-microembossing of the SCPBAEs reported in previous chapter was carried out as described in section 5.4.3. The PDMS molds of different shapes such as channels, squares pillar and cylindrical pillars with different aspect ratio and pattern density were used to process SCPBAEs.

5.5.2.1 UV-microembossing of SCPBAE in PDMS channels

The polymeric micro channel scaffolds have been used for vasculature and guided nerve generation. These scaffolds can also be used for tissue engineering of tubular organs such as blood vessels and esophagus (He and Park 2005, Shen et. al. 2006).

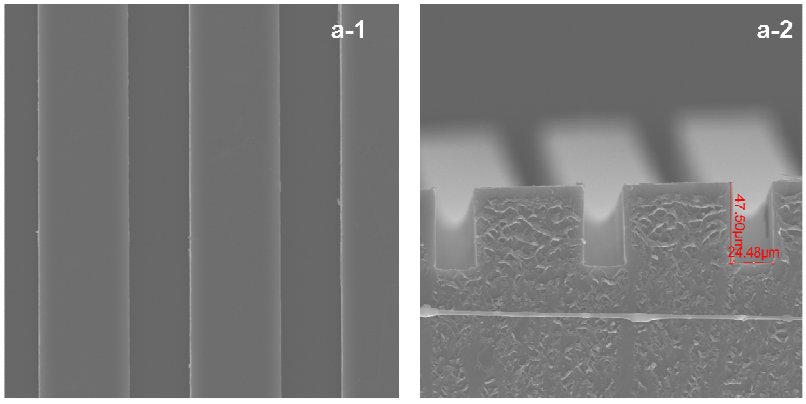

Figure 5.13: SEM images of a-1) microembossed polymer film and a-2) cross-section

In vitro culture of smooth muscle cells and skeletal muscle cells on flat culture plates leads to loss of spindle shape and contractility. Polyurethane based three dimensional scaffolds containing microchannels were fabricated to grow smooth muscle cells and skeletal muscle cells in vitro. It was noticed that cells show resistance to growth at narrower channel size (10 µm) and exhibit more fibroblast like morphology as observed on flat surface. The investigations showed that the skeletal muscle cells merged together to form myofibers when cells were seeded on scaffolds having channel width 40 µm (Shen et. al. 2006). Hence in this work more stringent PDMS mold with channel 25 µm wall width X 50 µm channel depth X 55 µm channel width was selected to evaluate performance of SCPBAEs.

Table 5.3: Replication of SCPBAES in PDMS channel mold

Polymers	w µm	s µm	d µm	AR
PDMS	25.00	55.00	50.00	2.00
Poly (PETA-Co-Pz)	24.46	57.83	48.32	1.97
Poly (PETA-Co-TMDP)	24.48	57.75	48.20	1.97
Poly (TMPTA-Co- Pz)	24.45	57.78	48.00	1.96
Poly (TMPTA-Co-TMDP)	24.48	57.80	47.50	1.94
Poly (TMPMADA-Co-TMDP)	24.46	57.85	47.80	1.95

AR-Aspect ratio, w- wall or channel width, s-distance between two walls or channels and d-height of wall or depth of channel.

The SCPBAEs evaluated using PDMS mold selected for this study showed identical performance irrespective of their molecular structure and degree of crosslinking. It may be noted that the values of *s* for SCPBAE patterns are greater than those for PDMS molds and the values for *w* as well as *d* are slightly lower. These could be attributed to small errors in measurement of dimensions. It is unlikely that the differences are due to shrinkage of the resins since the values of s for SCPBAE patterns are greater than those for PDMS molds. In any case the variations in pattern dimensions are comparable or lower than those reported in literature (Shen 2006). However, these variations need to be considered during scaffold fabrication by UV-microembossing. The representative SEM picture of the scaffold fabricated using poly (TMPTA-Co-TMDP) is given in figure 5.13.

5.5.2.2 UV-microembossing of SCPBAE in isolated PDMS square and cylindrical pillars

The fabrication of small independent microreservoir structures or containers is critical for the development of micro-chip based drug delivery system. Further these microreservoirs can be loaded with drugs, and be easily tracked, programmed or controlled (Randall et. al. 2007; Santini et. al. 1999). Tao and Desai (2003) developed silicon membrane by micro fabrication technique for sustained release of drugs and to develop implantable biocapsules for immunoisolation of pancreatic islet cells. However these devices once placed inside the body need to be removed again by surgical intervention as materials used for device fabrication are not biodegradable. We propose use of biodegradable SCPBAEs as materials for fabrication of such devices to eliminate to the need for second surgery. To demonstrate the utility of SCPBAEs synthesized by us for above applications we selected PDMS molds having isolated square posts and cylindrical pillars.

1. UV-microembossing of SCPBAE in PDMS square posts

Four PDMS molds (Sq1, Sq2 Sq3 and Sq4) containing square post pattern with varying aspect ratios as mentioned in table 5.2 were used for UV-microembossing of SCPBAEs. All SCPBAEs were processed by UV-microembossing using PDMS mold

and results are listed in tables 5.4 – 5.7. SEM images of representative Poly (TMPTA-Co-TMDP) for the corresponding PDMS mold are provided along with each table.

Table 5.4: PDMS mold Square pillars (Sq1) and polymer scaffolds

Polymers	w µm	s µm	d µm	AR	PD
PDMS	50.00	95.00	20.00	0.40	0.11
1. Poly (PETA-Co-Pz)	47.95	94.82	20.61	0.43	0.11
2. Poly (PETA-Co-TMDP)	46.75	94.73	21.63	0.46	0.11
3. Poly (TMPTA-Co- Pz)	48.65	94.38	21.07	0.43	0.12
4. Poly (TMPTA-Co-TMDP)	48.75	94.73	21.63	0.44	0.12
5. Poly (TMPAEDA-Co-TMDP)	50.28	87.13	19.63	0.39	0.13
6. Poly (TMPMADA-Co-TMDP)	48.53	94.21	21.58	0.44	0.12
7. Poly (TMPMADA (25%)-Co-TMDP (50%)-Co-CHDMDA (25%))	48.75	93.73	20.6	0.42	0.12
8. Poly (TMPMADA (12.5%)-Co-TMDP (50%)-Co-CHDMDA (37.5%))	48.58	94.83	21.74	0.45	0.11
9. Poly (TMPMADA (5%)-Co-TMDP (50%)-Co-CHDMDA (45%))	48.57	94.32	20.45	0.42	0.12

AR-Aspect ratio and PD-Pattern density, w- post or trench width, s-distance between two posts or trenches and d-height of post or depth of trench.

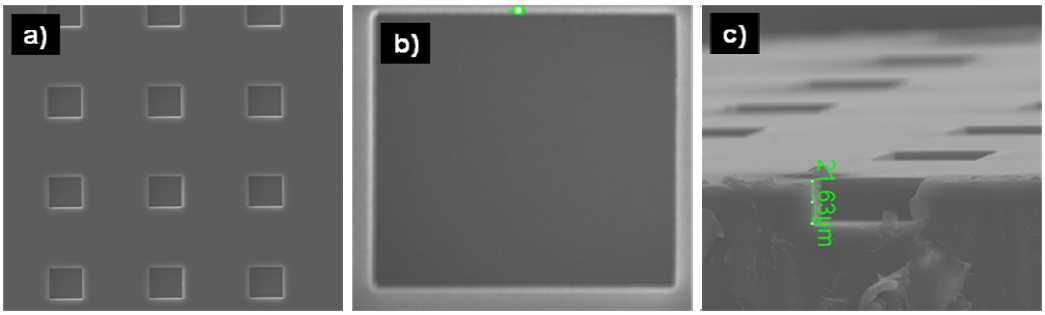

Figure 5.14: SEM images of the UV-micro embossed polymer film (PSq1) a) square wells, b) enlarged top view of single well and c) vertical cross section

Table 5.5: PDMS mold with square pillars (Sq2) and polymer scaffolds

Polymers	w µm	s µm	d µm	AR	PD
PDMS	50.00	50.00	20.00	0.40	0.25
1. Poly (PETA-Co-Pz)	48.08	46.54	20.88	0.43	0.26
2. Poly (PETA-Co-TMDP)	48.08	46.63	21.73	0.45	0.26
3. Poly (TMPTA-Co- Pz)	48.92	46.76	21.23	0.43	0.26
4. Poly (TMPTA-Co-TMDP)	48.08	46.63	21.73	0.45	0.26
5. Poly (TMPAEDA-Co-TMDP)	48.52	46.69	21.87	0.45	0.26
6. Poly (TMPMADA-Co-TMDP)	48.38	46.53	21.84	0.45	0.26
7. Poly (TMPMADA (25%)-Co-TMDP (50%)-Co-CHDMDA (25%))	48.08	46.63	21.73	0.45	0.26
8. Poly (TMPMADA (12.5%)-Co-TMDP (50%)-Co-CHDMDA (37.5%))	48.92	46.31	21.73	0.44	0.26
9. Poly (TMPMADA (5%)-Co-TMDP (50%)-Co-CHDMDA (45%))	48.72	46.29	21.52	0.44	0.26

AR-Aspect ratio and PD-Pattern density, w- post or trench width, s-distance between two posts or trenches and d-height of post or depth of trench.

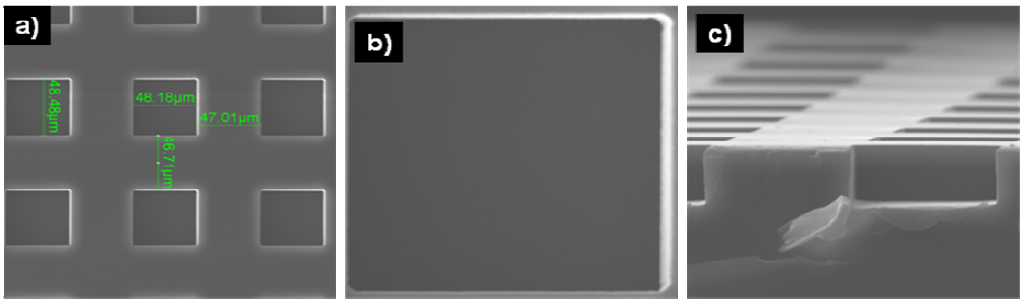

Figure 5.15: SEM images of the UV-micro embossed polymer film (PSq2) a) square wells, b) enlarge top view of single well and c) vertical cross section

Table 5.6: PDMS mold with square pillars (Sq3) and polymer scaffolds

Polymers	w µm	s µm	d µm	AR	PD
PDMS	50.00	45.00	20.00	0.40	0.27
1. Poly (PETA-Co-Pz)	49.00	46.32	21.26	0.43	0.26
2. Poly (PETA-Co-TMDP)	48.72	46.46	21.44	0.44	0.26
3. Poly (TMPTA-Co- Pz)	47.64	44.52	19.48	0.41	0.27
4. Poly (TMPTA-Co-TMDP)	48.72	46.46	21.44	0.44	0.26
5. Poly (TMPAEDA-Co-TMDP)	48.48	44.74	20.34	0.42	0.27
6. Poly (TMPMADA-Co-TMDP)	48.92	46.76	21.23	0.43	0.26
7. Poly (TMPMADA (25%)-Co-TMDP (50%)-Co-CHDMDA (25%))	48.72	46.46	21.44	0.44	0.26
8. Poly (TMPMADA (12.5%)-Co-TMDP (50%)-Co-CHDMDA (37.5%))	48.61	46.00	21.59	0.44	0.26
9. Poly (TMPMADA (5%)-Co-TMDP (50%)-Co-CHDMDA (45%))	48.39	46.83	21.43	0.44	0.26

AR-Aspect ratio and PD-Pattern density, w- post or trench width, s-distance between two posts or trenches and d-height of post or depth of trench.

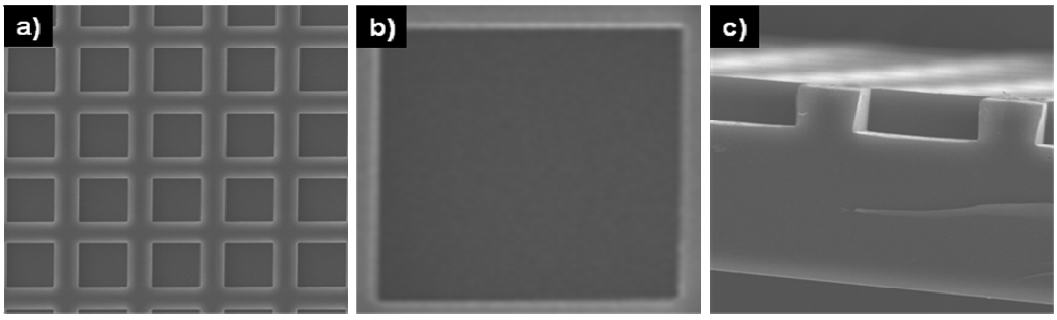

Figure 5.16: SEM images of the UV-micro embossed polymer film (PSq3) a) square wells, b) enlarge top view of single well and c) vertical cross section

Table 5.7: PDMS mold with square pillars (Sq4) and polymer scaffolds

Polymers	w µm	s µm	d µm	AR	PD
PDMS	50.00	20.00	20.00	0.40	0.51
1. Poly (PETA-Co-Pz)	48.18	24.06	20.45	0.42	0.44
2. Poly (PETA-Co-TMDP)	48.31	23.31	20.52	0.42	0.45
3. Poly (TMPTA-Co- Pz)	48.08	20.57	22.82	0.47	0.49
4. Poly (TMPTA-Co-TMDP)	48.08	22.44	23.03	0.48	0.46
5. Poly (TMPAEDA-Co-TMDP)	49.77	22.44	22.55	0.45	0.48
6. Poly (TMPMADA-Co-TMDP)	48.39	22.82	21.62	0.45	0.46
7. Poly (TMPMADA (25%)-Co-TMDP (50%)-Co-CHDMDA (25%))	48.08	22.44	23.03	0.47	0.46
8. Poly (TMPMADA (12.5%)-Co-TMDP (50%)-Co-CHDMDA (37.5%))	48.93	23.47	20.29	0.41	0.46
9. Poly (TMPMADA (5%)-Co-TMDP (50%)-Co-CHDMDA (45%))	48.58	23.92	20.1	0.41	0.45

AR-Aspect ratio and PD-Pattern density, w- post or trench width, s-distance between two posts or trenches and d-height of post or depth of trench.

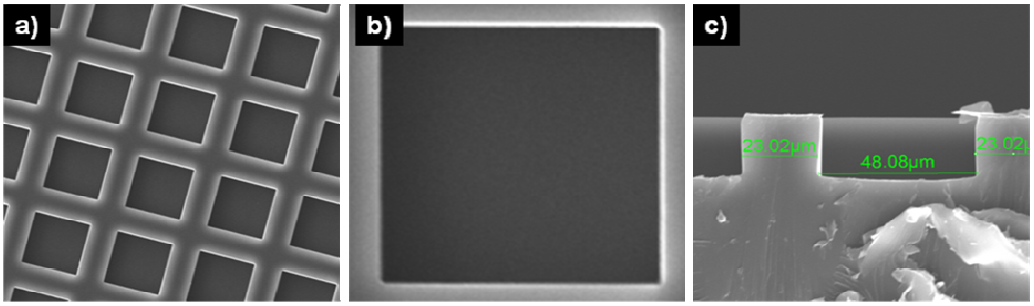

Figure 5.17: SEM images of the UV-micro embossed polymer film (PSq4) a) square wells, b) enlarge top view of single well and c) vertical cross section

The SEM images show that the polymers replicated patterns on PDMS molds with good fidelity. The enlarged image of single square well shows no cracking along the edges of the feature replicated in polymer film. The results obtained for UV-microembossing of SCPBAEs in PDMS molds with square posts suggest that all polymers replicated the patterns on PDMS molds with good fidelity and that there was no systematic correlation between the polymer structures, even when the pattern density of PDMS mold was varied four folds from 0.11 to 0.51. Once again variations in the measurement of w, s and d are reflected in the values of aspect ratios and pattern densities of SCPBAE structures. Unfortunately there are no parallel studies in the literature for UV-microembossing of polymers with which our findings could be compared. All that can be said at this stage is that these need to be taken in to consideration during designing these materials for processing by UV-microembossing.

2. UV-microembossing of SCPBAE in PDMS molds: cylindrical pillars

Four PDMS molds (Ci1, Ci2, Ci3 and Ci4) containing cylindrical pillars with varying aspect ratios, pattern density and feature size as mentioned in table 5.2 were used for UV-microembossing of SCPBAEs. These patterns are more stringent than square patterns used in previous study. The purpose was to investigate upto what pattern dimensions, could SCPBAEs be processed with good replicability. For this study we selected PDMS molds with cylindrical pillars having high aspect ratio 5.4, and pattern density 0.45 but smaller pillar diameter viz. 3.7 μm.

As mentioned earlier in case of PDMS molds Ci1 and Ci2 patterns were satisfactorily reproduced whereas in Ci3 and Ci4 lateral collapse of cylindrical pillars was observed. When SCPBAEs synthesized by us were processed in these PDMS molds we observed that the lateral collapse of pillars was not directly reflected in the SEM images of the polymer film. The micro wells appeared well separated even for the PDMS molds where lateral collapse of micropillars had taken place. Results for each PDMS mold are listed in tables 5.8 to 5.11 and SEM images of Poly (TMPTA-Co-TMDP) are provided for respective PDMS mold.

Table 5.8: PDMS mold with circular pillars (Ci1) and polymer scaffolds

Polymers	w µm	s µm	d µm	AR	PD
PDMS	10.00	4.00	25.00	2.50	0.40
1. Poly (PETA-Co-Pz)	9.18	3.40	23.32	2.54	0.42
2. Poly (PETA-Co-TMDP)	9.15	3.80	22.31	2.44	0.39
3. Poly (TMPTA-Co- Pz)	9.22	3.87	24.04	2.61	0.39
4. Poly (TMPTA-Co-TMDP)	9.50	5.01	20.85	2.19	0.34
5. Poly (TMPAEDA-Co-TMDP)	9.15	3.80	22.31	2.44	0.39
6. Poly (TMPMADA-Co-TMDP)	9.47	3.40	22.08	2.33	0.43
7. Poly (TMPMADA (25%)-Co-TMDP (50%)-Co-CHDMDA (25%))	9.20	4.20	23.31	2.53	0.37
8. Poly (TMPMADA (12.5%)-Co-TMDP (50%)-Co-CHDMDA (37.5%))	9.98	4.30	24.86	2.49	0.38
9. Poly (TMPMADA (5%)-Co-TMDP (50%)-Co-CHDMDA (45%))	9.15	3.70	22.29	2.44	0.40

AR-Aspect ratio and PD-Pattern density, w- post or trench width, s-distance between two posts or trenches and d-height of post or depth of trench.

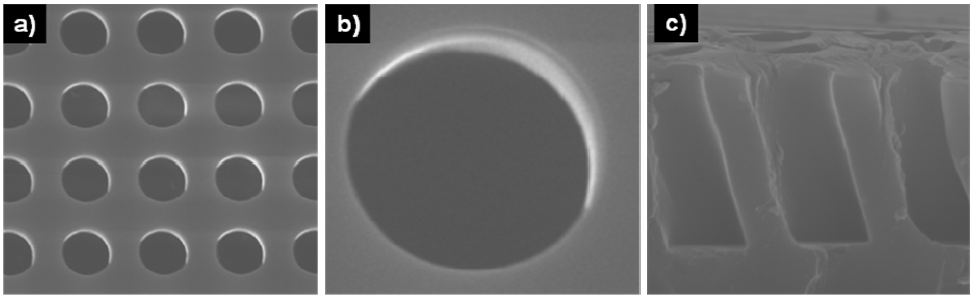

Figure 5.18: SEM images of the UV-micro embossed polymer film (PCi1) a) circular wells, b) enlarged top view of single well and c) vertical cross section

Table 5.9: PDMS mold with circular pillars (Ci2) and polymer scaffolds

Polymers	w µm	s µm	d µm	AR	PD
PDMS	10.00	7.00	25.00	2.50	0.27
1. Poly (PETA-Co-Pz)	9.50	6.50	21.39	2.25	0.28
2. Poly (PETA-Co-TMDP)	9.50	6.80	19.43	2.05	0.27
3. Poly (TMPTA-Co- Pz)	9.70	6.45	22.17	2.29	0.28
4. Poly (TMPTA-Co-TMDP)	9.50	6.80	19.43	2.05	0.27
5. Poly (TMPAEDA-Co-TMDP)	9.33	5.78	19.43	2.08	0.30
6. Poly (TMPMADA-Co-TMDP)	9.50	5.80	20.93	2.20	0.30
7. Poly (TMPMADA (25%)-Co-TMDP (50%)-Co-CHDMDA (25%))	9.72	5.92	23.43	2.41	0.30
8. Poly (TMPMADA (12.5%)-Co-TMDP (50%)-Co-CHDMDA (37.5%))	9.71	6.92	21.85	2.25	0.27
9. Poly (TMPMADA (5%)-Co-TMDP (50%)-Co-CHDMDA (45%))	9.50	6.72	19.37	2.04	0.27

AR-Aspect ratio and PD-Pattern density, w- post or trench width, s-distance between two posts or trenches and d-height of post or depth of trench.

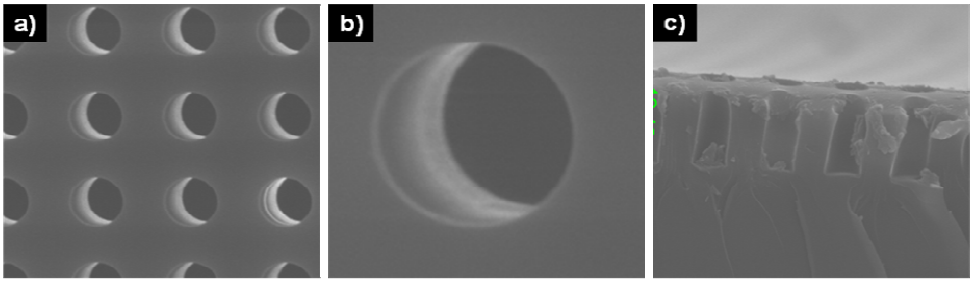

Figure 5.19: SEM images of the UV-micro embossed polymer film (PCi2) a) circular wells, b) enlarged top view of single well and c) vertical cross section

Table 5.10: PDMS mold with circular pillars (Ci3) and polymer scaffolds

Polymers	w µm	s µm	d µm	AR	PD
PDMS	9.50	2.50	25.00	2.60	0.45
1. Poly (PETA-Co-Pz)	9.46	2.72	21.00	2.22	0.34
2. Poly (PETA-Co-TMDP)	9.50	2.55	20.85	2.19	0.34
3. Poly (TMPTA-Co- Pz)	9.48	2.67	20.54	2.17	0.33
4. Poly (TMPTA-Co-TMDP)	9.15	2.8	22.31	2.44	0.46
5. Poly (TMPAEDA-Co-TMDP)	9.50	2.56	20.99	2.21	0.34
6. Poly (TMPMADA-Co-TMDP)	9.80	2.73	20.42	2.08	0.34
7. Poly (TMPMADA (25%)-Co-TMDP (50%)-Co-CHDMDA (25%))	9.60	2.66	20.73	2.16	0.33
8. Poly (TMPMADA (12.5%)-Co-TMDP (50%)-Co-CHDMDA (37.5%))	9.70	2.79	22.33	2.30	0.34
9. Poly (TMPMADA (5%)-Co-TMDP (50%)-Co-CHDMDA (45%))	9.50	2.58	20.78	2.19	0.33

AR-Aspect ratio and PD-Pattern density, w- post or trench width, s-distance between two posts or trenches and d-height of post or depth of trench.

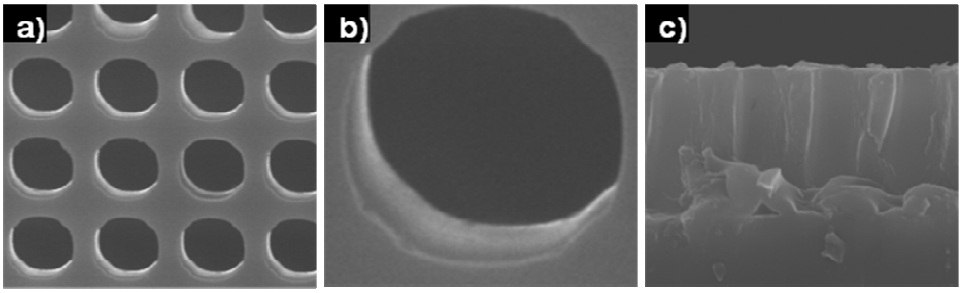

Figure 5.20: SEM images of the UV-micro embossed polymer film (PCi3) a) circular wells, b) enlarged top view of single well and c) vertical cross section

Table 5.11: PDMS mold with circular pillars (Ci4) and polymer scaffolds

Polymers	w µm	s µm	d µm	AR	PD
PDMS	3.7	2.3	20.00	5.40	0.29
1. Poly (PETA-Co-Pz)	3.4	2.2	19.08	5.61	0.29
2. Poly (PETA-Co-TMDP)	3.5	2.1	18.19	5.20	0.31
3. Poly (TMPTA-Co- Pz)	3.5	2.2	19.01	5.43	0.30
4. Poly (TMPTA-Co-TMDP)	3.5	2.1	18.19	5.20	0.31
5. Poly (TMPAEDA-Co-TMDP)	3.5	2.1	18.19	5.20	0.31
6. Poly (TMPMADA-Co-TMDP)	3.4	2.6	19.87	5.84	0.25
7. Poly (TMPMADA (25%)-Co-TMDP (50%)-Co-CHDMDA (25%))	3.2	2.1	18.26	5.71	0.29
8. Poly (TMPMADA (12.5%)-Co-TMDP (50%)-Co-CHDMDA (37.5%))	3.5	2.1	17.74	5.07	0.31
9. Poly (TMPMADA (5%)-Co-TMDP (50%)-Co-CHDMDA (45%))	3.5	2.25	19.97	5.71	0.29

AR-Aspect ratio and PD-Pattern density, w- post or trench width, s-distance between two posts or trenches and d-height of post or depth of trench.

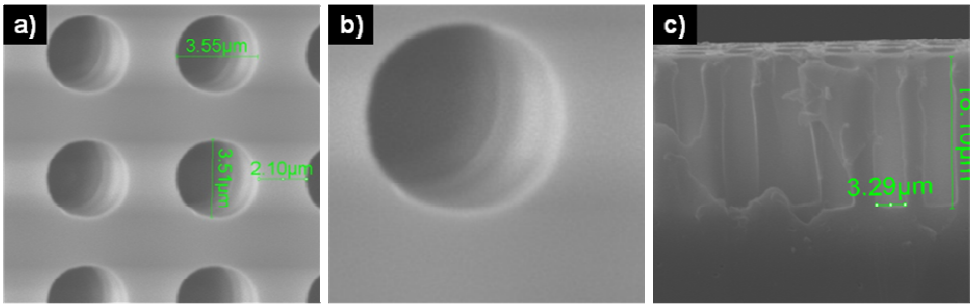

Figure 5.21: SEM images of the UV-micro embossed polymer film (PCi4) a) circular wells, b) enlarged top view of single well and c) vertical cross section

Once again the dimensions of the SCPBAE patterns are comparable to those of the PDMS patterns, within measurement errors and no systematic correlation with the diameter of pillars, aspect ratio and pattern density was observed. However SEM examination of the cross-section of the molds revealed that in case of Ci3 and Ci4 lateral collapse of PDMS pillars was observed. Upper portion of pillars was bent and only the tips adhered to each other. However the dimensions and position of the micro pillars base attached to PDMS substrate were unchanged. Hence once the viscous polymer was poured over PDMS mold, it crept down along laterally collapsed micro pillars to fill the cavities. After UV curing of SCPBAEs crosslinked films were peeled from PDMS mold. Micropatterns on the polymer film surface were complementary to micro pillars' base attached to PDMS substrate. Hence SEM images (figure 5.20a and 5.21a) for UV embossed polymeric films which were fabricated using PDMS molds containing laterally collapsed pillars, showed well isolated micro wells. However cross section of micropatterned polymer film (figure 5.20c and 5.21c) showed that micro wells formed in SCPBAE were fused. This however is limitation of PDMS used and not SCPBAEs resins. This can be overcome by using hard PDMS (h-PDMS) as reported by (Lee et. al 2005)

After UV curing, the micropatterned SCPBAE's films could be readily peeled from the PDMS molds, which is critical in the biomedical applications. Typically, a polyester film which has good adhesion to the acrylate resin (e.g. Melinex 454, DuPont) is needed as a carrier film to peel off microembossed structure from PDMS mold. Some of the additives used for peeling off are usually cytotoxic and difficult to fully get rid off after demolding (Shen et. al. 2006, Zhu et. al. 2006).

The overall shape, aspect ratio and pattern density of patterns replicated on crosslinked SCPBAEs films are in good agreement with those on parent PDMS molds. We observed small difference in dimension than the patterns present on parent PDMS molds. The variations in molecular structure of polymers did not exhibit any systematic influence on processing of SCPBAEs by UV-microembossing. However change in polymer molecular structure significantly influences the rate of degradation of crosslinked polymers under physiological conditions as shown in previous chapter. From these results we conclude that SCPBAEs with varying degradation patterns can be use to fabricate biodegradable polymeric scaffolds with 25 μm channels useful to produce elongated skeletal muscle cells (Shen et. al. 2006). Also these polymers can

be used to fabricate biodegradable polymeric scaffolds containing independent microreservoirs needed for the development advanced drug delivery technology (Randall et. al. 2007; Santini et. al. 1999).

5.6 Conclusions

UV-microembossing is a convenient technique for processing solvent free SCPBAEs. PDMS mold with different pattern geometry such as 1) microchannel, 2) square pillars and 3) cylindrical pillars were fabricated using replica moulding technique. The aspect ratio and the pattern density of the features presented on PDMS mold was varied from 0.11 to 5.4 and 0.4 to 5.4 to investigate upto what feature dimensions SCPBAEs could be processed without pattern failure. The UV-microembossing results of the SCPBAEs revealed that variation in polymer molecular structures did not influence the performance of the polymers. However difference in pattern dimensions needs to be considered while fabricating micropatterned polymeric scaffolds.

5.7 References

Anderson D. G., Lynn D. M., and Langer R. Angew. Chem. Int. Ed., **2003**, 42, 3153.

Anderson D. G., Tweedie C. A., Hossain N., Navarro S. M., Brey D. M., Vliet K. J., Langer R., Burdick J. A. *Materials, Adv. Mater.* **2006**, 18, 2614.

Brey D. M., Erickson I., Burdick J. A. *J Biomed Mater Res.* **2008[a]**, 85A, 731.

Brey D. M., Ifkovits J. L., Mozia R. I., Katz J. S., Burdick J. A. *Acta Biomaterialia*, **2008[b]**, 4 , 207.

Dawson E., Mapili G., Erickson K., Taqvi S., Roy K. *Advanced Drug Delivery Reviews*, **2008**, 60, 215.

Gates B. D., Xu Q., Stewart M., Ryan D., Willson C. G., Whitesides G. M. *Chem. Rev*. **2005**, 105, 1171.

Green J. J., Langer R., Anderson D. G. *Accounts of chemical research*, **2008**, 41, 749.

He B., Park M. B. *Macromolecules*, **2005**, *38,* 8227.

Jason D. C., Jessica M. S., Robert F. M., Guymon C. A. *Polymer*, **2007**, 48, 6554.

Langer R., Vacanti J. P., *Science*, **1993**, 260, 920.

Laus M., Angeloni A. S., Galli G., Chielhi E., *Makromol. Chem.*, **1988**, 189, 743.

Lee T-W., Mitrofanov O., Hsu J-W. P. *Adv. Fun. Mat.* **2005**, 15, 1683.

Lynn D. M., Langer R. *J. Am. Chem. Soc.*, **2000**, *122,* 10761.

Lynn D. M., Anderson D. G., Putnam D., Langer R. *J. Am. Chem. Soc*., **2001**, *123,* 8155.

Okada M. *Prog. Polym. Sci.,* **2002**, 27, 87.

Park M. B.,Yan Y., Neo W. K., Zhou W., Zhang J., Yue C. Y., *Langmuir* **2003,** *19,* 4371.

Park M. B., Zhu A. P., Shen J. Y., Fan A. L., *Macromol. Biosci.,* **2004**, 4, 665.

Randall C. L., Leong T. G., Bassik N. a, Gracias D. H. *Advanced Drug Delivery Reviews*, **2007**, 59 , 1547.

Santini Jr. J. T., Cima M. J., Langer R. T. *Nature*, **1999**, 397, 335.

Sawhney A. S., Chandrashekhar P. P., Hubbell J. A. *Macromolecules*, **1993**, 26, 581.

Shen J-Y., Park M. B., Feng Z-Q., Chan V. , Feng Z-W. *J Biomed Mater Res Part B: Appl Biomater*, **2006**, 77B, 423.

Tao S. L., Desai T. A. *Advanced Drug Delivery Reviews*, **2003,** 55, 315.

Vert M. *Biomacromolecules*, **2005,** 6, *538.*

Wang G-J., Hsu Y-F., Hsu S-H., Horng R. H. *Biomed Microdevices* , **2006**, 8,17.

Xia Y., Rogers J. A., Paul K. E., Whitesides G. M. *Chem. Rev*., **1999**, 99**,** 1823.

Xia Y., Whitesides G. M. *Annu. Rev. Mater. Sci.,* **1998**, 28,153.

Yan Y., Park M. B., Gao J., Yue C. Y. *Langmuir***, 2004**, *20,* 1031.

Zhu A., Chen R., Park M. B. *Macromol. Biosci.*, **2006**, 6, 51.

Chapter 6

Soft lithography technique to fabricate unusual patterns

6.1 Introduction

The micropatterned polymers can be used in tissue engineering scaffolds (Naughton and Mansbridge 2004), and biosensors (Tsai et. al. 2009) applications. Micropatterned stimuli sensitive polymeric biomaterials find applications in bio-mimetics (Peppas and Ward 2004). In addition to advanced techniques such as electron-beam, X-ray, extreme UV/deep UV, and focused ion-beam lithography (Ito and Okazaki 2000) soft lithography techniques such as replica molding, self-assembly of organic molecules, template deposition and size reduction are used in microfabrication (Xia and Whitesides 1998).

For micropatterning of polymer surfaces, UV-microembossing and hot embossing techniques are commonly used (Yan et. al. 2004). Typically a Polydimethylsiloxane (PDMS) stamp or mold bearing the desired micropattern is used as a template for replication (McDonald and Whitesides 2002). PDMS is an inert, non-toxic, and optically transparent material, and has chemical and physical properties suitable for non-planar and large area patterning. PDMS stamps can be generated by casting a precursor solution against a suitable mold, usually a silicon master fabricated by photolithography. In previous chapter we discussed UV- microembossing technique for solvent free processing of SCPBAEs to fabricate biodegradable scaffolds having channel, square trenches and circular wells patterns. However pattern geometries that can be processed by replication are limited to those that can be obtained by optical lithography. Features such as squares, rectangles, cylinders can be readily fabricated with PDMS stamps. More complex topologies such as spheres or ellipsoids are difficult to fabricate. Hence creative modifications of existing patterning techniques as well as new innovative approaches are needed to develop cost competitive solutions which can be practiced on large scales (Xia et. al. 1999). During the past decades this strategy has been pursued rather aggressively by materials scientists to create technologically useful ordered patterns using chemical and physical routes (Bunz 2006; Rabani et. al. 2003). Such complex patterns are often desired for the fabrication of tissue engineering scaffolds for directed growth, microdevices for drug delivery, microbioreactors, microlens arrays and many other applications.

In this chapter we describe processing of SCPBAES containing solvents to show how incarporation of solvent helps to develop features not initially present in the PDMS mold. This technique helps to generate complex patterns on the surface of polymer film which is otherwise difficult to create on parent silicon masters or

PDMS molds. Before we discuss how the use of solvent helps us to develop more complex structure during soft lithography processing, we briefly review some of the soft lithograhy techniques modified to fabricate complex features.

6.1.1 Mechanical deformation of polymer molds

In this technique the patterns which were difficult to prepare using conventional lithographic as well micromolding technique were fabricated. This was achieved by first deforming the PDMS molds followed by replication of the patterns present on the surface of the mold. To attain the topologically difficult microstructures, the elastomeric PDMS mold bearing simple regular and planar structure was deformed by three means 1) compression, 2) bending and 3) streching as shwon in figure 6.1. These techniques have broad applications including applied optics, grafting on non-planar surface, cell culture and MEMS (Xia et. al. 1996).

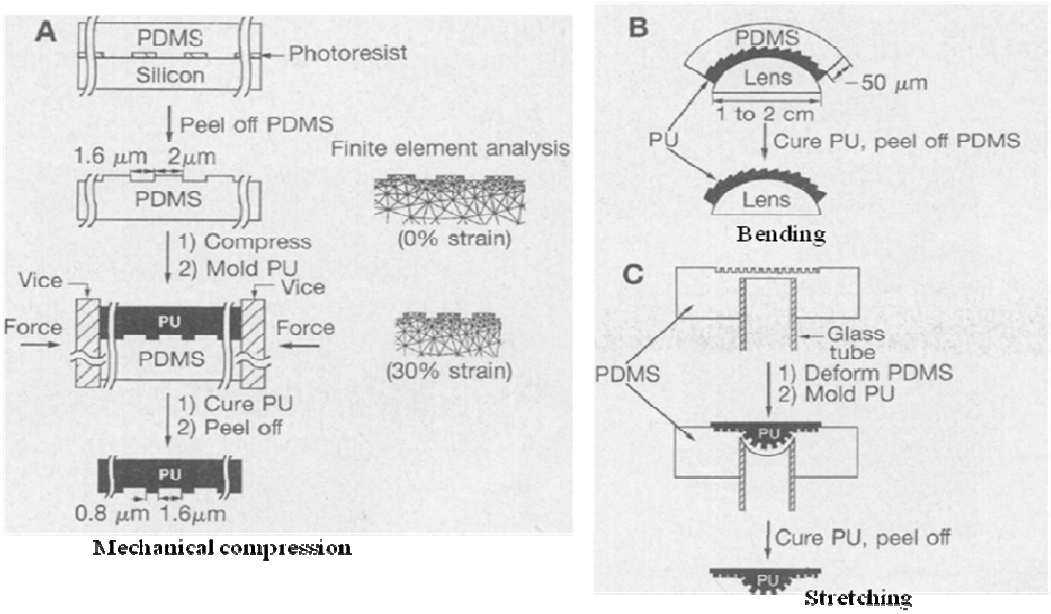

Figure 6.1: Schematic of molding-replication against an elastomeric master (adapted from Xia et. al. 1996)

6.1.2 Liquid filled microlens arrays

This micromolding technique was developed to fabricate arrays of microlens having size from hundreds of microns to several mililmeters (Chronis et. al. 2003) . It involves two steps,

1) Fabrication of PDMS molds consisting circular chambers which are

interconnected via microchannels (figure 6.2).

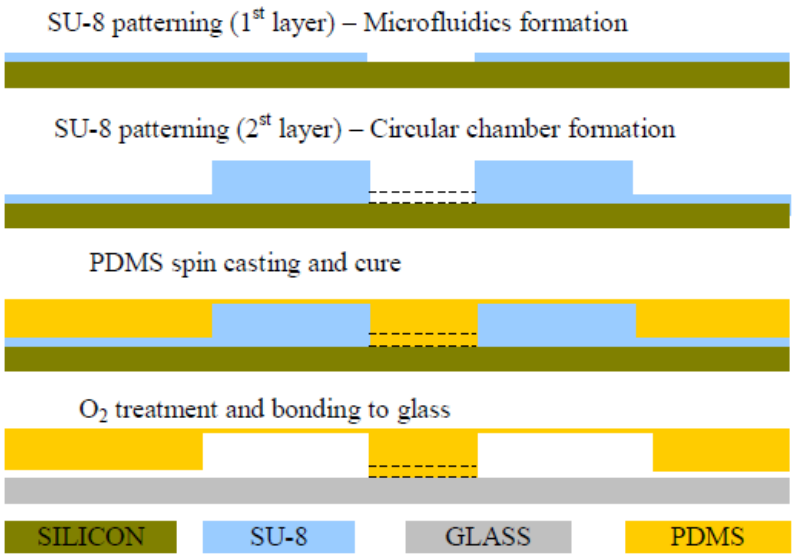

Figure 6.2: The fabrication process for integrating microfluidics on bottom of the microlens arrays (adapted from Chronis et. al. 2003)

2) Preparation of microlens array by pressure filling the liquid having higher refractive index than PDMS in the microchambers (figure 6.3).

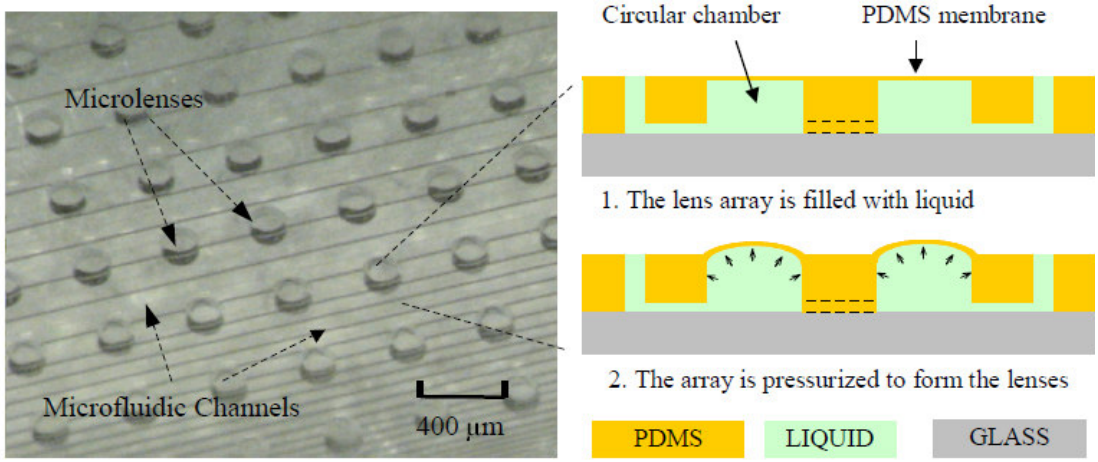

Figure 6.3: Optical micrograph of the microlens array (adapted from Chronis et. al. 2003)

6.1.3 Thermal reflow processes

The thermal reflow techinique was developed to fabricate spherical and square

microlens array (Yang et. al. 2004). The process involved the fabrication of either cylindrical or square resist post on substrate followed by heating the material above its glass transition temperature to attain spherical or square microlens array (figure 6.4).

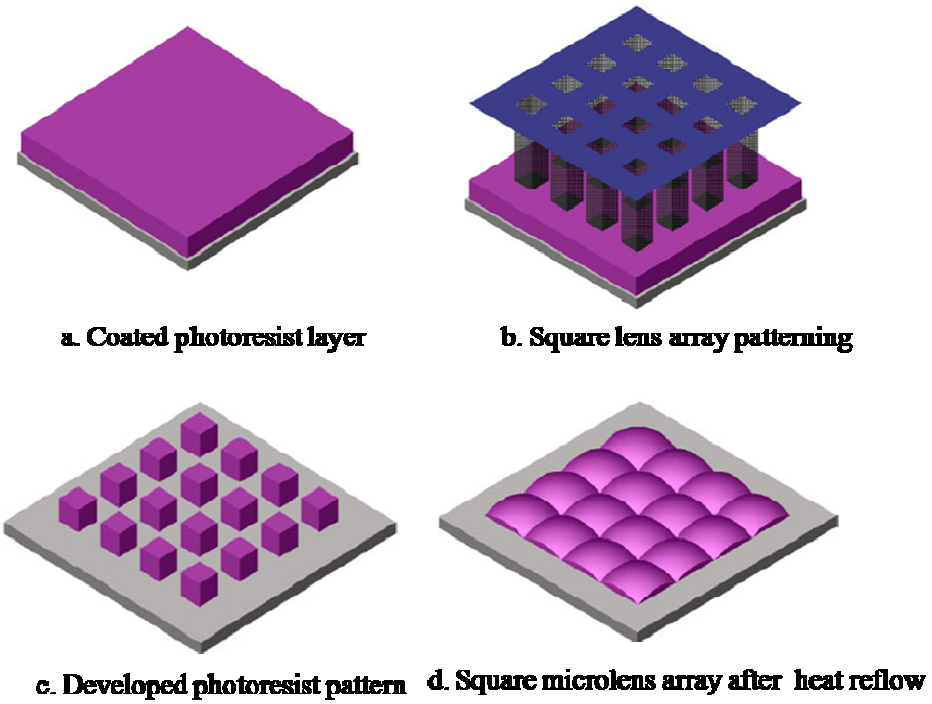

Figure 6.4: Schematic of square microlens array fabrication process (adapted from Yang et. al. 2004).

These microlens arrays have been used in photolithography, imaging, optical communications and recently for a lab-on-a-chip systems (Chronis et. al. 2003; Yang et. al. 2004).

6.1.4 Gel entrapment

The entrapment technique was developed to produce ordered microlens array (Cayre and Paunov 2004). This techniques involves three steps,

1) Formation of self assembled monolayer of charged latex particles (polystyrene sulfate) at oil-water interface.
2) Replication of self assembled monolayer on PDMS resin by gel trapping technique.
3) Fabrication of microlens array bearing shape complementary to PDMS template via replica molding of photopolymer.

Schematic of gel entrapment technique is shown in figure 6.5.

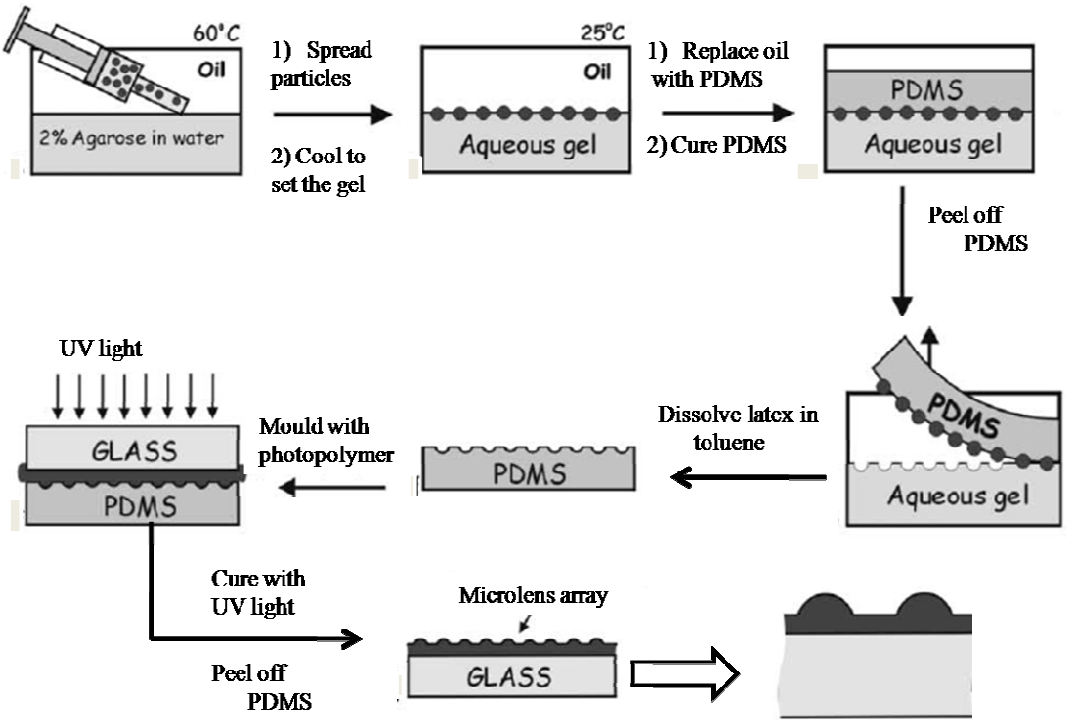

Figure 6.5: Gel entrapment process for fabrication of microlens array (adapted from Cayre and Paunov 2004)

6.1.5 Silicon mould with high aspect ratio patterns

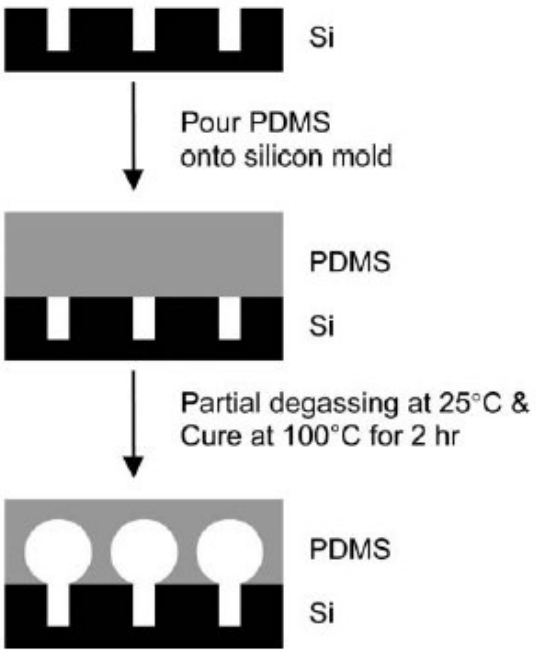

Figure 6.6: Cavity formation process (adapted from Giang et. al. 2007)

In this technique silicon wafer mold comprising deep reactive ion etched (DRIE) trenches was used to create smooth concave cavities in polydimethylsiloxane (figure 6.6). This technique enabled manipulation of radius of curvature of the cavities formed. These cavities are further used to create either shallow pits or spherical cavities. Such structures are useful in microlens molding and to create microbioreactor array (Giang et. al. 2007).

6.1.6 Deformation of PDMS membrane using air pressure through SU-8 shadow mask

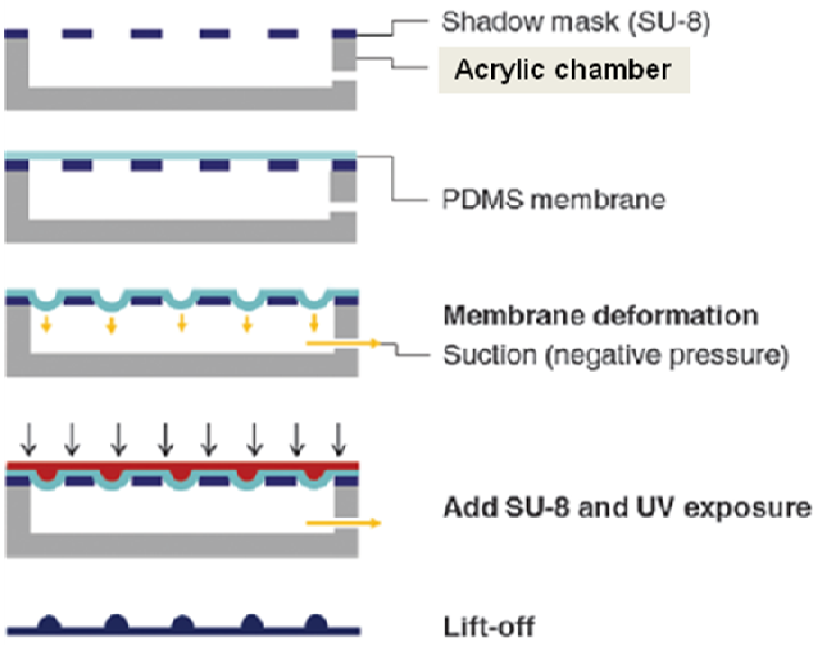

Figure 6.7: Fabrication of convex and concave microstructures (adapted from Park et. al. 2009)

In this microfabrication technique a thin (10–20 μm) PDMS membrane, SU-8 shadow mask, and compressed air are used to fabricate convex and concave microstructures. Briefly, a simple acrylic vacuum device is connected to an air compressor. SU-8 mask with patterned microholes (size in the range of 100 to 300 μm) is fabricated using photolithography. This mask is clamped onto the vacuum device followed by placing a thin elastic PDMS film on the top of SU-8 mask and suction applied. The suction pressure is adjusted to fabricate the arrays of concave and convex chambers varying in diameter and curvature (figure 6.7). The patterns generated using this

microfabrication technique is expected to be useful in bio-MEMS applications such as microbioreactors, microlenses and also in cell differentiation (Park et. al. 2009).

6.1.7 Elastic contact induced self organized patterning of soft polymer films

This technique is used to engineer variety of self-organized, ordered structures such as channels, posts, and wells, patterned in PDMS elastomeric films. A simple stamp consisting of parallel channels is used to prepare more complex structures, such as an array of femto-liter beakers and doubly periodic channels. This technique uses elastic stamp hence in-situ tuning, manipulation, and reconfiguration of the microstructures is easy. The conventional photolithography needs radiation cross-linkable polymers. In contrast the elastic contact lithography can be used for any soft polymer, including hydrogels and the glassy polymers softened by heating or plasticizers (Gonuguntla et. al. 2006).

6.1.8 Patterning through selective inversion of a liquid–liquid bilayers

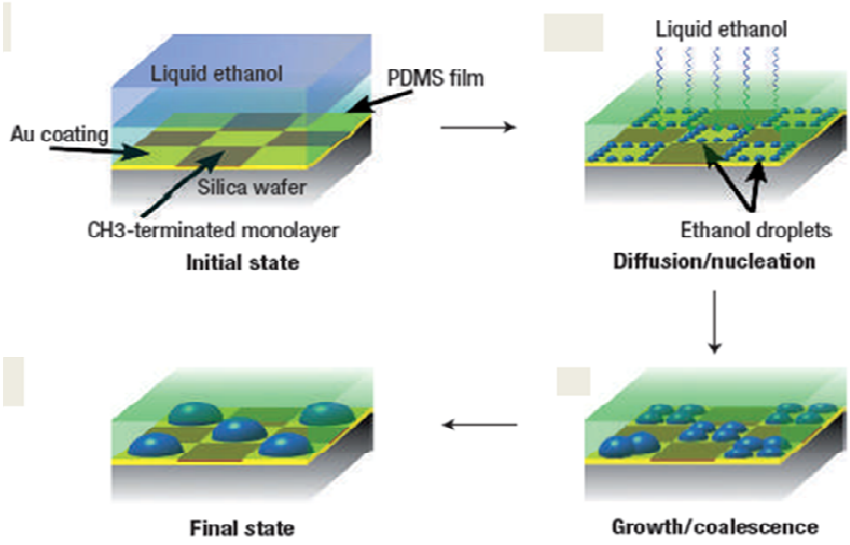

Figure 6.8: Schematic of PDMS film patterning (adapted from Léopoldés and Damman 2006)

In this process viscous PDMS is applied on silica wafer with gold / self-assembled monolayer of hexadecanethiol chessboard type surface. This PDMS coated wafer is then immersed in ethanol solution for 24 hrs. Ethanol diffuses through PDMS layer and coalesces to form 3D structured PDMS layer (figure 6.8). After patterning, the

PDMS film is UV-cured and peeled off from the substrate. This system is promising for creating patterns useful for microfluidics and biosensor applications (Léopoldés and Damman 2006).

In the context of recent efforts to fabricate more complex patterns, we present in this chapter a simple new approach for the creation of unique highly ordered mixed microcavity patterns. Patterns generated using this approach comprise the replica of the parent mold and an additional pattern not present in the parent mold, formed through template modulated solvent vapour back-pressure. A viscous polymer solution is poured onto a PDMS mold bearing simple geometric pattern replicated from a silicon master. Evolution of solvent vapours through the viscous polymer solution concurrently with cross-linking, results in the generation of the patterns not present in the parent PDMS mold. We further show that the modified pattern thus generated in the polymer can be subsequently transferred to another PDMS mold to generate multiple copies of the said pattern. We demonstrate the technique using a biodegradable polymer [poly (β-amino ester)] having pendant unsaturated C=C bonds, (figure 6.9). The specific polymer used was Poly (trimethylolpropane triacrylate - Co - 4, 4'-trimethylenedipiperidine) [poly (TMPTA-Co-TMDP)].

6.2 Experimental section

6.2.1 Materials

Trimethylolpropane triacrylate (TMPTA), 4, 4'-trimethylenedipiperidine (TMDP) and 1-hydroxy cyclohexyl phenyl ketone were purchased from Aldrich Chemicals and Sylgard 184 from Dow Corning. Aluminum chloride ($AlCl_3$), benzoyl chloride were purchased from Merck India ltd. and used without further purification. Dichloromethane (DCM), dichloroethane and tetrachloroethylene were purchased from Merck India ltd. and further purified and dried using standard methods. The silicon masters were provided by Dr. Rabah Boukherroub from Institut de recherché Interdisciplinaire (IRI) France.

6.2.2 Polymer synthesis

Synthesis of poly (TMPTA-Co-TMDP)

In a 100 ml jacketed reactor 2.96 g (1.00×10^{-2} moles) of TMPTA was dissolved in 150 ml chloroform. 2.10 g (1.00×10^{-2} moles) of TMDP was first dissolved in 50 ml chloroform and added dropwise to the acrylate solution with constant stirring at 53 °C. The reaction mixture was maintained at this temperature for 5 days. It was then cooled to room temperature and extracted thrice with aqueous brine solution. The organic layer was dried over night on anhydrous sodium sulphate. Chloroform was evaporated under reduced pressure. The polymer was precipitated twice in pet ether, and vacuum dried prior to analysis. The polymer poly (TMPTA-Co-TMDP) was characterized using ^{1}H NMR and FTIR spectroscopy to confirm the presence of unsaturations.

6.2.3 Fabrication of PDMS mold by replica molding

Poly (dimethylsiloxane) (PDMS) was used for elastomeric stamp fabrication. The two parts were mixed in 10:1 weight ratio, thoroughly mixed and degassed in vacuum for 30 minutes to ensure the removal of the air bubbles created during stirring. After degassing, the prepolymer mixture was poured onto the silicon master and degassed for 5 minutes in vacuum to remove the air bubbles created during pouring. The stamp was cured thermally at 80 °C for 1 hour. After curing PDMS turned into an elastomeric rubber and could be easily removed from the silicon master. These PDMS molds were characterized using scanning electron microscope (SEM). The schematic of fabrication process is shown in figure 6.10 and dimensions of the PDMS molds are summarized in table 6.1.

Table 6.1: Pattern dimensions of silicon master and PDMS mold

Patterns	Silicon masters*			PDMS molds#		
	w µm	s µm	d µm	w µm	s µm	d µm
Sq1	50	100	45	50	100	45
Sq2	50	50	45	50	50	45
Sq3	50	100	20	50	45	20

** Pattern dimensions provided by suppliers, # pattern dimensions measured using SEM. Sq – squares, w- post or trench width, s-distance between two posts or trenches and d-height of post or depth of trench.*

6.2.4 Fabrication of polymeric scaffolds

Poly (TMPTA-Co-TMDP) along with the photo-initiator 1-hydroxycyclohexyl phenyl ketone were dissolved in dichloromethane and poured in the PDMS mold. Typically PDMS mold having square posts of height 50 µm, width 50 µm and distance between two posts 100 µm was used for fabrication of UV-microembossed polymeric film. After 1 min polymer was cured under UV light for 15 min and cured. Patterned polymeric film was peeled off from PDMS mold.

6.2.5 Effect of fabrication parameters on morphology and position of microcavities

Following experiments were carried out to study the effect of variations in fabrication parameters on morphology and position of microcavities evolved in the polymeric scaffolds from PDMS molds.

6.2.5.1 Variations in polymer solution viscosity

Polymer solutions having varying viscosities in the range 24 - 250 cP were prepared. The polymer was dissolved in different amounts of dichloromethane and viscosity was measured using Brookfield Viscometer LVDV-II + PRO (Brookfield Engineering Laboratories, USA), spindle type CPE 42, spindle speed 0.3 RPM, solvent dichloromethane, temperature 25 ºC and sample volume 1 ml. These polymer

solutions having different viscosities were used to fabricate microcavity patterned polymer films.

6.2.5.2 Variations in solvent vapor pressure

Polymer solutions having viscosity ~250 cP were prepared using three different solvents varying in boiling points (BP) and vapor pressure (VP). (a) dichloromethane [BP. 39.8 °C, VP. 349 mm Hg (20 °C)]; (b) dichloroethane [BP. 83 °C, VP. 60.98 mm Hg (20 °C)] and (c) tetrachloroethylene [BP. 121 °C, VP. 13 mm Hg (20 °C)].

6.2.5.3 Variations in polymer film thickness

Polymer solution of viscosity ~250 cP was prepared in dichloromethane. This was poured in PDMS molds to fabricate micropatterned polymeric films of different thickness and crosslinked subsequently by UV light. Three micropatterned films having thickness 150, 300 and 700 µm were fabricated

6.2.5.4 Variations in pre-curing time

During the pre-curing time solvent partially evaporates before the polymer film is exposed to UV light. Three pre-curing times 1 min, 7 mins and 30 mins were selected to study the effect of pre-curing time on the shape and alignment of microcavity.

6.2.5.5 Variations in aspect ratio and pattern density of PDMS mold

Three PDMS molds of varying pattern density and aspect ratio were selected to study effect of these parameters on microcavity morphology and position. The dimensions of the micropatterns present on PDMS molds used for these studies are listed in table 6.1.

6.2.6 Fabrication of microembossed PDMS molds

Patterns generated on polymer film were subsequently transferred on PDMS film by replica molding technique. The micropatterned polymeric film was placed in flat glass petri dish with pattern cavity opening facing upward. The PDMS prepolymer and curing agent were mixed in the ratio 10:1 by weight, degassed by vacuum to remove air bubbles created during stirring. After degassing the PDMS prepolymer, the

mixture was poured carefully over the patterned polymer film and degassed for 5 minutes in vacuum to remove the air bubbles created during pouring. PDMS was then cured at 80 ℃ for 1 hr. Micropatterned polymer film was separated from cured PDMS film in dichloromethane carefully. Mushroom type features along square posts complementary to microcavities and square trenches present on polymer film were reproduced on PDMS film surface.

6.2.7 Polymeric scaffolds characterization by ESEM

Scanning electron microscopy (Quanta 200 3D, FEI) was used to observe the microstructures on PDMS moulds and polymer films. Optical images of polymer films were taken with Nikon Eclipse, E600-POL (Japan).

6.3 Results and discussion

6.3.1 Synthesis of Poly (TMPTA-Co-TMDP)

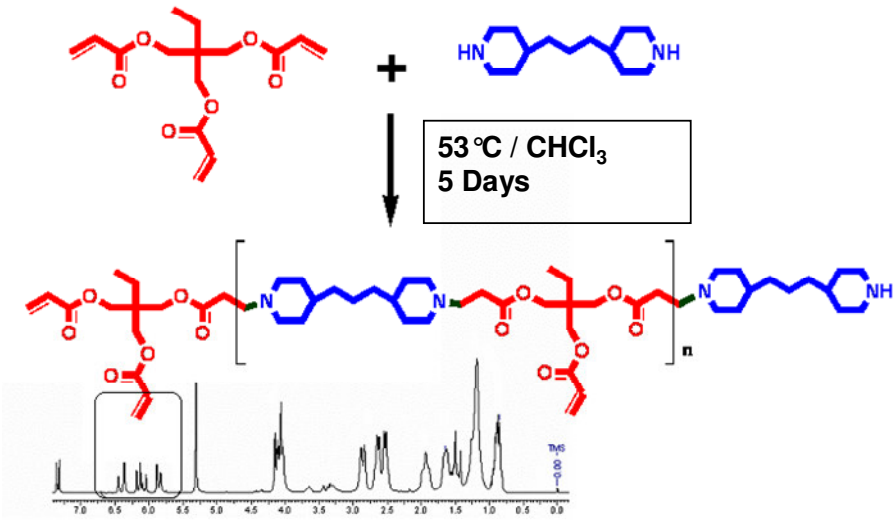

Figure 6.9: Synthesis of Poly (TMPTA-Co-TMDP)

As reported in the earlier chapter, we used a single step methodology for the synthesis of biodegradable poly (β-amino esters) having pendant unsaturated C=C bonds (figure 6.9)**.** Poly (trimethylolpropane triacrylate-Co-4 4'-trimethylene dipiperidene) was further evaluated, using soft lithography technique.

6.3.2 Fabrication of PDMS mold

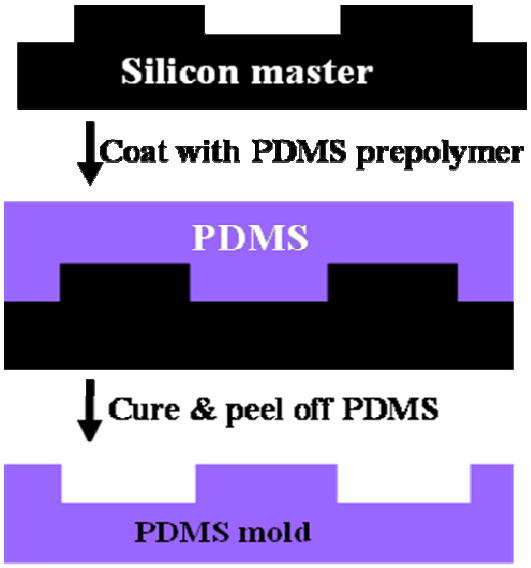

Figure 6.10: fabrication of PDMS mold via replica molding

PDMS molds with raised square micropillars were fabricated using silicon master via replica molding technique discussed earlier (table 6.1). The schematic of fabrication technique is shown in figure 6.10. Out of these molds Sq1 was used to explore the microcavity formation during the UV-microembossing.

6.3.3 Fabrication of micropatterned polymer film

PDMS mold with square micropillars pattern on the surface was selected to fabricate micropatterned polymer film. Poly (TMPTA-Co-TMDP) solution in dichloromethane having a viscosity of 250 cP was poured in to the PDMS mold. Polymer was cured by UV irradiation for 15 mins to yield micropatterned crosslinked film. The film was easily peeled off from PDMS mold. When observed under optical microscope the film revealed unusual self-organized highly ordered uniformly sized microcavities aligned along the original pattern, figure 6.11a shows an optical image of such a polymeric film.

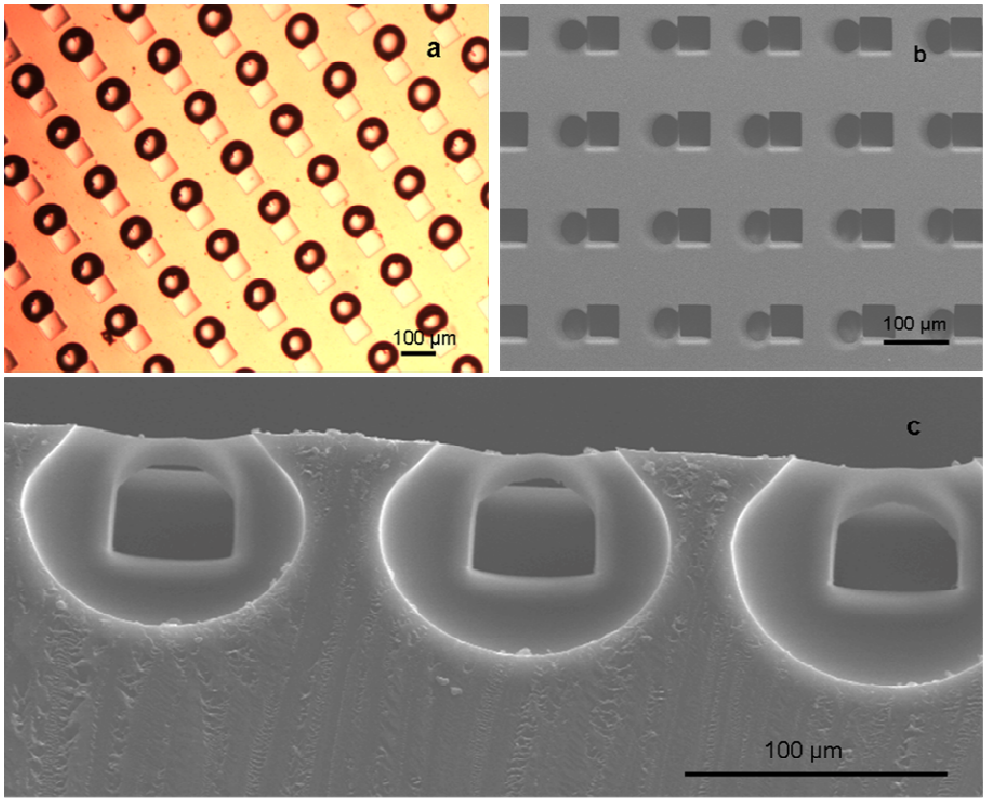

Figure 6.11: (a) Optical (b) SEM images of self assembled microcavities in micropatterned Poly (TMPTA-Co-TMDP) (c) cross section image

These polymeric films were further characterized using SEM to study surface morphology. The SEM results revealed that the microcavity evolved along the square trenches corresponding to square pillars of PDMS mold fused with each other. This led to the formation of patterns which were not present on the parent mold (figure 6.11b). Cross section of these patterns also showed that the mouth of the microcavity was smaller than the body of the cavity and appeared like a balloon and clearly showed the connectivity between balloon like and square cavity (figure 6.11c).

6.3.4 Effect of variations in fabrication parameters on microcavity morphology and position

It has been observed that formation of microcavity depends on the fabrication parameters such as viscosity of the polymer solution, nature of the solvent, thickness of the film, precuring time, aspect ratio and pattern density of PDMS molds. The influence of the parameters was examined to study the dependence on size, position and morphology of microcavities evolved. This would also help to understand the mechanism of microcavity formation.

6.3.4.1 Effect of solution viscosity

We used polymer solutions in the range 24 -250 cP to investigate the dependence on viscosity. It was observed that the diameter of the mouth of the microcavity decreased systematically with increasing solution viscosity and that its location vis a vis the pillar position changed as well. As shown in figure 6.12 the mean approximate mouth size of the cavities decreased from 75 µm to 40 µm as the solution viscosity increased from 24 cP to 250 cP. When solution viscosity was 24 cP and 132 cP each cavity was located at the center of the four adjacent square trenches (figure 6.12a,b), whereas at 250 cP viscosity the cavities were aligned next to the square trench (figure 6.12c). It is interesting to note that the positions of microcavities are highly reproducible. The location of the cavity vis a vis the pillars appears to be guided by hydrodynamic gradients and strains as discussed later.

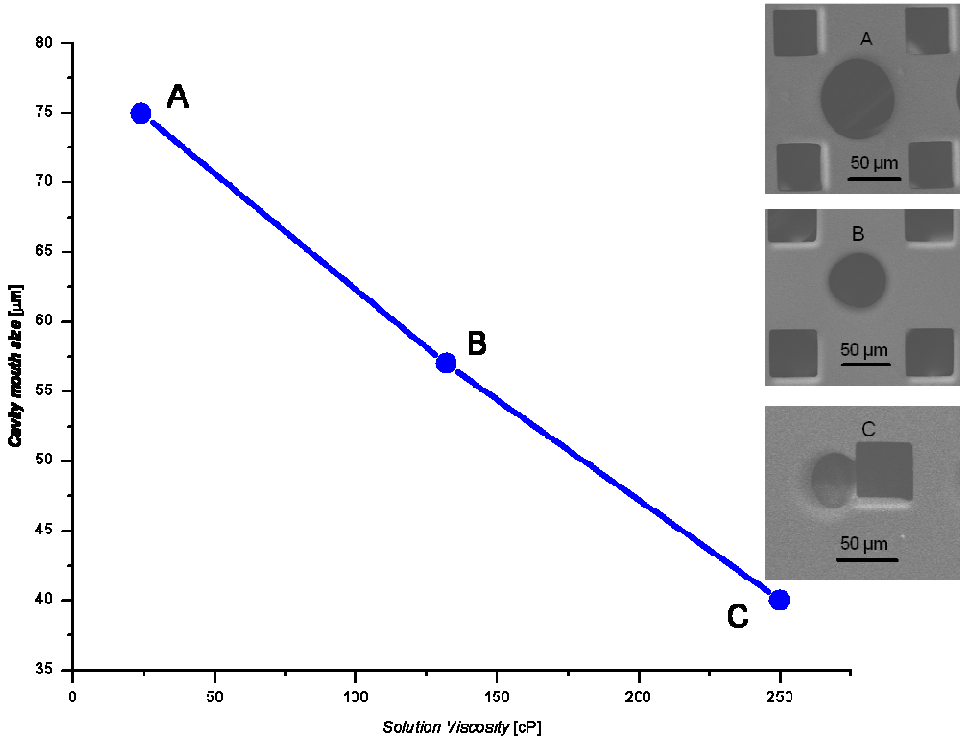

Figure 6.12: Evolution of microcavity mouth size with polymer solution viscosity

6.3.4.2 Effect of aspect ratio and pattern density

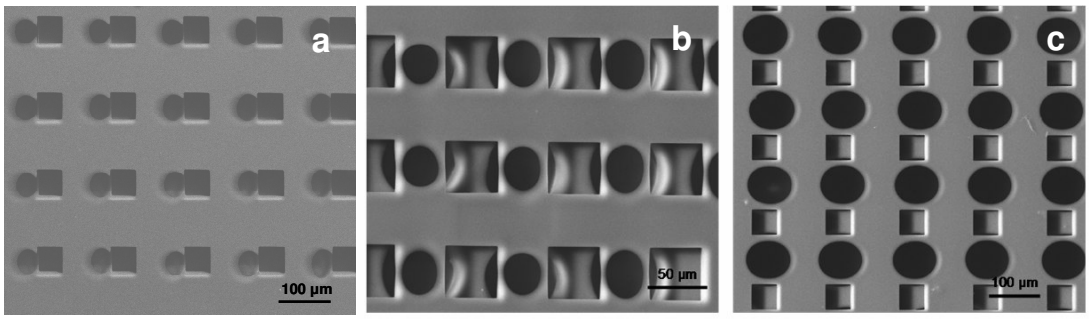

Figure 6.13: Variation in the size and shape of microcavities along with pattern dimensions

With varying pattern dimensions and density, the alignment and size of the cavities also varied. Figure 6.13 shows SEM images of microcavities obtained for different pattern dimensions. Interestingly with this technique it is also possible to manipulate fabrication of isolated or interconnected cavities beneath the original patterns. PDMS molds of higher pattern density facilitate formation of cavities that are internally connected to the square trench in the polymer replica. One such case is shown in figure 6.13b. When the height of the pillar is reduced to half of the initial, as shown in figure 6.13c, ellipsoidal cavities are formed with increased size.

6.3.4.3 Effect of solvent vapor pressure

In order to study the effect of solvent properties, especially their vapor pressure at the processing temperature, we used three solvents dichloromethane, dichloroethane and tetrachloroethylene having increasing boiling points. There was no significant difference between the nature of microcavities obtained using dichloromethane (39.8 ºC) (figure 6.14a) and dichloroethane (83 ºC) (figure 6.14b). However when tetrachloroethylene (121 ºC) was used as solvent the resulting microcavities did not evolve homogeneously throughout the polymer film (figure 6.14c)

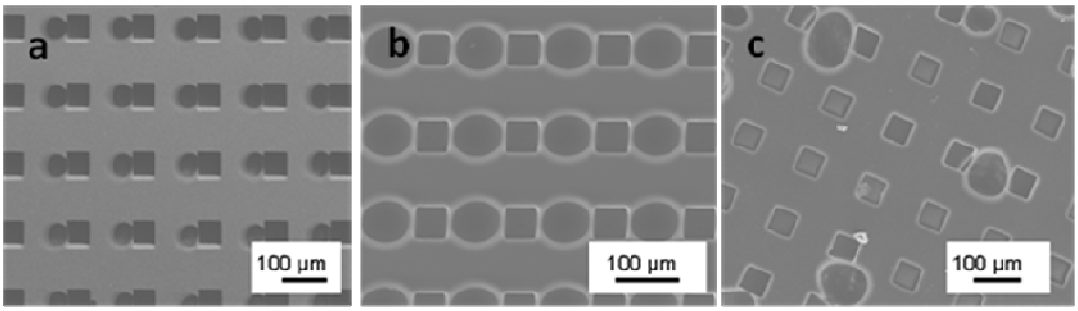

Figure 6.14: SEM images of microcavity pattern in polymer films fabricated by using (a) dichloromethane, (b) dichloroethane and (c) tetrachloroethylene

6.3.4.4 Effect of film thickness

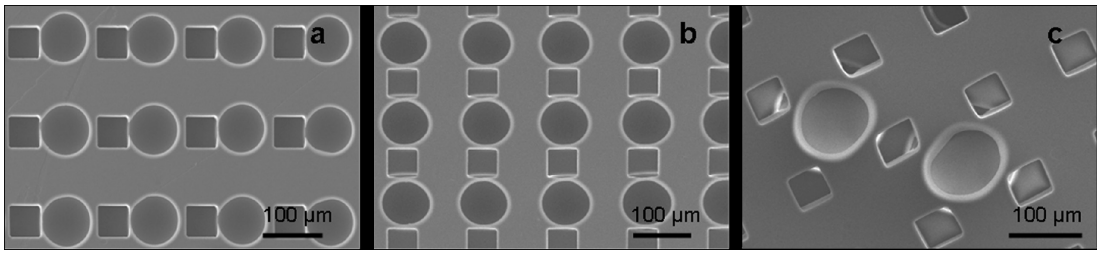

Figure 6.15: SEM images of microcavity pattern occurred in polymer films of the thickness (a) 150 ± 5 µm (b) 300 ± 20 µm (c) 700 ± 30 µm

Experiments were carried out to explore the effect of film thickness on size and position of microcavity mouth size. Polymer films of thickness ~ 150 ± 5 µm, 300 ± 20 µm and 700 ± 30 µm were obtained by controlling initial liquid spreading. Figure 6.15 shows that in the polymer film having a thickness of 150 ± 5 µm, the mouth of microcavity is 56.22 ± 5µm in dia and the microcavities are evenly distributed. Each microcavity is fused to a square trench (figure 6.15a). For a film thickness of 300 ± 20 µm the mouth of microcavity is 85 ± 5 µm in dia and evenly distributed. Each microcavity is located in between two square trenches attached to both the trenches (figure 6.15b). In case of 700 ± 30 µm thick UV-cured film, mouth of microcavity is 100 ± 5µm in dia. However, these microcavities are not evenly distributed in the film but each balloon is located at the centre of four square trenches (figure 6.15c). The results are best understood in terms of mechanism proposed below.

6.3.4.5 Effect of pre-curing time

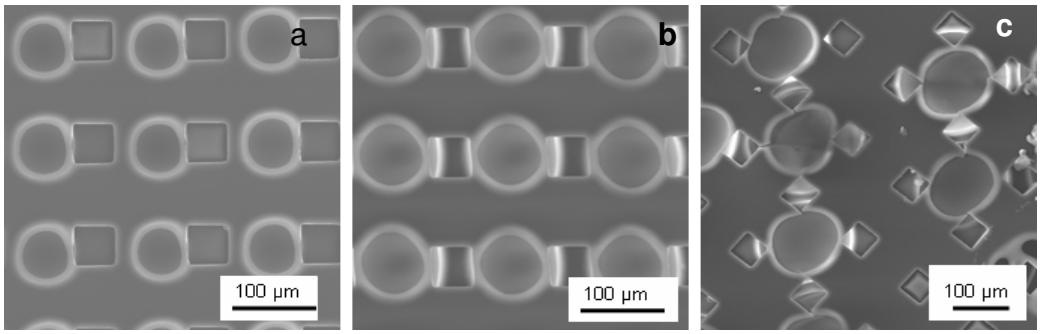

Figure 6.16: SEM images of microcavity pattern in polymer films. Precuring time (a) 1 min, (b) 7 min, (c) 30 min

Figure 6.16 shows that the precuring time also has an effect on the size and alignment of microcavities. In this case, prepolymer solution was spread over the three different PDMS molds having same pattern dimensions. The film thickness of the polymer was also maintained uniform (150 ±5 µm). Pre-curing time was varied between 1-30 mins to study the effect of precuring time on size and position of microcavity. When precuring time was 1 min the microcavity mouth size was small 60 ±5 µm and each microcavity was fused to the square trench (figure 6.16a). When pre-curing time was increased to 7 min the mouth of microcavity increased to 80 ± 5 µm in diameter and each microcavity was located in between two square trenches attached to both the trenches (figure 6.16b). In case of 30 min pre-curing time further increase in microcavity mouth size to 110 ± 5µm in diameter was noted. Microcavities were located at the centre of four square trenches (figure 6.16c).

6.4 Mechanism of bubble formation

Initially we considered the possibility of formation of microbubbles and their coalescence leading to microcavities, which would depend on solution vapor pressure. Dichloroethane having a boiling point (83˚C) higher than that for dichloromethane (39˚C) was tried. No significant differences between the basic features of the patterns were noted. The diameter of microcavity mouth was different for dichloromethane (45 µm) and dichloroethane (80 µm) as expected (figure 6.14). The possibility of microbubble formation was refuted since the cavity patterns were not seen when soft lithography was performed on non-

patterned PDMS surface.

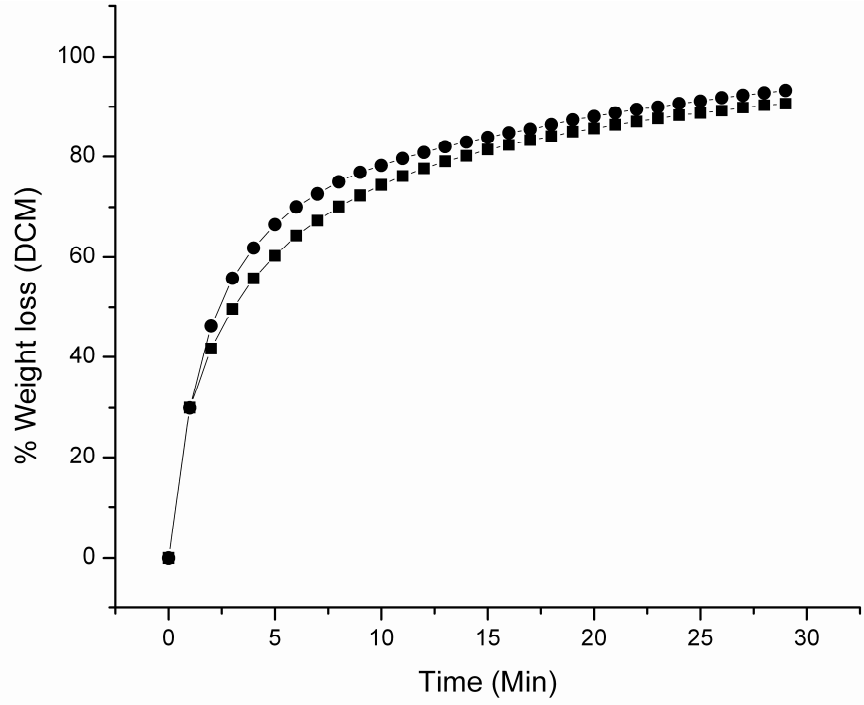

Figure 6.17: Weight loss of dichloromethane from –●–plane and –■–pattern PDMS surface

In order to estimate a possible time period over which the microcavity formation may take place, the rate of loss of fluid from the polymer film was monitored during the course of curing. Figure 6.17 summarizes weight loss of fluid for the polymer film formed on a plane PDMS surface and when formed on the patterned surface, a condition under which the microcavities were actually formed. We could get excellent fits to the curves with second order exponential $1- e^{-\alpha 1t} - e^{\alpha 2t}$ type behavior. The time constants ($1/\alpha 1$ and $1/\alpha 2$) obtained from fitting (χ^2~0.55) are 1.35 mins and 9 mins for the case of fluid loss from the liquid film on plane PDMS, and 0.88 mins and 7.95 mins ((χ^2 ~0.45) for fluid loss from the patterned PDMS surface, respectively. This implies that the microcavity formation must be taking place in the first few minutes of the process. Interestingly the difference observed between the two curves in figure 6.17 is rather small even when for the given pillar geometry, 88% of the bottom surface of the liquid film on patterned surface is open to the cavities below. In fact, the loss of fluid is slightly lower in the case of pattern supported film, which can be attributed to the fact that a portion of such a supported liquid film is not in thermal contact with the substrate.

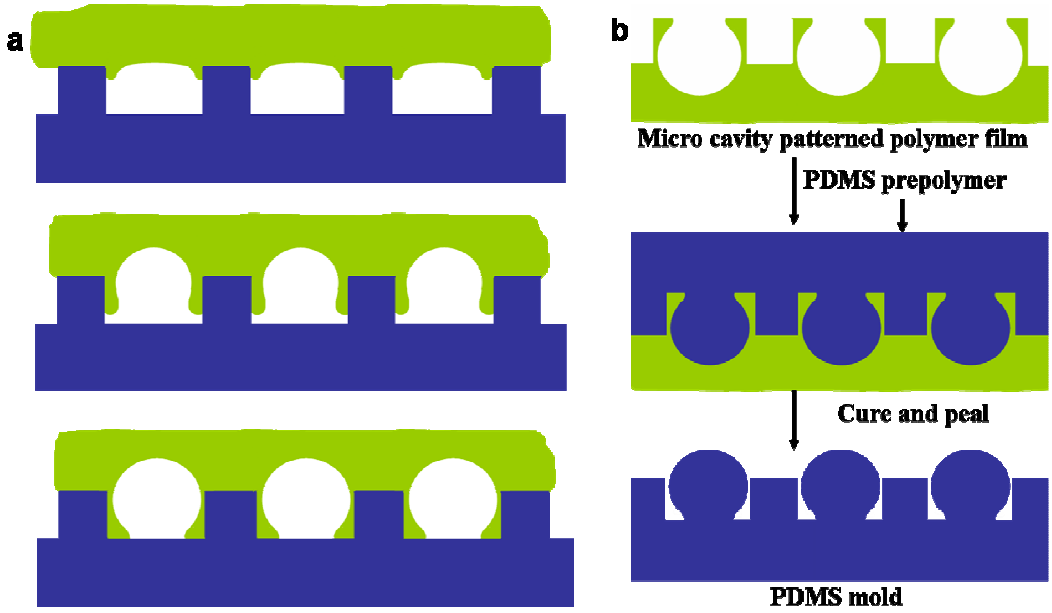

Figure 6.18: Schematic of (a) the possible mechanism of cavity formation, (b) replication of cavities to form complementary micromushroom patterns in PDMS

These observations suggest that the solvent vapor emerging from the bottom surface does not leave the system laterally at a rapid rate, a condition that enables the system to sustain some solvent vapor back pressure. We argue that this pressure holds back the polymer liquid film from flooding into the entrapped microcavities under self weight. The polymer solution can then creep down along the side walls as shown in figure 6.18. This will then push the lower surface profile of the liquid upwards as shown, forming a mushroom like balloon. The basic balancing forces involved under this condition and which would lead to the final observed pattern are thus the gravitational force and the force due to the solvent vapour back pressure (Laplace balance).

Given the dynamically evolving nature of the visco-elastic forces in the gradually drying solution however, there will be lateral tension forces within the film which will be modulated by the pillars and the self generated mushroom like cavities. The interplay of these forces will not only guide the manner in which a microcavity will locate itself vis a vis the pillar pattern, but will also induce long range ordering to minimize energy. One could in principle envision the thin visco-elastic film as a stretched membrane and seek the vertical displacement “u” as a function of lateral location by solving an equation,

$\nabla^2 u = - f/t$ (here "t" is the line tension, namely lateral in-plane force/length and "f" is the net upward the external force) with the boundary conditions provided by pillar geometry and the external forces stated above. Consolidating these plausibility arguments further in quantitative terms is clearly a complex problem, especially due to the high density of the pillars in relation to the length scale of the cavity feature formed, and would need computer modelling which is outside the scope of this work.

Also, in this case one can expect that depending on the viscosity of the solution and solvent evolution during drying, the size of the local microcavity can vary. To elaborate this point we briefly discuss the shapes and locations of the microcavities with respect to the pillar geometry for some cases of interest. The corresponding results are shown in figure 6.19. We have observed that when the solution viscosity is high (~250 cP), tiny ordered cavities attached to individual pillars are seen (Case-1). On the other hand when the viscosity is decreased progressively, the microcavity size can grow and strain interactions between cavities attached to two or four pillars can play a role. When the viscosity is high the size of the microcavity would be small and such a balloon nucleated at a random location would be pulled towards a pillar and get attached there to lower elastic energy via interface attachment (figure 6.19, Case-1). It can also move towards the face centre of the pillar and achieve further lowering of energy depending on the conditions and availability of such opportunity in the drying process. As the viscosity is lowered progressively, the size of microcavities would grow and it would begin to feel the strain fields of two or four pillars, thereby adjusting its location and shape gradually as shown for Cases 2, 3 and 4 in figure 6.19. It is also important to point out here that as one microcavity moves towards a particular location or organizes itself vis a vis the pillar configuration, the strains in the nearby region are bound to be influenced and this would lead other nearby cavities to organize themselves systematically to induce long range order and uniformity, as observed.

Self assembled microcavities fabricated by this technique can be useful in several applications. These cavities can be effectively used as microreservoirs for controlled drug delivery (Razzacki et. al. 2004; Grayson et. al. 2004; Santini et. al. 1999). Specifically, such narrow mouth and wide bottom reservoirs cannot be fabricated by any other microfabrication technique. These enhanced surface area architectures

formed beyond the area afforded by the original pattern should be useful in tailoring novel adhesion schemes as well as selective nanoparticle loadings for biosensors

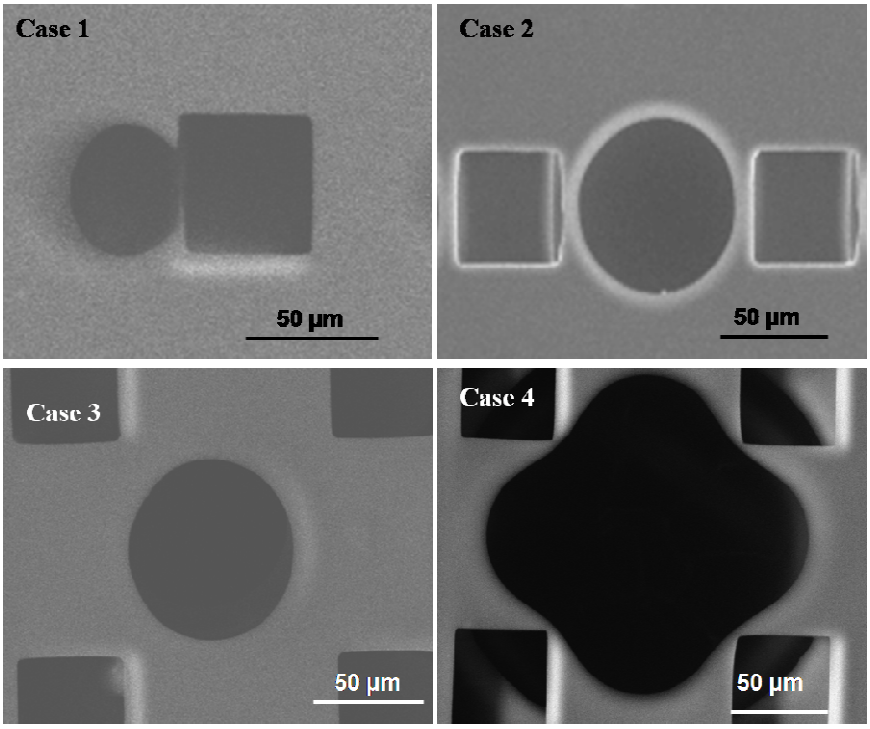

Figure 6.19: SEM pictures of shapes and locations of the microcavities with respect to the pillar geometry

6.5 Fabrication of microembossed novel PDMS molds

Polymer films bearing modified microcavities and the parent patterns were then used as templates to replicate these pattern in PDMS. PDMS moulding technique is discussed in section 6.2.6 and a schematic of process is shown in figure 6.18 b. Mushroom-like microstructures, which complement the microcavities, are seen to evolve concurrently in juxtaposition with the micropillars (figure 6.20). These PDMS molds show that the complementary patterns are also highly regular in their size, shape and placement. We believe that such patterns are interesting for many applications such as sensors, MEMS devices, microlens molding (Lee et. al. 2009), or to fabricate microbioreactor (Giang et. al. 2008). It would be interesting to study this approach with PDMS templates of different patterns i. e. microcircles, tapered microstructures, etc.

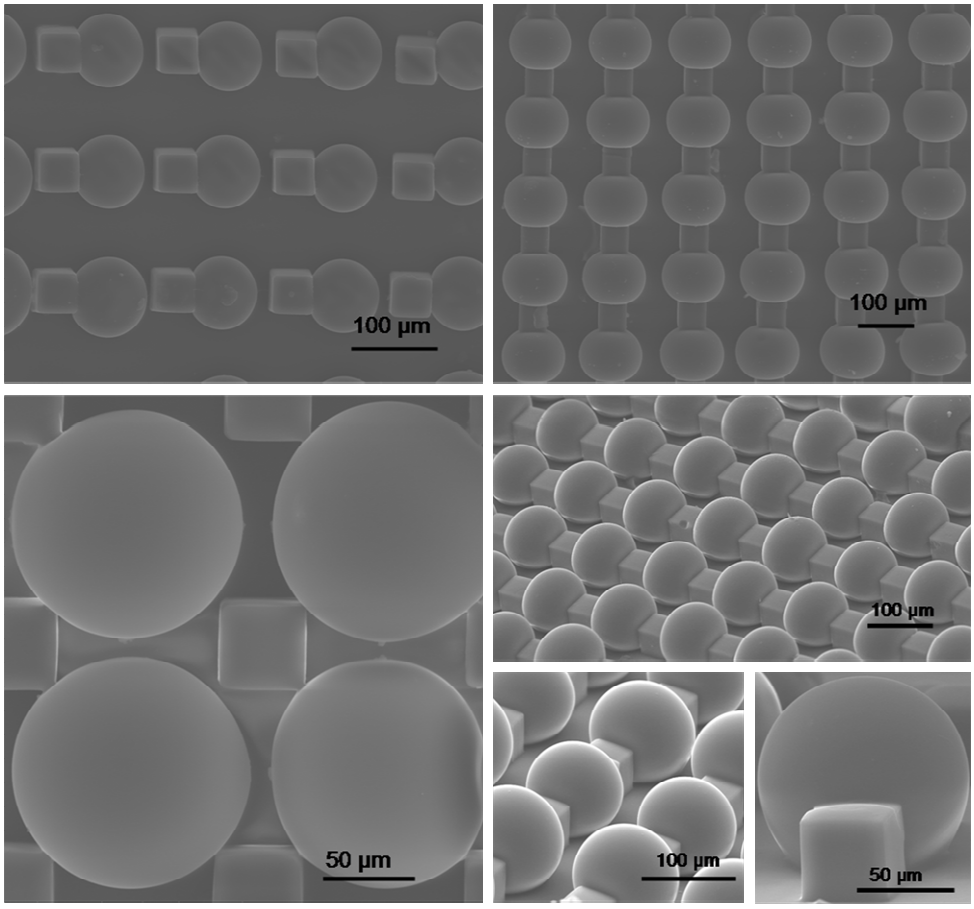

Figure 6.20: SEM images of complementary micromushroom PDMS patterns

6.6 Conclusions

In summary we have developed a novel ‘‘Template modulated solvent vapor back-pressure’’ route for the fabrication of very ordered highly regular assembly of microreservoirs concurrently with the replica of the parent pattern. Parametric dependence of the pattern formation process is examined and control of the pattern features through the control of aspect ratio and pattern density of PDMS mould, solution viscosity, polymer film thickness, solvent vapor pressure, polymer film thickness and pre curing time is demonstrated. These films are then used as templates to replicate the structures on PDMS mold, which are in the form of mushroom-like configurations plus pillars. We believe that such patterns are interesting for many applications such as sensors, MEMS devices, microlens molding (Lee et. al. 2009), or to fabricate microbioreactors (Giang et. al. 2008). It would be interesting to study this approach with PDMS templates of different patterns i.e. microcircles, tapered microstructures, etc.

6.7 References

Bunz U. H. F. *Adv. Mater*. **2006**, 18, 973.

Cayre O. J. ,Paunov V. N. *J. Mater. Chem.* **2004**, 14, 3300.

Chronis N. , Liu G. L. , Jeong K. H., Lee L. P. *Opt. Express*, **2003**, 11, 2370.

Giang U.B.T. , Lee D. , King M. R., DeLouise L. A. *Lab Chip,* **2007**, 7, 1660.

Giang U.B. T., King M. R., DeLouise L. A. *J. Bionic Eng*. **2008**, 5, 308.

Gonuguntla M., Sharma A., Mukherjee R., Subramanian S. A. *Langmuir*, **2006**, 22, 7066.

Grayson A. C. , Shawgo R. S. , Johnson A. M. , Flynn N. T. , LI Y. , Cima M. J., Langer R. T. *Proc. IEEE*, **2004**, 92, 6.

Ito T., Okazaki S. *Nature*, **2000**, 406, 1027.

Lee J. Y., Hong B. H., Kim W. Y., Min S. K., Kim Y., Jouravlev M. V., Bose R., Kim K. S., Hwang I.C., Kaufman L. J., Wong C. W., Kim P., Kim K. S. *Nature,* **2009**, 460, 498.

Léopoldés J., Damman P. *Nat. Mater*., **2006**, 5, 957.

McDonald J. C., Whitesides G. M. *Acc. Chem. Res*., **2002**, 35, 491.

Naughton G. K., Mansbridge J. N. *Clin. Plast. Surg*., **1999**, 26, 579.

Park J. Y., Lee D. H., Lee E. J., Lee S. H. *Lab Chip*, **2009**, 9, 2043.

Peppas N. A., Ward J. H. *Adv. Drug Delivery Rev*., **2004**, 56, 1587.

Rabani E., Reichman D. R., Geissler P. L., Brus L. E. *Nature*, **2003**, 426, 271.

Razzacki S. Z., Thwar P. K., Yang M., Ugaz V. M., Burns M. A. *Adv. Drug Delivery Rev*., **2004**, 56, 185.

Santini J. T., Cima M. J., Langer R. T. *Nature,* **1999**, 397, 335.

Tsai H. K., Moschou E. A., Daunert S., Madou M., Kulinsky L. *Adv. Mater*., **2009**, 21, 656.

Xia Y. , Kim E. , Zhao X. M. , Rogers J. A. , Prentiss M., Whitesides G. M. *Science*, **1996**, 273, 347.

Xia Y., Whitesides G. M. *Angew. Chem., Int. Ed.*, **1998**, 37, 550.

Xia Y., Rogers J. A., Paul K. E., Whitesides G. M. *Chem. Rev.*, **1999,** 99*,* 1823.

Yan Y. H. , Chan-Park M. B., Gao J. X., Yue C. Y. *Langmuir*, **2004**, 20, 1031.

Yang H., Chao C.K. , Wei M.K., Lin C.P. *J. Micromech. Microeng*., **2004**, 14, 1197.

Chapter 7

Conclusions and recommendations for further work

During the course of this work we developed a synthetic methodology for the preparation of poly (β-amino esters) using Lewis acid catalysts. This synthetic methodology was further extended to incorporate weak β-amino esters link within PLA /PCL chains and to introduce hydrophobic pendant chains in poly (β-amino esters) structure. Liquid sequentially crosslinkable poly (β-amino esters) containing pendant vinyl functionality were synthesized. These polymers were subsequently photochemically crosslinked. UV-microembossing technique was used to fabricate different types of patterns. We also demonstrated the utility of new approach to fabricate unusual patterns in PDMS molds using soft lithography.

Significant findings

The significant findings from the investigation undertaken can be summarized as follows.

1. Lewis acid catalysts helped to reduce Michael addition reaction time from 5 days to 1 day at room temperature without affecting yield and molecular weight of resulting polymers (Chapter 3).
2. Michael addition reaction was successfully used for chain extension of oligomers of PLA and PCLA and to introduce hydrophobic pendant chains in the polymer structure (Chapter 3).
3. Polymer dissolution study revealed that the rate of dissolution is higher at acidic pH as compared to that at neutral pH (Chapter 3).
4. Poly (β-amino esters) containing pendant acrylate, methacrylate and allyl ether groups can be synthesized using appropriate triacrylate monomers (Chapter 4).
5. The extent of incorporation of pendant vinyl groups can be manipulated by reacting a mixture containing varying ratios of triacrylate and diacrylate with stoichiometric (1:1) ratio of amine (Chapter 4).
6. Liquid poly (β-amino esters) containing pendant vinyl groups can subsequently be crosslinked by thermal or photochemical methods (Chapter 4).
7. Polymers which degrade in few days to upto 3 months can be synthesized based on choice of hydrophilic and hydrophobic monomers (Chapter 4).

8. Sequentially crosslinkable poly (β-amino esters) can be patterned using UV-microembossing technique in absence of solvents (Chapter 5).
9. The patterns such as channels, square post and cylindrical pillars having pattern density and aspect ratio varying from 0.4 to 5.4 and 0.11 to 0.51 respectively can be fabricated (Chapter 5) .
10. The variation in polymer molecular structures did not influence the performance of the polymers during UV-microembossing. However while fabricating micropatterned polymeric scaffolds, small variations in pattern dimensions due to measurement errors was observed (Chapter 5).
11. The UV-microembossing of SCPBAEs in presence of solvents resulted in new micro patterns, which comprise the patterns present on parent mold along with newer patterns generated during processing as a result of solvent release (Chapter 6).
12. The morphology of these additional microcavities can be manipulated in predictable manner by manipulating fabrication parameters such as polymer solution viscosity, film thickness, solvent vapor pressure, pre-curing time and aspect ratio of parent pattern (Chapter 6).
13. These novel patterns created on the polymer film can be subsequently transferred to another PDMS mold and can then be used to generate multiple copies of the said patterns (Chapter 6).

Recommendations for further work

A research investigation of this kind cannot address all the issues, especially those arising during the course of the investigation. These could form the basis for subsequent investigations. In this context following recommendations can be made for the future work in this area.

1. In this work we have demonstrated the proof of concept. Specific applications of these polymers in drug delivery and tissue engineering need to be identified. Polymers which will meet desired mechanical properties and degradation profiles for these applications can be then synthesized and evaluated for the selected applications.
2. SCPBAEs synthesized in this work can also be used to fabricate nano-fibers via electrospining. Biodegradable nano-fibers are desirable for wound healing, tissue engineering and drug delivery applications.

3. Investigations on biocompatibility and cytotoxicity of the polymers and their degradation products need to be under taken so that further specific applications can be identified.
4. Evaluation of these polymers to demonstrate their utility in the fabrication of nano structure will widen scope of these polymers in soft lithography.
5. Use of polymeric inter-connected scaffolds with cavity for guided cell growth could be evaluated.
6. The mechanism of formation of new patterns from polymer containing solvent needs to be investigated more systematically. This will help to fabricate new unusual patterns which will find applications in other fields as well.
7. Efforts need to be made to synthesize polymers which will reproduce the patterns more precisely.

List of publications

Patent Applications

Novel degradable co-polymer compositions, crosslinked polymers and process for preparation thereof, *1221/DEL/2004*

Santosh L. Hire and Mohan G. Kulkarni.

Communications

1. Template assisted highly ordered novel self assembly of micro-reservoirs and its replication, Hire S.L. et al, **Lab on a Chip**, 2010, 10, 1902 – 1906.

2. Biodegradable UV-micro-embossed polymeric scaffolds for tissue engineering
   Hire S.L et al, Manuscript under preparation.

National / International Conferences

1. pH sensitive biodegradable polymers: Synthesis and applications.
   Oral presentation, at Macro 2004, Thiruvananthapuram, Kerala, India, Dec 14-17, 2004.
2. Sequentially crosslinked biodegradable poly (β-amino esters) for drug delivery.
   Poster Accepted at CRS 2007, Long Beach, California, USA, July 07-11, 2007